Academia Arena

学术争鸣

http://www.sciencepub.net

ISSN: 1553-992X

Volume 1 - Number 1 (Cumulated No. 1), January 1, 2009

Marsland Press, The United States

Academia Arena

学术争鸣

Academia Arena is published bi-linguistically with Chinese and English for the scientists and Engineers by Marsland Press in USA. The journal founded in January 1, 2009 aims to present an arena of science and engineering. The Editor-in-Chief, Deputy Editor and editors have backgrounds in Science, Technology, Civil, Electrical, Chemical, Mechanical Engineering and Physics, Chemistry, Math, Biology and Medicine. Papers submitted could be reviews, objective descriptions, research reports, opinions/debates, news, letters, and other types of writings that are nature and science related.

学术争鸣于2009年元月1日在美国纽约马斯兰德出版社发刊，主要目标为提供科学家与工程师学术辩论的发表园地，专业领域包含科学、技术、土木、电机、化工、机械工程以及物理、化学、数学和医学，编辑群将以最专业客观的立场为所有投稿作者服务。

Information for Authors

Manuscripts Submission

(1) Submission Methods: Electronic submission through email, on line submission and regular mail with formatted computer diskette would be accepted.
(2) Software: The Microsoft Word file is preferred.
(3) Font: Normal, Times New Roman, 10 pt, single space.
(4) Indent: Type 4 spaces in the beginning of each new paragraph.
(5) Manuscript: Don't use "Footnote" or "Header and Footer".
(6) Cover Page: Put detail information of authors and a short running title in the cover page.
(7) Title: Use Title Case in the title and subtitles, e.g. "**Debt and Agency Costs".**
(8) Figures and Tables: Use full word of figure and table, e.g. **"Figure 1.** Annul Income of Different Groups**", Table 1. List Data".**
(9) References: Cite references by "last name, year", e.g. "(Smith, 2003)". References should include all the authors' last names and initials, title, journal, year, volume, issue, and pages etc.

Reference Examples:

Journal Article: Hacker J, Hentschel U, Dobrindt U. Prokaryotic chromosomes and disease. Science 2003;301(34):790-3.

Book: Berkowitz BA, Katzung BG. Basic and clinical evaluation of new drugs. In: Katzung BG, ed. Basic and clinical pharmacology. Appleton & Lance Publisher. Norwalk, Connecticut, USA. 1995:60-9.

(10) Submission Address: Marsland Company, 525 Rockaway PKWY, #B44, Brooklyn, New York 11212, The United States; Telephone: (347) 321-7172; Email: editor@sciencepub.net,

.

(11) Reviewers: Authors should suggest 2-8 competent reviewers with their name and email.

2. Manuscript Preparation

Each manuscript should be formatted to include the following components :

(1) Title page: including the complete article title; each author's full name; institution(s) with which each author is affiliated, with city, state/province, zip code, and country; and the name, complete mailing address, telephone number, facsimile number (if available), and e-mail address for all correspondence.
(2) Abstract: including Background, Materials and Methods, Results, and Discussions.
(3) Key Words.
(4) Introduction.
(5) Materials and Methods.
(6) Results.
(7) Discussions.
(8) References.
(9) Acknowledgments.

Journal Address:

Marsland Press
525 Rockaway PKWY, #B44
Brooklyn, New York 11212
The United States
Telephone: (347) 321-7172
E-mail: sciencepub@gmail.com;
editor@sciencepub.net
Websites: http://www.sciencepub.org

Academia Arena

http://www.sciencepub.net
ISSN: 1553-992X

The **Academia Arena** is an international journal with a purpose to enhance our natural and scientific knowledge dissemination in the world under the free publication principle. Papers submitted could be reviews, objective descriptions, research reports, opinions/debates, news, letters, and other types of writings that are nature and science related. All manuscripts submitted will be peer reviewed and the valuable papers will be considered for the publication after the peer review. The Authors are responsible to the contents of their articles.

Introductions to Authors

1. General Information

(1) Goals: As an international journal by Chinese and English published both in print and on internet, The **Academia Arena** is dedicated to the dissemination of fundamental knowledge in all areas of nature and science. The main purpose of **Academia Arena** is to enhance our knowledge spreading in the world under the free publication principle. It publishes full-length papers (original contributions), reviews, rapid communications, and any debates and opinions in all the fields of nature and science.

(2) What to Do: **Academia Arena** provides a place for discussion of scientific news, research, theory, philosophy, profession and technology - that will drive scientific progress. Research reports and regular manuscripts that contain new and significant information of general interest are welcome.

(3) Who: All people are welcome to submit manuscripts in any fields of nature and science.

(4) Distributions: Web version of the journal is freely opened to the world, without any payment or registration. The journal will be distributed to the selected libraries and institutions for free. For the subscription of other readers please contact with: aarena@gmail.com or sciencepub@gmail.com.

(5) Advertisements: The price will be calculated as US$400/page, i.e. US$200/a half page, US$100/a quarter page, etc. Any size of the advertisement is welcome.

2. Manuscripts Submission

(1) Submission Methods: Electronic submission through email is encouraged and hard copies plus an IBM formatted computer diskette would also be accepted.

(2) Software: The Microsoft Word file will be preferred.

(3) Font: Normal, Times New Roman, 10 pt, single space.

(4) Indent: Type 4 spaces in the beginning of each new paragraph.

(5) Manuscript: Don't use "Footnote" or "Header and Footer".

(6) Cover Page: Put detail information of authors and a short title in the cover page.

(7) Title: Use Title Case in the title and subtitles, e.g. **"Debt and Agency Costs".**

(8) Figures and Tables: Use full word of figure and table, e.g. **"Figure 1.** Annul Income of Different Groups**", Table 1. Annual Increase of Investment".**

(9) References: Cite references by "last name, year", e.g. "(Smith, 2003)". References should include all the authors' last names and initials, title, journal, year, volume, issue, and pages etc.

Reference Examples:

Journal Article: Hacker J, Hentschel U, Dobrindt U. Prokaryotic chromosomes and disease. Science 2003;301(34):790-3.

Book: Berkowitz BA, Katzung BG. Basic and clinical evaluation of new drugs. In: Katzung BG, ed. Basic and clinical pharmacology. Appleton & Lance Publisher. Norwalk, Connecticut, USA. 1995:60-9.

(10) Submission Address: aarena@gmail.com or sciencepub@gmail.com, Marsland Company, P.O. Box 21126, Lansing, Michigan 48909, The United States, 517-980-4106.

(11) Reviewers: Authors are encouraged to suggest 2-8 competent reviewers with their name and email.

2. Manuscript Preparation

Each manuscript is suggested to include the following components but authors can do their own ways:

(1) Title page: including the complete article title; each author's full name; institution(s) with which each author is affiliated, with city, state/province, zip code, and country; and the name, complete mailing address, telephone number, facsimile number (if available), and e-mail address for all correspondence.

(2) Abstract: including Background, Materials and Methods, Results, and Discussions.

(3) Key Words.

(4) Introduction.

(**5) Materials and Methods**.

(**6) Results**.

(**7) Discussions**.

(**8) References**.

(**9) Acknowledgments**.

Journal Address:

Marsland Press
P.O. Box 21126
Lansing, Michigan 48909
The United States
Telephone: (517) 349-2362
E-mail: aarena@gmail.com;
sciencepub@gmail.com
Websites: http://www.sciencepub.net

Academia Arena

Volume 1 - Number 1, January 1, 2009, ISSN 1553-992X
Cover Page, Introduction, Contents, Call for Papers, All papers in one file

Contents

Marsland Press, the United States, editor@sciencepub.net

Design investigation of a magnetic hollow cathode discharge for general laboratory applications

Djamel Boubetra[1], Hartmut Kerkow[2]

[1]LMSE Centre Universitaire de Bordj Bou Arreridj, Algeria
[2]Alt Karow 17 HUB Berlin, Germany
E-Mail: boubetra@gmail.com

Abstract: We present in this work a model of design gas discharges with cold and magnetic hollow cathode, which can be useful for the experiments of sputtering and perforation of the layers solid bodies. It would use the physical principle of crossing electrical and magnetic fields so to increase the ionization way electrons and to guarantee a long maintenance of the discharge. This arrangement has potential application in a wide variety of laboratory research and development projects. [Academia Arena, 2009;1(1):1-3]. ISSN 1553-992X.

Keywords: magnetic hollow cathode, sputtering, plasma

1. Introduction

The magnetic hollow cathode (MHC) is an element for the construction of gas discharges arrangement for different purposes, which are still functional with relatively gas pressures (Boubetra, 2007), the MHC has been studied in order to improve the life-time of a discharge and of an ion source for an implanter (Tonegawa et al, 1986) and it would used for an Penning ion source (Joshua, 2008).

2. Experimental and results

It's consists of the magnetic hollow cathode, the cylindrical anode and a (anti-cathode), those simultaneous is the magnetic pole piece of the magnetic field in anode region. The potential of the anti cathode could be selected in voltage range between 200 V and 1 kV, concerning the anode is freely, without the ion stream would have changed considerably. The polarity of the two magnetic fields to each other had crucial influence on the shape of the plasma in the anode region. Were the fields antivalent, then arose a strong bundling of the plasma, this can be explained with the fact that the magnetic flux lines penetrate inside the used hollow cathode and to be pushed by the permanent magnet.

A strong magnetic scattering field develops directly under the cover of the hollow cathode, there takes place a strong gas reinforcement of discharge, and all electrons from this range are collected by participation of the outside field in the plasma production and transferred into anode region. Special characteristic for this field geometry is the low gas pressure; witch can be lowered up to 0, 1 Pa.

Against it if the two magnetic fields are positioned in series, then the plasma is transferred into the Anode region according to the cross section of the hollow cathode opening.

In the anti cathode develops an even glowing seam, for its distance becomes larger with increasing suction tension for the ions (space charge layer). In this field arrangement the spraying installation must be operated with somewhat higher gas pressures, which shows that the gas reinforcement is not so effective for this magnetic field arrangement.

In Figure 2 is to shown 200 µm thick Si-disk, which was also bombarded in different times with Ar-Ions. The sample were perforated after two hours radiation, after four hours the hole diameter rose of 2 mm to 4mm, from which a certain radiation not homogeny in outer zone is to be read off, with the arrangement of parallel magnetic field was tried a homogeneous demolition , however the homogeneity of the demolition was not satisfying because the deviation were over a sample diameter more than 10%, also attempts were to tested by a sample shift a diagonal cross section not very successful and only by accident one could receive an edge sharp edge at evaporated films.

The power conversion at the samples was substantial by the high ion current density of several 100 mA/cm², the sample heating up played a large role with the attempts sometimes then it came also to bubbling at the surface, which resulted from current charges of the sample by to high loss rates.

The form of the plasma is determined by the polarity of the two magnetic fields to each other. If the magnetic fields of the hollow cathode and the anode region are arranged against each other for plasma focusing, then a focal spot develops on the Anticathode and/or anode. If the magnetic fields lie parallel to each other, then the plasma is transferred wide into the anode region.

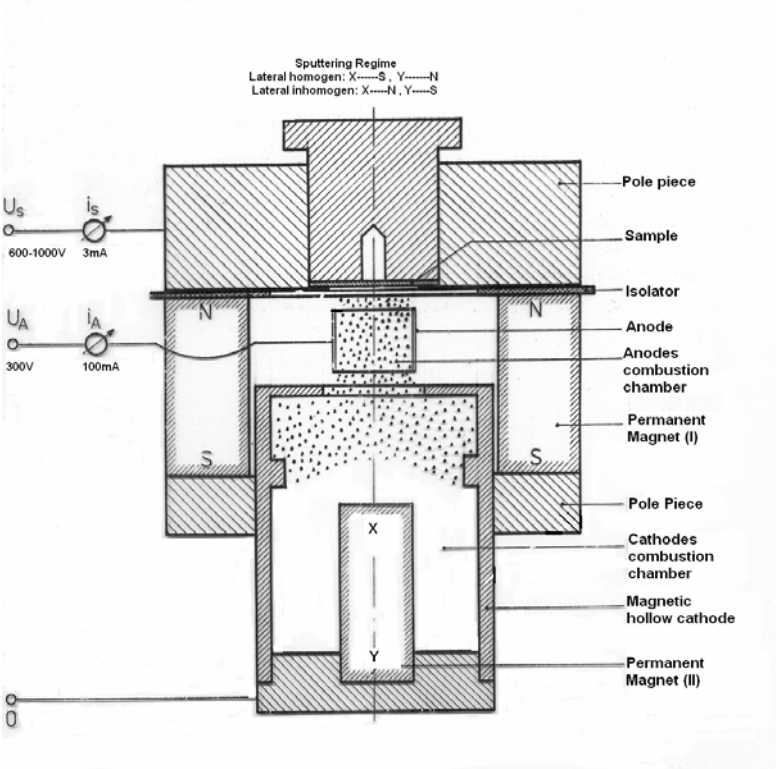

Figure 1. Sputtering arrangement with magnetic hollow cathode

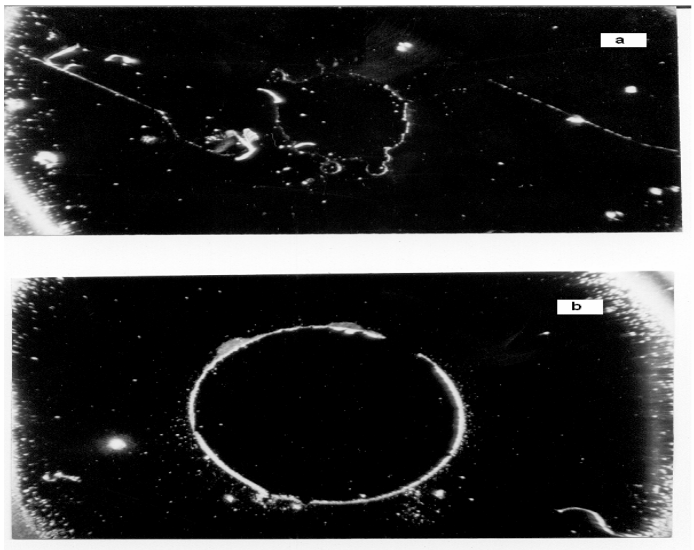

Figure 2. Photography of perforation by sputtering from 200 μm thick Si samples
a) after 2h/5mA/800V - ion bombardment
b) after 4h/5mA/800V–ion bombardment

Conclusion

By use this arrangement with crossed electrical and magnetic fields the gas pressure can be reduced likewise according to the extension of the ionization ways by the circulation of the electrons in the magnetic field , This leads then to a smaller gas need for the maintenance discharges and a decrease the gas load of the recipient in the vacuum installation This magnetic hollow cathode is an element with which one different ion source types can realize like Penning ion source, sheet ion source and duoplasmatron.

Acknowledgments

This work was supported in part by the Company Antar Trade Condor BBA, Algeria.

Correspondence to:
Dr. Boubetra Djamel
LMSE, Centre Universitaire Bordj Bou Arreridj
El Anasser 34265, Algeria
boubetra@gmail.com

References

1. Boubetra, Dj., J. of American Sci. 3(4), 15-19, (2007).
2. Tonegawa, A. et al., Vacuum, Vol. 36, Issues 1-3,15-18, (1986).
3. Tonegawa, A. et al., NIM B Vol. 6 Issues 1-2, 129-132, (1985)
4. Joshua, L.R., Plasma Sources Sci. Technol.17 035009 (7pp) (2008)

A Procedural Schedule For Groundwater Flow In Porous Media

Odunaike R. K. Usman M. A. Hammed F. A. Adeosun T. A. and Olayiwola, M.O.

[1]Department of Mathematical Sciences,
Olabisi Onabanjo University, Ago-Iwoye, Nigeria.
2 Department of Mathematics, Yaba College of Technology, Lagos, Nigeria

Dr. Usman M A
Dept. of Mathematical Sciences
Olabisi Onabanjo University, Ago-Iwoye, Nigeria.
usmanma@yahoo.com

ABSTRACT: The classical Darcy,'s law is generalized by regarding groundwater flow as a function of the hydraulic head; which is' a quantity of primary interest. This generalized law and the law of conservation of mass are then used to derive the generalized form of the groundwater flow equation. Analytical solution of this groundwater flow equation for which a fractal dimension for the flow is assumed. Equation of unsteady flow in a leaky aquifer is discussed. Prediction of groundwater flow with illustrations of contouring the water table map helps to predict the direction of flow. [Academia Arena, 2009;1(1):4-12]. ISSN 1553-992X.

Keywords: Porous media, Darcy's law, Hydraulic Head Introduction

INTRODUCTION

A problem that arises naturally in groundwater investigation is to choose an appropriate geometry for the geological system in which the flow occurs. For example, one can use a model based on unsteady state radial flow to simulate the flow in porous media with a very large pore i1uid density (Black *et aI*, 1986). This is in particular the case with the delineation of freshwater aquifer in the Coastal area of Lagos State (lkoyi, Lekki, Apapa and Victoria Island), characterized by the presence of boreholes drilled in these area that serve as the main drawdown in pumping wells. Attempts to fit in analytical solution of the groundwater flow equation with a one dimensional flow and fit a Conventional radial flow model to the observed drawdown at early times underestimates and later times over estimates[1– 4].

The derivation of a generalized groundwater flow equation from the law of mass Conservation and energy balance is usually an indication that the theory is not implemented correctly or does not fit the observations. To investigate the possibility on the Lagos coastal areas. A generalized equation of groundwater flow in three-dimensional equation is expressed as[6-10]

$$\frac{\partial}{\partial x}\left(K\frac{\partial h}{\partial x}\right)+\frac{\partial}{\partial y}\left(K\frac{\partial h}{\partial y}\right)+\frac{\partial}{\partial z}\left(K\frac{\partial h}{\partial z}\right)=S_s\frac{\partial h}{\partial t} \qquad (1)$$

A fractal one-dimensional groundwater flow equation is assumed as an hypothetical case of a closed aquifer for which the flow is essentially horizontal direction and independent of y and z- axis.

$$\frac{\partial}{\partial x}\left(K\frac{\partial h}{\partial x}\right)=S_s\frac{\partial}{\partial t}$$

$$\nabla.[k\nabla h]=S_s\,\partial_1 \text{ h} \qquad (2)$$

Where S_S the specific storativity
Where K the hydraulic conductivity tensor of the aquifer
Where h(x,t) the hydraulic head with x and t the usual spatial and time coordinate
Where ∇ the gradient operator
Where ∂_1 the time derivative

The model showed that the dominant flow in these aquifers is essentially horizontal and linear and not vertical and radial as commonly assumed. However, more recent investigations (Cloot and Botha, 2006) suggest that the flow is also influenced by the geometry of the bedding parallel fractures, a feature that Equation (3) cannot account for. It is therefore possible that equation may not be application flow in fractured rock other than a porous media[I 1- 15].

In an attempt to circumvent this problem, we introduced a conventional geometry of the aquifer, which assumed a fractal one dimensional flow (Figure I). Although this model has been applied with reasonable success in the analysis of the hydraulic head from borehole in the Lagos' Coastal Area[16].

As a review of the derivation of Equation (2) will show [Bear, 1972], Darcy's Law is used as a keystone in the derivation of Equation (2)[5].

$$q(x,1) = -k\nabla h \qquad \ldots (3)$$

This law proposed by Darcy early in the 19th century, is relying on experimental results obtained from the flow of water through a one-dimensional sand column, the geometry of which differs completely from that of a fracture [17]. There is therefore a possibility that the Darcy's law not be valid for flow in fractured rock formation but is only a very crude idealization of reality. Nevertheless, the relative success achieved by (Cloot and Botha, 2006) to describe many of the properties of Karoo aquifer on the campus of the university of free State, suggests also that the basic principle underlying this law may be correct: the observed draw down is to be related to either a variation in the hydraulic conductivity of the aquifer or a change in the hydraulic head. Any new form of the law should therefore be reduced to the classical form under a more common condition. Because K is essentially determined by the permeability of the porous medium and not the flow pattern, the gradient term in Equation (3) is the most likely cause for the deviation between the observed and the theoretical drawdown observed in the Karoo formation. In this work, the possibility is further investigated for a flow symmetry form of Equation (2) by creating an artificial vertical fault that divides the aquifer into two compartments of length L, on the left and L_1 on the right. The fault gauge is sufficiently low in hydraulic conductivity that acts as a flow barrier. Thus, the left compartment is hydraulically isolated from the right compartment. Initially, the hydraulic head is h_1 in the left compartment and h_2 in the right compartment. Assume that at time t = 0, the fault is ruptured by an eat1hquake, so that the two compartments are now hydraulically connected. The earthquake would deform the aquifer causing changes in hydraulic head. The question we want to answer is, what happens to the hydraulic head distribution in the aquifer after the fault rupture? [19]

Therefore, when the fault ruptures, we expect groundwater to flow from compartment with higher head to compartment with lower head, in other word, flow would occur essentially in horizontal x-direction. Analytically, if we set the original length of the x-axis at the left hand boundary, then the How domain is for one-dimensional flow in a homogenous aquifer, the governing in equation (4).

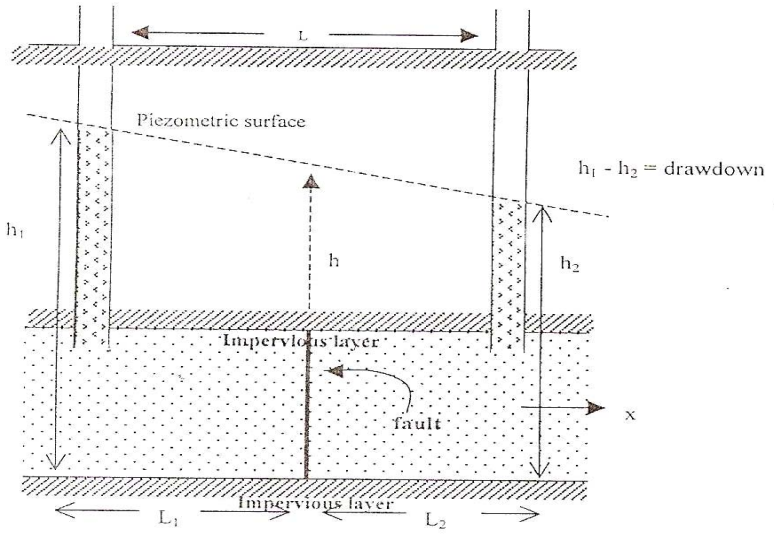

Figure 1. Flow through a confined aquifer

The boundary condition are $\frac{\partial^2 h}{\partial x^2} = \frac{S_s}{K}\frac{\partial h}{\partial t}$ (4)

$$0 < x < L_1 + L_2$$

$$\frac{\partial h}{\partial x} = 0 \text{ at } x = 0$$

$$\frac{\partial h}{\partial x} = 0 \text{ at } x = L_1 + L_2$$

The initial conditions are

$$h(x,0) = h_1 \quad \text{for } 0 \le x \le L_1$$

$$h(x,0) = h_1 \quad \text{for } L_1 \le x \le L_1 + L_2$$

Separation of variables is employed and the solution is assumed as:

$$h(x,t) = f(x) \,.\, g(t) \quad (5)$$

where:

$$a = \frac{S_s}{K} \text{ and } f(0) = 0 \text{ for } K_1 = \frac{n\pi}{L}$$

Using these in solution of (5), we have,

$$h(x,0) = A_0 + Cos\frac{n\pi}{L}x\lambda\frac{n^2 n^2 Kt}{S_s L^2}$$

Initial condition, we have,

$$h(x,0) = A_0 + \sum_{n=1}^{\infty} A_n Cos\frac{n\pi}{L}x\lambda\frac{n^2 n^2 Kt}{S_s L^2} \quad (6)$$

Substitute for A_0 and A_n from Fourier integral, we have

$$A_0 = \frac{1}{L}\int_0^L f(x)dx \quad \text{and}$$

$$A_0 = \frac{2}{L}\int_0^L f(x)\text{Cos}\frac{\text{n}\,\pi}{\text{L}}dx$$

$$h(x,t) = \frac{1}{L}\int_0^L f(x)dx + \frac{2}{L}\sum_{n=1}^{\infty}\lambda\frac{n^2 n^2 Kt}{S_s L^2}\text{Cos}\frac{\text{n}\,\pi x}{\text{L}}\int_0^L f(x)\text{Cos}\frac{\text{n}\,\pi x}{\text{L}}dx \quad (7)$$

Let x be a dummy variable of integration. To find the solution to the flow equation, we replace L in Equation (7) by L_1+L_2 and in addition, we replace f(x) by h(x,0) as defined. The integral inside the summation on the right hand side of equation (7) and substituting the preceding integral, we have.

$$h(x,t) = \frac{h_1 L_1 + h_2 L_2}{L_1 + L_2} + \frac{2}{L_1 + L_2}\sum_{n=1}^{\infty}\lambda\frac{n^2 n^2 Kt}{S_s L_1 + L_2}Cos\frac{n\pi x}{L_1 + L_2}\frac{(h_1 - h_2)(L_1 + L_2)}{n\pi}\text{Sin}\frac{n\pi L_1}{L_2 + L_2}$$

$$h(x,t) = \frac{h_1 L_1 + h_2 L_2}{L_1 + L_2} + \frac{2(h_1 - h_2)}{\pi}\sum_{n=1}^{\infty}\frac{1}{n}\lambda\frac{n^2 n^2 Kt}{S_s (L_1 + L_2)^2}Cos\frac{n\pi x}{L_1 + L_2}\ \text{Sin}\frac{n\pi L_1}{L_2 + L_2} \quad \ldots.(8)$$

This solution can be expressed in dimensionless form as:

$$h_D(x_D, t_D) = L_D + \frac{2}{\pi}\sum_{n=1}^{\infty}\frac{1}{n}\lambda^{-n^2\pi^2 t_D}Cos(n\pi x_D)Sin(n\pi L_D)\ldots \quad (9)$$

Where:

The dimensionless distance- $$x_D = \frac{x}{L_1 + L_2}$$

The dimensionless time - $$t_D = \frac{Kt}{(L_1 + L_2)^2 S_s}$$

The dimensionless - $$L_D = \frac{L_1}{L_1 + L_2}$$

One advantage of a closed form analytical solution is that it allows us to examine the behaviour of the flow system. There are several interesting features in this solution. The first term on the' right hand side is the steady state part of the solution. It gives the head in the aquifer when *t* is very large (Figure 3). The second term on the right hand side is the transient part of the problem. Because *t* appears in the argument of the exponential function, the second term tends to zero as *t* becomes large. Furthermore, note that the second term goes to zero at a faster rate if K/Ss (hydraulic diffusivity) is large. Thus, the hydraulic diffusivity is a quantity that controls the rate of hydraulic head.

Unsteady Flow in a Leaky Aquifer

The generalized groundwater flow equation in a leaky aquifer is of the form,

$$S_s \frac{\partial h}{\partial t} = K\nabla^2 h - G \qquad (10)$$

where $G = \frac{e}{T}$, and $\mathrm{e} = \mathrm{K}^1 \frac{h_0 - h}{b^1}$ can determined form Darcy's law.

Under this condition, the above equation becomes a radial flow,

$$T\left(\frac{\partial^2 S}{\partial r^2} + \frac{1}{r}\frac{\partial S}{\partial r}\right) - S\frac{\partial}{\partial t} - q = 0$$

where

$$q = \frac{K^1}{b^1} S = \frac{S}{C} \qquad (11)$$

Using the same approach as the solution for the confined (Theis) solution, we obtained the leaky partial different equation:

$$u\left(\frac{\partial^2 S}{\partial u^2} + \frac{\partial S}{\partial u}\right) + \frac{\partial S}{\partial u} - \frac{r^2}{4uL^2} S = 0 \qquad \ldots(12)$$

and from separation of variables, we obtain an appropriate solution

$$S = \frac{Q}{4\pi T} W\left(u, \frac{r}{B}\right) \qquad \ldots(13)$$

The quantity $\frac{r}{B}$ is given by $\frac{r}{\sqrt{T/(K^1/b^1)}}$

Which holds as long as $U < 0.01$

Where W $\left(u, \frac{r}{B}\right)$ is dimensionless form from a logarithm plot chart.

The plot of S = *hi - h;* versus *t* at various observation wells, since drawdown is the hydraulic heads measured the level of the water table in wells relative to the piezometric surface (Figure I). The change in water table in the pumping well or in observation well nearby is referred to as drawdown (Figure 5).

APPLICATION

Set of drawdown data was analyzed in order to validate the new method. The examples were obtained from borehole drilled along the coastal area of Lagos State. The boreholes belong to companies operating along the coastal area. The examples were to illustrate the application using equations developed in this case.

Example 1

A well is located in an aquifer with a conductivity of 15 meters per day and a storativity of 0.005. The aquifer is 20 meters thick and is pumped at a rate of 2725 cubic meters per day. What is the drawdown at a distance of 7 meters from the well after one day of pumping?

- Hydraulic conductivity = 15 metres per day
- Storativity = 0.005
- Aquifer thickness = 20 metres
- Pumping rate = 2,725 cubic metres per day
- Distance from the well = 7 metres

T=Kb = m/day x 20m = 300 m^2/day

$$u = \frac{r^2 S}{4Tt} = \frac{(7m)^2 \times 0.005}{4 \times 300m^2 / day \times 1day} = 0.0002$$

From the table of W(u) and u, if u = 2 x10^{-4}, w(u) = 7.94:

$$h_1 - h_2 = \frac{Q}{4\pi T} W(u) = \frac{2727m^3 / day \times 7.94}{4 \times \pi \times 300m^2 / day} = 5.73m$$

The draw is 5.73 meters after one day.

Example 2

A well in a confined aquifer was pumped at a rate of 220 gallons per minute for about 8 hours. The aquifer was 18 feet thick. Time drawdown data for an observation well 824 feet away are given in table 2. Find T, K, and S.

W(u) = 1

I/u = 1

$h_1 - h_2$

$t/r^2 = 6.06 \times 10^{-6}$

Radial Diameter d = 20ft

Pumping Rate = 220 gallons per day for 8 hours

Aquifer thickness = 18 feet

Transmissivity:

$$T = \frac{114.6QW(u)}{h_0 - h} = \frac{114.6 \times 220 \times 1.0}{2.4} = 10{,}500 \ \ galonsgpd \, \text{l ft}$$

Hydraulic Conductivity:

$$K = \frac{T}{b} = \frac{10{,}500}{18} = 580gpd \ / \ \text{ft}^2$$

Storativity

$$S = \frac{Tu}{2693} \times t / r^2 = \frac{10{,}500 \times 1}{2693} \times 6.06 \times 10^{-6} = 0.00002 \ldots. \quad \text{(Theis method)}$$

$$S = \frac{Qr^{1-n}}{4\pi Td} = \frac{220}{4\pi(10{,}500)(20)} = 0.000018 \quad \ldots \quad \text{(Cloot \& Botha method)}$$

$$S = \frac{QW(u)}{4\pi Td} = \frac{220 \times 1.0}{4 \times \pi \times 10{,}500} = 0.0016 \quad \ldots. \quad \ldots.. \quad \text{(Observation)}$$

(See fig 4 & 5)

Example 3

An aquifer 10 meters thick is penetrated by a well It is overlain by a semipervious layer I meter thick with a K" of I 0^{-5} centimeter per second. There is no storage in the leaky confining layer. The aquifer has a K of] $0.^{2}$ centimeter per second and an S of 0.0005. If a well pumps at 500 cubic meters per day, compute values of drawdown at I, 5, 10, 50, 100, 500, and 1000 meters. (see Table 2)

Aquifer Thickness = 10 metres
Storativity = 0.0005
Pumping rate = 500 cubic metres per day
Various depths = I, 5, 10, 50, 100,500 & 1,000 metres
r = distance to the observation wells
t = time since pumping begin
K = 10^{-2} cm/sec x 60 sec/min x 1440 min/day x 10^{-2} m/cm = 8.64 m/day
K' = 10^{-5} cm/sec x 60 sec/min x 1440 min/day x 10^{-2} m/cm= 8.64x 10^{-3} m/day
b'=-lm
b'=l0m
T = Kb = 86.4 m^2/day
B = $(Tb'/K')^{1/2}$
= (86.4 m^2/day x 1 m /8.64 x $10.^{3}$/day)$^{1/2}$
$(10^{4})^{1/2}$
B = 100

$$u = \frac{r^2 s}{4Tt} = \frac{r^2 \times 0.0005}{4 \times 86.4 \times 1} = 1.44 \times 10^{-6} r^2$$

$$\frac{r}{B} = \frac{r}{100} = 10^{-2} r$$

$$h_1 - h_2 = \frac{2.6Q}{4\pi T} W\left(u, \frac{r}{B}\right) = 1.06 W\left(u, \frac{r}{B}\right)$$ (our observation) see Figure 5

As u = 1.44x $10^{-6}r^2$, we can find the value of u for each r-value

4.1 Discussion of Results:

All the three examples of drawdown data show that the new method underlying this law and the observed drawdown variations in hydraulic conductivity of the aquifer is correct. Each of the analytical solution describes the response to pumping in a very idealized representation of aquifer configurations. In the real world, aquifers are heterogeneous and isotropic: They usually vary in thickness; and they certainly do not extend to infinity. Where they are bounded, it is not by straight-line boundaries that provide perfect confinement. Aquifers are created by complex geologic processes that head to irregular stratigraphy and trendouts of both aquifers and aquitards. The Predictions that can be carried out with the analytical solution presented in this paper must be viewed as best estimates. In general, hydraulic head solutions are most applicable when the unit of study is a well.

They are less applicable on a large scale, where the unit of study is an entire aquifer.

The graphical method of solution starts with the construction of reversed type curve of W(u) against I/u on logarithm paper (Figure 4). Data from observation well located at different distances from the pumping wells were used. If there is only one observation well, then it is sufficient to plot hi - h_2 as a function of *t* (Table I). .

Using "Contouring the Water Table Map", we noticed that the contours form V's with the river and its tributaries. That's because the river is a "gaining" river. It is receiving recharge from the aquifer. The contours show that ground water is moving down the sides of the valley and into the river channel. The opposite of a gaining stream is a "losing" stream. It arises when the water table at the stream channel is lower than the stream's elevation or stage, and stream water flows downward through the channel to the water table. This is very common in dryer regions of the Southwest. In the case of a losing stream, the V will point downstream, instead of upstream. (Figure 6).

When making a water table map, it is important that your well and stream elevations are accurate. All elevations should be referenced to a standard datum, such as mean Sea level. This means that all elevations are either above or below the standard datum (e.g., 50 feet above mean sea level datum). It's also very important to measure all of the water table elevations within a short period of time, such as one day, so that you have a

"snapshot" of what's going on (Adeosun *et al* 2006). Because the water table rises and falls over time, you would be more accurate if readings are made before these changes occur.

Understanding how ground water flows is important when you want to know where to drill a well or a water supply, to estimate a well's recharge area, or to predict the direction of contamination is likely to take once it reaches the water table. Water table contouring can help groundwater developer to do all these things. Hence, groundwater flow through the subsurface is the whole essence of this paper and called for further investigation.

CONCLUSION

It has been clearly demonstrated that the study of flow in porous media was recognized in detailed through the physical behaviour of subsurface water and their interactions with the solid matrix (flow of groundwater was delineated through the presence of boreholes drilled along the coastal area of Lagos State for characterizing the flow in the subsurface aquifer. The classical Darcy's law governed the flow in porous media by regarding ground water flow as a function of the hydraulic head. A complete statement of this flow problem required specifying the extent of the flow domain, the governing equation, spatial distribution of properties, for example, hydraulic conductivity and specific storativity, boundary conditions and initial conditions. Analytical solution of this flow equation for which a fractal dimension was assumed to yield a closed form solution that could be written on paper and also be examined to understand the behaviour of the flow system in a typical limited homogeneous flow domain with relatively simple geometry.

The problem of solving fluid flow through porous media has proved analytically intractable and the problem of understanding flow and storage in aquifers is very complex. It was ·recognized that flow through' such a medium is very significantly influenced by the porous media characteristics such is porosity and permeability. A limitation of this work is the estimation of permeability (hydraulic conductivity) of the medium which can not be examined and investigated without being to the field, even if examined, permeability estimation has proved to be complex and this concept has limited the free flow of fluid within the porous medium. Therefore, this work is hoped to complement the study of flow through porous media that might have been done in other parts of the world and contributes to the unveiling knowledge of the applicability of flow in porous media. Prediction of this flow shows several interesting qualitative features such as graphs and contouring of water table map, which held to predict change in drawdown in pumping well and the direction of flow. The method becomes more accurate and easy to handle with little or no variations in the observed drawdown and water table flow prediction.

NOMENCLATURE

S = Storativity
T = Transimissivity (L^2T^1)
$h_1 - h_2$ = drawdown (L)
Q =pumping rate (L^3T^1)
t = time, (time since pumping began)
r = radial distance from pumped well (L)
e = leakage rate
B = leakage factor (Lb^{-1}) = thickness of leaky layer (L)
b^l = thickness of leaky layer (L)
K^1= vertical hydraulic conductivity of leaky layer (LT^{-1})
(X, y)= rectilinear coordinator
S_s = specific storage
h = head (L)
q = specific discharge (M^3d^{-1} per m^2)
K = hydraulic conductivity of aquifer (md^{-1})
h_2, h_1 = hydraulic heads measured along flow path
L = distance between head measurements (m)
W = width of cross - sectional flow (m)
D = height of cross-sectional flow (m)
W(u)= dimensionless form from chart
G = leakage factor
U = flow velocity

Table 1: Drawdown Table

Time After Pumping Started (min)	T/r^2	Drawdown (ft)
3	4.46×10^{-6}	0.3
5	7.46×10^{-6}	0.7
8	U8 x l0^{-5}	1.3
12	1.77×10^{-5}	2.1
20	2.95×10^{-5}	3.2
24	3.53×10^{-5}	3.6
30	4.42×10^{-5}	4.1
38	5.57×10^{-5}	4.7
47	6.94×10^{-5}	5.1
50	7.41 xl0^{-5}	5.3
60	8.85 x l0^{-5}	5.7
70	1.03×10^{-4}	6.1
80	1.18×10^{-4}	6.3
90	1.33×10^{-4}	6.7
100	1.47×10^{-4}	7.0
130	1.92×10^{-4}	7.5
160	2.36×10^{-4}	8.3
200	2.95×10^{-4}	8.5
260	3.83xl0^{-4}	9.2
320	4.72×10^{-4}	9.7
380	5.62×10^{-4}	10.2
500	7.35×10^{-4}	10.9

Table 2: Field Data

R	U		W
1m	1.44×10^{-6}	0.01	9.44
5m	3.6 x l0^{-5}	0.05	6.23
10 m	1.44×10^{-4}	0.1	4.83
50 m	3.6×10^{-3}	0.5	1.85
100m	1.44×10^{-2}	1	0.824
500 m	6×10^{-1}	5	0.007
1000 m	1.44	10	00001

From the computed values of W(u, r/u) at each observation point, the drawdown can be computed from $h_0 - h = 1.06$ W(u, r/b)

R	**$h_1 - h_2$**
1m	9.44m
5m	6.23m
10 m	4.83m
50 m	1.85m
100m	0.824m
500 m	0.007m
1000 m	00001m

REFERENCES

1. 1 Adeosun T.A., Nwonwu, A.C. and Oladapo, M.l. (2006): Delineation of Freshwater Aquifers in the Coastal Area of Lagos State (Ikoyi, Victoria Island, Lekki, Apapa): conference paper presented at 29th Annual Conference of the Institute of Physics, held in the Department of Physics, University of Nigeria, Nsukka.
2. Allen, R. and Cherry, *J.A.* C200 I): Groundwater, Prentice - Hal!, Inc, Englewood Cliffs. NJ.
3. Bear, J. (1972): Dynamics of fluids in porous media: Dover publication Inc., Mineola, New YorK. U. S. A.
4. Beltrami, E. (2004): Mathematics for Dynamic Modeling: Academic Press, lnc, N. Y. at Stony Brook, N. Y.
5. Cloot, A. and Botha J.F. (2006): A Generalised Groundwater Flow Equation Using The Concept of Non-Integer Order Derivatives, Institute of Groundwater Studies, Journal of Growldwater, SA Vol. 32 No.1. Department of Mathematics, University of the Free State, Bloemfontein, South Africa. www.wrc.org.za
6. Coat, J. and Smith, F. (2005): Reservoir Simulation, Dover Publication, New York.
7. Codinton, E.A. (1990): An Introduction to ordinary Differential Equation: Prentice-Hall, New Delhi.
8. Darton N. H. (1972): Preliminary Report on the Geology and Underground Water Resources of the Central Great Plains. U. S. A Geological Survey Professional Paper32, 433pp.
9. Douglas, J .F., Gasiorek, J. M. and Swaffield, J. A (1995): Fluid Mechanics: Longman Singapore Publishers, Third Edition, 1995.
10. Felter C. W. (1997): Applied Hydrogeology: Cambridge University Press, New York
11. Ferziger, J.R. and Milovon P. (2002): Computational Fluid Dynamics, 3rd edition, Springer- Verlag, New York
12. Fujita, K. (1997): Principle of Geophysics: Blackwell Science, Inc, U.S.A.
13. Harper, C. (1999): Introduction to Mathematical physics: Prentice- Hall, New Delhi,
14. Ogunleye L O. and Oni T.O. (2001): Simple Approach to Fluid Mechanics for Science and Engineering Students: Godliness Printing and Publishing Co. Vol. 1. University of Ado Ekiti, Ado Ekiti, Nigeria.
15. Oladapo M. 1. And Omosuyi O. (2000): Groundwater Geophysics: Lecture Note Series, Vol. I. Department of Applied Geophysics, Federal University of Technology, Akure.
16. Oteri A. U. (1988): Report on water pollution in the coastal area of Lagos State, Nigeria.
17. Wright, W.S. Wright, C.D. (1997): Differential Equations with Boundary Value Problems, Brooks and Cole Publishing Coy. N. Y.
18. Zhan, H. and Park, E. (2005): Modeling of Underground Water Flow, Department of Geophysics, Texas A & M, University College. Station, Tx 77843-3115, Corresponding Author (Zhan@hydrog.tamu.edu).

Wed, Aug 27, 2008 at 2:55 PM

Comparison of the Wehner Spots With Angle Distribution Sputtered Atoms Materials

Dj. Boubetra and L.Selmani

LMSE, Centre Universitaire de Bordj Bou Arreridj
El Anasser 34265, Algeria
boubetra@gmail.com

Abstract: The causes for the Anisotropy in the angle distribution sputtered atoms is yet extensively unexplained. Therefore experimental investigation should be carried out to this question. The ions beam was used for comparing investigation between the distributions of back steered ions and sprayed atoms. We know that the pulverization of crystals shows an anisotropic angular distribution of pulverized atoms. The appearance of these phenomena is initiated once Wehner spots are obtained by putting a receptor in front of the sample, which shows a correlation with the principal crystallographic axes. Other study shows that till now the studies and works already done are not strongly founded in the sense of the correspondence of the Wehner spots and the principal axes of the crystals. Measurements are represented in many works and during the last years detailed studies on gold crystals (111). Principally the gold atoms emissions have appeared in the directions (110) and (111) for which the intensity to energy ratio of projectile ions is modified. Emissions directions are to be maintained in addition to representation and for omitted raison directions changes have to be taken into account. After the studies of deviations in the emission direction appear during the copper crystals pulverization. The authors allocate this fact to the influence of the forces of superficial links which should generally lead to a preference of the particles emission in the normal direction to the surface. The question is who it makes that the link ratio for different crystals directions have a different response; however, it is shown that the application of an ionic beam emitter, to examine the interference of the direction emissions of the pulverized atoms with principal crystallographic axes is necessary. [Academia Arena, 2009;1(1):13-17]. ISSN 1553-992X.

Key words: Anisotropy, angular distribution, sputtering, crystallography

Experimental and Methods

The principle of the exact determination of the angle distribution sputtered atoms and the crystal direction was based up on the registration of the particle currents in the pulverisation through precipitation development on a transparent plastic foil and through photographic registration of the particle current reflected Proton arrangement shows in Fig.1. In a reason disk out of aluminium, a hole is bored in the middle to the reception of the copper-mono-crystals. Around the crystal as an axis, a cylindrical screen is mounted, that is connected with the circular disk firmly. This screen contains in the middle a hole through which the ions ray is arranged on the sample. The screen consists of a film stage, in which a transparent plastic film could be inserted to measure the angle distribution of sputtered atoms or a photographic film, with which an over energy, reflected Proton become (Protonogram) recorded.

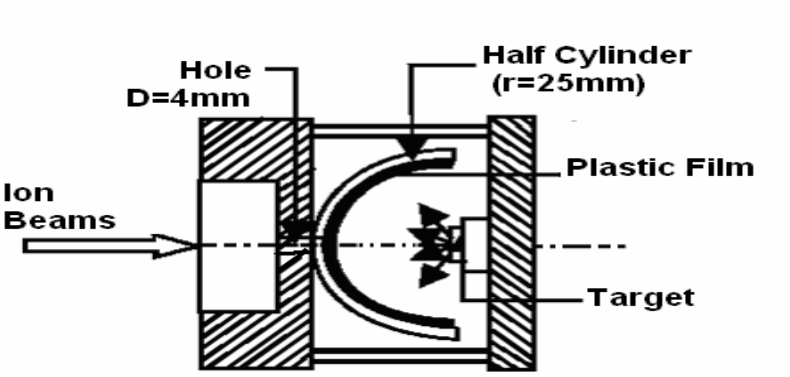

Figure 1: Schematic representation of radiation

Because in the two cases the disposal (arrangement) of the film support is the same with respect to the crystal, we can superpose the film and the transparent to observe that the correspondence of the emitted particles and the crystallographic axes of the sample.

Wehner Spots Apparition

To determine the angular distribution of the pulverised atoms, a transparent sheet is inserted in film carrier linked to the device in which is placed the sample (copper mono-crystal) with the wanted direction, the device being connected to the last electrode placed under the ions optics land of the beams emitter.

With a current of about 100μA, the sample is bombarded with Ne and Ar ions during 15-30 min., as a result we obtain the matter distribution on a plastic sheet and because it consists of a cylindrical arrangement, it is important to place the emission direction in the meridian plane of the device, in addition the crystal should be turned in parts around its axes until the geometry is optimal to measuring angle, this has been reached after 2-3 tests. With this arrangement and the desired image we undertake the copper crystal direction in the film carrier and this is done due to the angular distribution recording of the reflected protons.

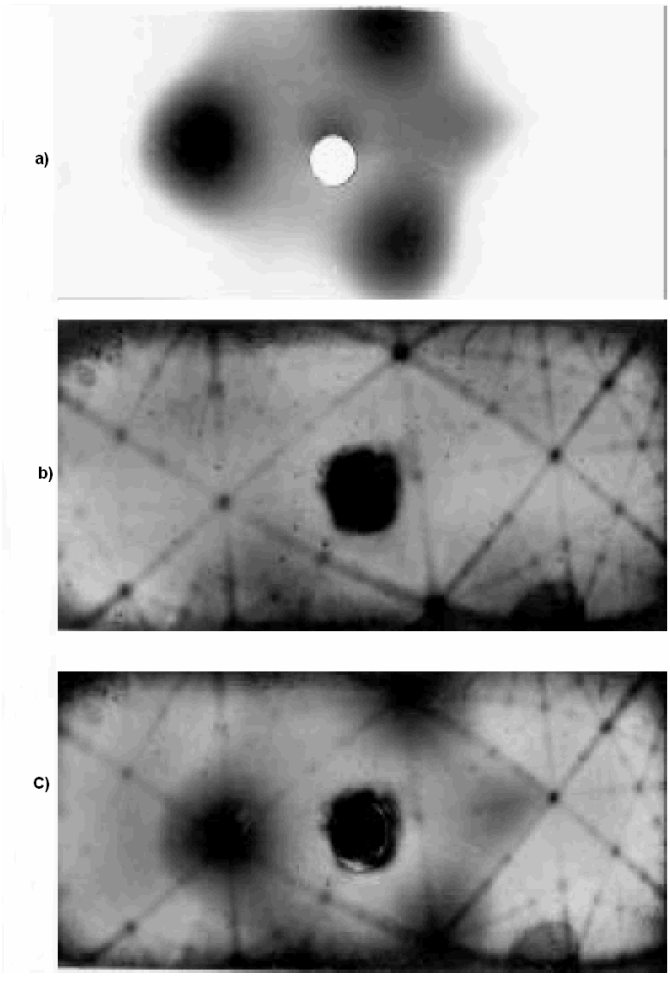

Figure 2**.** Comparative representation of the network plane structure of a mono-crystal Cu-(111) obtained by measurements of dispersion with protons (protonogram). With the arrangement of Wehner spots, during the same angle of deviation between the surface and the axis of the crystal, a)Wehner Spots by Protonogram c) Common copy of the two photography that shows clearly the Wehner spots deviation very weak compared to the desired emission direction according to the protonogram.

Determination of the Crystal Direction

We bombard the copper mono-crystal with weight and rapid particles; hence those penetrate deeply in the crystal. For protonogram photography we have taken 300kV protons with a 2μA current, an exposure time of 10s and a desensitized film, the desensitizing of the film necessitate the device installation in the dispersion room under the green light.

The protonogram is based on the reflection of the weight projectiles on the heavy atoms sample, the weight and rapid protons deeply penetrate in the mono-crystal. During a redispersion of the protons in the total angle sector around atoms network can be lighted up, a proton can be also reflected due to a collision with the atoms network in all the direction of observation, here however every atoms network is surrounded with adjacent atoms, regularly distributed and this for every adequate atom is repeated in the depth direction and the side. The protons can not be emitted by the effect protecting the adjacent atoms along their distribution direction. Even though, the protons are reflected in all the direction during the particular spreading process on the atoms network, they are however, stopped by the surrounding adjacent atoms in this direction of emission.

Because in this direction no proton is emitted, given rise on the gleam screen or on photographic film as an plane image of the network with darken films on the illuminated background plane which is produced by irregular spread protons. Because of the effect protecting adjacent atoms we call the process "Blocking Effect" or the "Shadow Effect" (Barett, 1973).

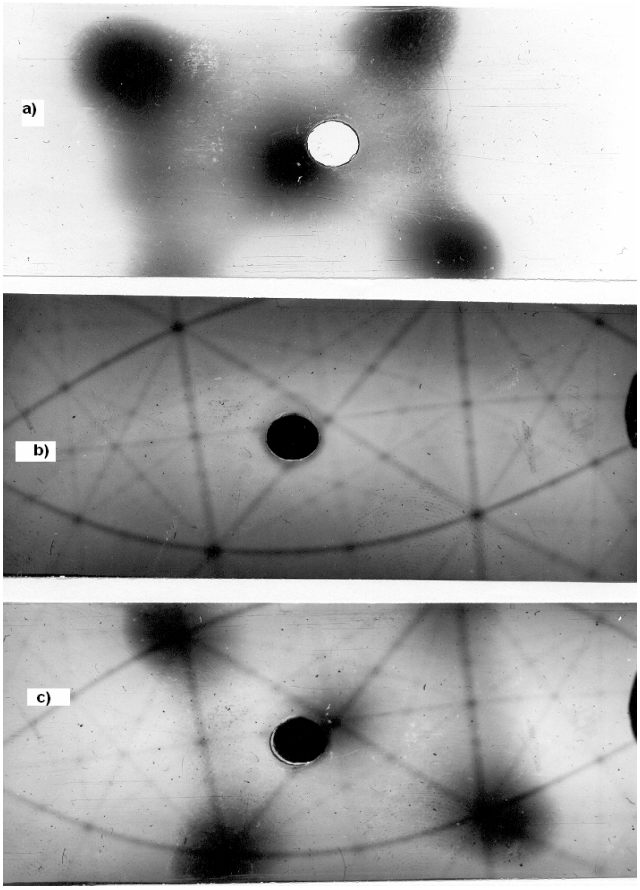

Figure 3. Comparative representation of the network plane structure of a mono crystal Cu-(001) obtained by the dispersion measurement using protons (protonogram). With the Wehner spots arrangement, during the same angle deviation between the surface and the axis of the crystal.

a) Wehner spots.

b) Protonogram .

c) Common copy of the two photographies: Wehner spots and mono-crystal principal axis directions that correspond well surface normals.

Discussion and Summary

As it is shown in the Fig. 3 that with direction crystals of surface (100), the emission direction and the crystallographic axes are well joined. On the other hand**,** for crystals (111) (Fig. 2) the directions correspondence with pulverisation images exist; while for the directions (100) a deviation is clearly observed with respect to (100) direction in the protonogram of around 2 mm with a radius of 25 mm of the film carrier of cylindrical form corresponds to a 20° of angle shifting. The emission direction of the normal is preferred. Similar observation are already done by the work (Niedrig et *al.,* 1987), if the cause should be the engagement energy of the surface, this should also affect the directions (100), because they passes also to the surface normal. For the other directions of the crystal also, we could observe the shifts. According to work (Robinson, 1981), overcoming the voltage barrier at the surface should cause angle enlargement at the output during the extraction of atoms relatively the normal, however the opposite shift is observed for centred crystals clear deviations of the position of Wehner spots is also observed. Consequently, it is evident to postulate to surface atoms relaxation,, this should be easily seen, because the atoms of the centred side position possess the shortest path of link compared to the atoms at the cubic corner points of the crystal network with centred fronts. If a crystal of this type is cut along the surface diagonals, these atoms arrive to the surface because they are under pressure due to their short link distances, they can be relaxed; this relaxation should be recovered on the first and the second atoms positions. Is it about the surfaces (100) or (110), the relaxations in the pulverisation image are not shifted, because the percussion direction coincide with the relaxation direction. If it is about however, more surface (111), the relaxation direction and the percussion direction between the atoms of the first and the second position do not correspond anymore.

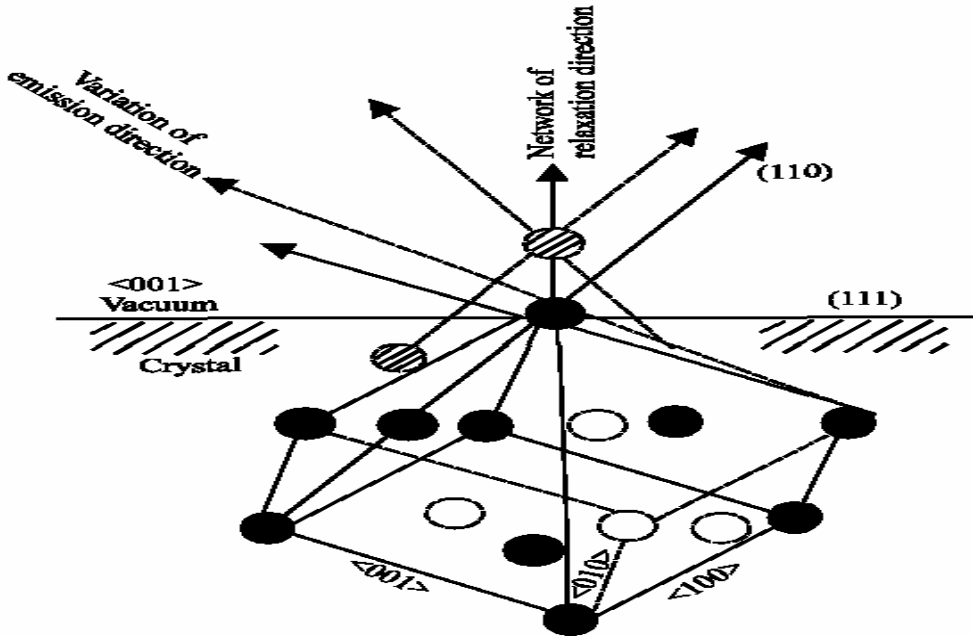

Figure 4. Schematic representation of the process. For the relaxation of atoms vertical with respect to the surface emerges a modification in the Wehner spots situation. While for the spot (100) stills not influenced by the relaxation, It is produced for the axe (001) a change in the particles emission direction.

If we evaluate quantitatively the shift on the basis of the model shown in Figure 4. A relaxation of atoms on the surface, 50% of this value is calculated by the adoption of the appearance or creation of Wehner spots comes from the percussion interaction between the adjacent atoms is always a central percussion, i.e.: There exist no preferred percussion direction of second position atoms, however the atoms possess percussion energy of second position atoms in the preferred direction, which coincide with the packed and close balls directions. Hence, the oblique percussion between adjacent atoms are also possible. In this case, the network atoms are not concerned, but the percussion radius which is crucial and the ratio between the distance and the percussion radius of atoms which decide on the percussion oblique if it increases or decreases. With percussion radii which are small with respect to network gap, the oblique deviation increases concerning the central percussion, because the transferred energy of the

surface atoms during the pulverisation increase in a multiple of links energy, the percussion radius can be ten times less than network distances, hence the network relaxation values are reduced from 50 to 5%. Similar values have been found (Davies et al., 1975; Saris, 1982) with the measurement of Surface-Blocking-Effect, h s method is relatively expensive and necessitate very high vacuum conditions, the arrangement of the Wehner spots relaxation process is in the other hand simpler and possible under the high vacuum conditions, if we increase also the sensitivity of the measurement method with the use of a particle test, it can be possible not only to determine the metals structure, but also the arrangement arbitrary matters atoms on the surface, if it is sufficiently regular. Consequently, it appears very important also to examine very far the mono-crystals surface particles emission question and other matters, because new structural analysis methods of solid bodies' surfaces can emerge.

Acknowledgement

This research was supported in part by the Department of physics, Humboldt University Berlin.

Correspondence to:
Dr. Djamel Boubetra
Centre Universitaire de Bordj Bou Arreridj
El Anasser 34265 Algeria
E-Mail : boubetra@gmail.com

References

1. Barett, C.S., 1973. In: Scattering (Blocking) Patterns Applied to Crystallography, (Eh.) Morgan, D.V. and Wiley and Son, London, N.Y., Sydney, Toronto.
2. Niedrig, H., I. Linders, M. Steinberg and M. Edermann, 1987. In: Detection of Angular Atomic Emission Distribution from Sputtered Single Crystals, Scanning Microscopy Supplement, 1: 23.
3. Robinson, M.T., 1981. In: Sputtering by Particle Bombardment I, (Ed.) R. Behrisch Topics in Applied Physics, Springer, Berlin, 47: 73.
4. Davies, J. A., D.P. Jackson, J.B. Mitchell, P.R. Northon and R.L. Tapping, 1975 Phys. Letters 54A, 239.
5. Saris F. W., 1982, Nucl. Instr. And Meth. 194, pp 625-632

8/30/2008

Chlorophyll *a* dynamics and environmental factors in a tropical estuarine lagoon

*Onyema, I.C. and Nwankwo, D.I.

Department of Marine Sciences, University of Lagos, Akoka.
*e-mail: iconyema@gmail.com

Abstract: The chlorophyll *a* dynamics and environmental factors of the Iyagbe lagoon, Lagos was investigated for 2 years (Oct., 2004 - Sept., 2006). The environmental indices reflected seasonal changes related to rainfall distributive pattern and tidal seawater incursion. Air temperature (26 - 34°C), surface water temperature (26 - 33°C), total dissolved solids (90 - 25,000mgl^{-1}), transparency (22 - 231cm), sulphate (20.8 - 1140mgl^{-1}), silica (0.9 - 6.0mgl^{-1}), dissolved oxygen (4 - 5.6mgl^{-1}), conductivity (110 - 40850 S/cm), salinity (0.06 - 35.1%), chloride (20.5 - 15,015mgl^{-1}), pH (6.7 - 8.42), acidity (3.8 - 44mgl^{-1}), alkalinity (15.3 - 30mgl^{-1}), total hardness (18 - 6875mgl^{-1}), calcium (10 - 720.1mgl^{-1}) and magnesium (1.4 - 900mgl^{-1}) recorded increased values in the dry than wet season. On the other hand chemical oxygen demand, biological oxygen demand, total suspended solids(18 - 2310mgl^{-1}), nitrate (3.3 - 59.8mgl^{-1}), phosphate (0.01 - 1.68mg), copper (0.001 - 0.079mgl^{-1}), zinc (0.001 - 0.015mgl^{-1}) and iron (0.06 - 1.08mgl^{-1}) recorded higher values in the wet season. Values for chlorophyll *a* were higher in the dry than wet season for the lagoon. Positive correlation coefficient was recorded between chlorophyll *a* and salinity, total dissolved solids, alkalinity, pH, conductivity total hardness, chloride, transparency, acidity, nitrate, sulphate, calcium and magnesium levels. Recorded chlorophyll *a* values places the Iyagbe lagoon between the mesotrophic and eutrophic status. It is suggested that increasing tidal influence associated with reduced rain events may have encouraged elevated salinities and created conditions for the development of more algal cells, hence higher chlorophyll *a* records. [Academia Arena, 2009;1(1):18-31]. ISSN 1553-992X.

Keywords: Physico-chemical factors, brackish, microalgae, hydroclimatic factors, Nigeria.

Introduction

Lagoons are ecologically and economically important aquatic ecosystems in South-western Nigeria. They provide natural food resources rich in protein which includes an array of fish and fisheries. They are also important in water transportation, energy generation, exploitation and exploration of some mineral resources including sand (FAO, 1969; Kirk and Lauder, 2000; Onyema *et al*., 2003, 2007; Chukwu and Nwankwo, 2004; Onyema, 2008a). Lagoons also inadvertently serve as sinks for the disposal of both domestic, municipal and industrial wastes in the region. There are nine lagoons in South-western Nigeria namely: Yewa, Ologe, Badagry, Iyagbe, Lagos, Kuramo, Epe, Lekki and Mahin lagoons from the west to the east (FAO, 1969, Webb, 1958a; Nwankwo, 2004b; Onyema, 2008).

Furthermore, chlorophyll *a* is an essential plant pigment and concentrations of it could be used to reflect algal biomass and hence, level of primary production. Chlorophyll *a* can be an effective measure of trophic status (Lee, 1999). However, elevated chlorophyll *a* concentrations often indicate poor water quality and low levels often suggest good conditions (Ogamba, *et. al*., 2004). According to Lee (1999), higher Phytoplankton biomass would directly reflect in a higher level of chlorophyll *a* in such regions. One method to determine the amount of plant materials present in a water sample is to filter out the phytoplankton, count the cells and multiply the number counted by the average mass per individual cell (Sverdrup *et al*., 2006). A less tedious method is to extract the chlorophyll from a sample of phytoplankton and determine the concentration of pigment present. Hence chlorophyll concentration can be used to estimate the total quantity of plant material or biomass (Sverdrup *et al*., 2006).

The immense ecological significance of phytoplankton diversity studies especially in relation to aquatic trophic relationships cannot be understated (Smith, 1950; Lee, 1999; Nwankwo, 1984, 2004a). Coastal areas are generally more productive than the open oceans because rivers and land run-offs supply nutrients along coasts and adjoining estuarine systems. With regard to the annual rates of global primary production and productivity, Lagos offshore falls under the high productivity category (= 300gC/m^2/yr) (Sverdrup *et al*., 2006).

Determination of primary production in the Lagos lagoon has primarily been by biomass estimation using cells number of phytoplankton (Nwankwo, 2004). With regard to chlorophyll *a* in Nigeria, there exist a report by Kadiri (1993) on the Ipkoba reservoir in Benin and another by Ogamba *et al*., (2004) on chlorophyll *a* levels and variations in the Niger Delta region. Hence studies in Nigeria using chlorophyll *a* method are limited.

At present, there is no report on any of the nine lagoons of South-western Nigeria with regard to the chlorophyll *a* method of estimation. The aim of this study was to investigate the seasonality in chlorophyll *a* concentration and relate findings to environmental factors in the Iyagbe lagoon.

Materials and Methods

Description of Study Site

The Iyagbe lagoon (Fig 1) is located in Lagos state, Nigeria and is one of the nine lagoons in South-western Nigeria (Webb, 1958a; Nwankwo, 2004b; Onyema, 2008a). It is located between Latitude 6^0 26'N Longitude 3^0 19' E and Latitude 6^0 23'N Longitude 3^0 06' E (Webb, 1958a; Onyema, 2008a,b). It is majorly made up of the Porto-Novo and Badagry creeks. The Iyagbe lagoon is centered about the town of Iyagbe (Webb, 1958a). The lagoon is shallow at some point especially in the Badagry creek arm and is open all year round via the Lagos harbour to the sea (Webb, 1958b; Webb and Hill, 1958; Sandison, 1966; Sandison and Hill, 1966). Like all parts of South-western Nigeria, the Iyagbe lagoon is exposed to two distinct seasons namely the wet (May – October) and the dry season (November – April) (Nwankwo, 2004b; Sandison and Hill, 1966). The harmmattan, a short season of dry, dusty North-East Trade winds are experienced sometimes between November and January in the region reducing visibility and lowering temperatures (Onyema *et al.*, 2003). Dense rain forest zone vegetation preceded by littoral mangrove assemblages is the common macrofloral assemblages especially in areas with reduced anthropogenic influence. The lagoon deposits are varied, and are reflected in the pattern and type of vegetation in the region. Most of the Iyagbe lagoon area away from the Tin can Island and Apapa Ports are colonized by a recognizable riparian mangrove swamp community especially where man made structure are absent. These mangrove environments are inhabited by amphipods, polychaetes, isopods, barnacles, oysters, periwinkles, nematodes, fiddler crabs, sea cucumbers, mangrove crabs, mudskippers and shrimps among others (Sandison and Hill, 1966; Onyema, 2008b). The notable macro-floral species in the area include *Rhizophora racemosa, R. harrisoni, Avicennia germinans, Phoenix reclinata, Raphia hookeri, Elaeis guineensis, Acrotiscum aureum* and *Cocos nucifera* (Akinsoji *et al*., 2002).

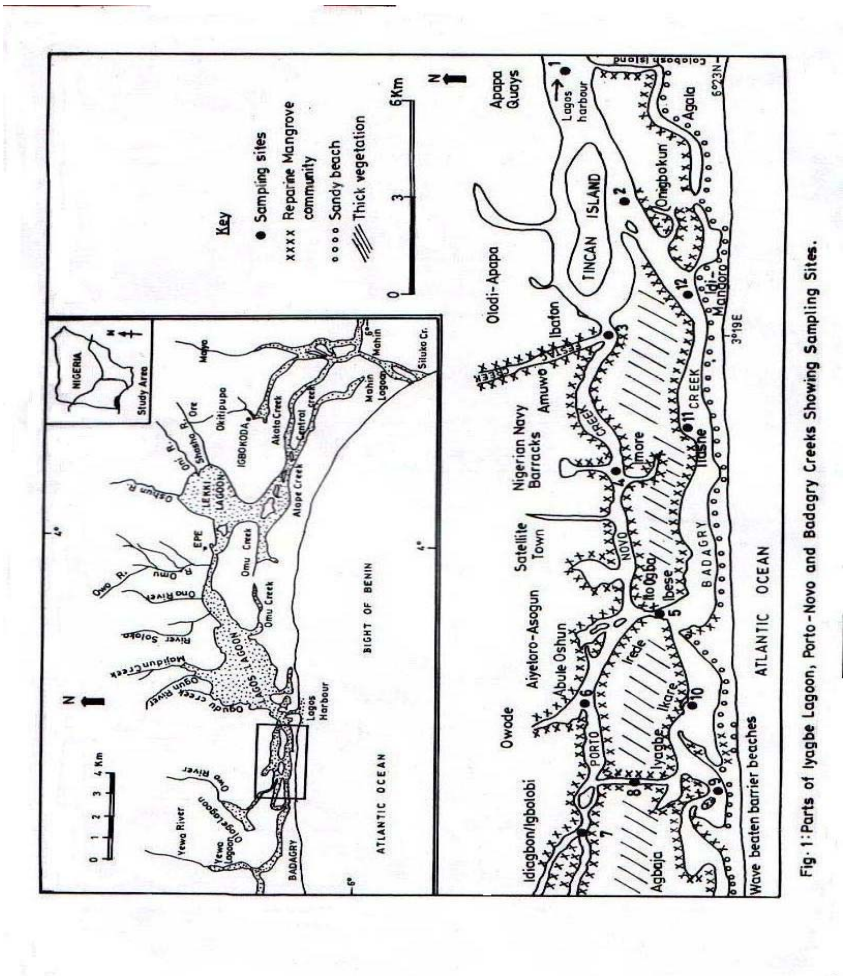

Fig. 1: Parts of Iyagbe Lagoon, Porto-Novo and Badagry Creeks Showing Sampling Sites.

Collection of samples.

Collection of water samples

Twelve sampling stations were selected to cover the lagoon area and for the collection of samples. Table 1 shows the G.P.S. location, names and number of sampling stations. Monthly surface water samples was collected for twenty-four consecutive months (October, 2004 – September, 2006) for physico-chemical characteristics analysis using 500ml plastic containers with screw caps. Collection of samples from the stations was always between 10 and 15hr each time. Water samples were collected just a few centimeters below the water surface at each of the twelve stations. The plastic containers was then labeled appropriately and transported to the laboratory immediately after collection for to further analysis. Water samples for Dissolved Oxygen was collected also in 50cl bottles and fixed on site with white and black ampoules.

Table 1: G.P.S. location and station name of sampled areas in the Iyagbe lagoon.

Table 2 below presents the methods / device used in estimating the various environmental factors for this study with corresponding references.

Station No.	Station name	G.P.S. locations
Station 1	Calabash Island	Latitude 6^{o} 25^{1}.987 N, Longitude 3^{o} 23^{1}.400 E
Station 2	Tin-can Island	Latitude 6^{o} 25^{1} .833 N, Longitude 3^{o} 21^{1} .532 E
Station 3	Ibafon	Latitude 6^{o} 25^{1} .964 N, Longitude 3^{o} 19^{1} .244 E
Station 4	Imore	Latitude 6^{o} 25^{1} .755 N, Longitude 3^{o} 19^{1} .915 E
Station 5	Ito-ogba	Latitude 6^{o} 25^{1} .409 N, Longitude 3^{o} 14^{1} .624 E
Station 6	Abule-oshun	Latitude 6^{o} 26^{1} .134 N, Longitude 3^{o} 13^{1} .224 E
Station 7	Idiagbon / Igbolobi	Latitude 6^{o} 26^{1}.214 N, Longitude 3^{o} 11^{1} .826 E
Station 8	Iyagbe	Latitude 6^{o} 25^{1} .603 N, Longitude 3^{o} 11^{1} .990 E
Station 9	Agbaja	Latitude 6^{o} 24^{1} .473 N, Longitude 3^{o} 12^{1} .744 E
Station 10	Ikare	Latitude 6^{o} 24^{1} .632 N, Longitude 3^{o} 13^{1} .705 E
Station 11	Ilashe	Latitude 6^{o} 24^{1} .676 N, Longitude 3^{o} 16^{1} .938 E
Station 12	Idimangoro	Latitude 6^{o} 24^{1} .717 N, Longitude 3^{o} 19^{1} .307 E

Table 2: Summary of environmental factors and method/device used for their estimation

	Parameter/ Unit	Method / Device	Reference(s)
1	**Air temperature (^oC)**	Mercury – in – glass thermometer	Nwankwo (1984)
2	**Water temperature (^oC)**	Mercury – in – glass thermometer	Onyema (2008)
3	**Transparency (cm)**	Secchi disc method	Onyema (2008)
4	**Depth (cm)**	Graduated pole	Brown (1998)
5	**Rainfall (mm)**	Acquired from NIMET, Oshodi, Lagos	
6	**Total Dissolved Solids (mgL^{-1})**	Cole Palmer TDS meter	
7	**Total Suspended Solids (mgL^{-1})**	Gravimetric method	APHA (1998)
8	**Chloride (mgL^{-1})**	Argentometric method	APHA (1998)
9	**Total hardness (mgL^{-1})**	Titrimetric method	APHA (1998)
10	**pH**	Electrometric / Cole Parmer Testr3	
11	**Conductivity (µS/cm)**	Philip PW9505 Conductivity meter	
12	**Salinity (‰)**	HANNA Instrument	APHA (1998)
13	**Alkalinity (mgL^{-1})**	Titration method	APHA (1998)
14	**Acidity (mgL^{-1})**	Titration method	APHA (1998)
15	**Dissolved oxygen (mgL^{-1})**	Titration method	APHA (1998)
16	**Biological oxygen demand (mgL^{-1})**	Incubation and Titration	APHA (1998)
17	**Chemical oxygen demand (mgL^{-1})**	Titration method	APHA (1998)
18	**Nitrate – nitrogen (mgL^{-1})**	Colorimetric method	APHA (1998)
19	**Phosphate – phosphorus (mgL^{-1})**	Colorimetric method	APHA (1998)
20	**Sulphate (mgL^{-1})**	Turbidimetric method	APHA (1998)
21	**Silica (mgL^{-1})**	Colorimeter (DR2010)	APHA (1998)
22	**Calcium (mgL^{-1})**	Titrimetric method	APHA (1998)
23	**Magnesium (mgL^{-1})**	Titrimetric method	APHA (1998)
24	**Copper (mgL^{-1})**	Atomic Absorption Spectrophotometer Perkin Elmer 5000 AAS	Perkin Elmer Application methods (2002)
25	**Iron (mgL^{-1})**	Atomic Absorption Spectrophotometer Perkin Elmer 5000 AAS	Perkin Elmer Application methods (2002)
26	**Zinc (mgL^{-1})**	Atomic Absorption Spectrophotometer Perkin Elmer 5000 AAS	Perkin Elmer Application methods (2002)
27	**Chlorophyll *a* (µg/L)**	Florometric method	APHA (1998)

Correlation Coefficient Values (r)

The Pearson correlation coefficient (r) (Ogeibu, 2005) for the relationship between the different environmental parameters and chlorophyll *a* were obtained using the formula:

$$r = \frac{n(\sum XY) - (\sum X)(\sum Y)}{\sqrt{(n(\sum X^2 - (\sum X)^2]\,[n\sum Y^2 - (\sum Y)^2}}$$

Where
r = Coefficient of correlation
X and Y = Variables under consideration

Results

The minimum and maximum values obtained for the estimates of environmental factors, their means and standard deviation are presents in Table 3. Also in Table 3 is whether each parameter recorded higher values in the wet or dry season for the two (2) years of study.

Air temperature values ranged between 26 and 34^{0}C throughout the sampling period. Whereas the lowest value estimated was 26^{0}C (September, 2006), the highest value obtained was 34^{0}C recorded in March of the same year. The lowest surface water temperature estimated was 25^{0}C (September, 2005) and the highest value obtained was 33^{0}C (May, 2005). Transparency was between 11 (March, 2006) and 280 cm (December, 2004). Total dissolved solids ranged between 90 and 25000 mg/L with the lowest value recorded in September, 2005 and the highest value in April, 2006. Total suspended solids values ranged between 18 (February, 2005) and 2310 mg/ L (August, 2005). Rainfall volumes showed both monthly changes and varied from one year to the next. In the first year the highest rainfall volume was recorded in June 2005 (330 mm) and the least was in February 2005 (8.9 mm). In the second year the highest rainfall was in June 2006 (315.7 mm) and the least in January 2006 (6.0 mm). Recorded chloride values were between 20.5 (October, 2005) and 17710mg/L (April, 2006). Whereas the lowest value estimated for total hardness was 18 mg/L (July, 2006) whereas the highest value obtained was 6875 mg/L (December, 2005). Hydrogen ion concentration (pH) values ranged between 6.7 (June, 2006) and 8.42 (February, 2006) throughout the sampling period. Whereas the lowest conductivity estimated was 110µS/cm and recorded in October, 2004, the highest value obtained was 33092 µS/cm recorded in April, 2006.

Salinity value ranged between 0.06 (October, 2004), and 35.1$^o/_{oo}$ (April, 2006). Alkalinity values were between 18 (August, 2006) and 311.2 mg/L (February, 2005). Acidity estimates ranged between 3.8 and 60 mg/L (November, 2005 and January, 2006) respectively.

Dissolved Oxygen values ranged between 4 (September, 2005) and 5.6 mg/L (January, 2006) throughout the sampling period. Biological Oxygen Demand values ranged between 2 (March, 2005) and 22mg/L (September, 2006) throughout the sampling period. Chemical oxygen demand ranged between 8 (March, 2005) and 211mg/l (Feburary, 2006). Nitrate-nitrogen values werebetween 3.3 (November, 2005) and 59.8 mg/L (June, 2006) whereas Phosphate-phosphorus recorded between 0.01 mg/L (January, 2006) and 1.68 mg/L (August, 2005). Sulphate values ranged between 20.8 (October, 2005) and 1160 mg/L (January, 2006) throughout the sampling period. Silica values fell between 0.9 (August, 2005) and 6.0mg/L (September, 2006). Calcium levels were between 10mg/L in October, 2005 and 720.1 mg/L in November, 2004. Magnesium estimates were between 1.4 mg/L in July, 2006 and 981.1 mg/L in January, 2005 and Copper values was between 0.001 (May through July 2005) and 0.09 mg/L (August, 2005). Iron levels ranged between 0.06 and 1.08 mg/L (October 2004). Zinc values ranged between 0.001 and 0.015 mg/L (August, 2005).

Chlorophyll *a* values were between 4.2 and 55 µg/L. whereas the lowest value estimated was in June, 2005, the highest value obtained was recorded in November 2005. Chlorophyll *a* values showed a positive relationship with salinity (r = 0.21), transparency (r = 0.24), chloride (r = 0.21), total dissolved solids (r = 0.22), water temperature (r = 0.18), air temperature (r = 0.09), pH (r = 0.23), conductivity (r = 0.23), acidity (r = 0.10), alkalinity (r = 0.27), calcium (r = 0.17), magnesium (r = 0.27), nitrate (r = 0.11), chemical oxygen demand (r = 0.03), iron (r = 0.05) and sulphate (r = 0.20). A negative relationship existed between chlorophyll *a* and biological oxygen demand (r = -0.16), zinc (r = -0.02), copper (r = -0.04), total suspended solids (r = -0.07) and phosphates (r = -0.13) estimates. Table 4 shows the Seasonal variation in Chlorophyll *a* values at the different stations in the Iyagbe lagoon from Dec., 2004 to Nov., 2006, Table 5 tabulates the Pearson correlation co-efficient matrix of environmental characteristics. Fig. 2: Seasonal variation in some environmental factors at four selected station each and chlorophyll *a* at the Iyagbe lagoon from Dec., 2004 to Nov., 2006. Stations represented were selected based on

their importance as confluence points and areas exposed to possible anthropogenic stresses or not. Furthermore, Fig. 3 shows the Pearson correlation coefficient between chlorophyll *a* and environmental factors.

Table 3: A summary of the minimum, maximum and mean / standard deviation estimate values for environmental factors from the Iyagbe lagoon (December, 2004 – November, 2006).

	Parameter/ Unit	Minimum value	Maximum value	Mean value ± S.D.	Higher values reported in the ….
1	Air temperature (^oC)	26	34	30.07 ± 1.98	Dry season
2	Water temperature (^oC)	26	33	29.42 ± 1.81	Dry season
3	Transparency (cm)	22	231	102.42 ± 51.47	Dry season
4	Total Dissolved Solids (mgL^{-1})	90	25000	8467.65 ± 6641.66	Dry season
5	Total Suspended Solids (mgL^{-1})	18	2310	172.48 ± 259.01	Wet season
6	Rainfall (mm)	6	315.7	141.83 ± 116.87	Wet season
7	Chloride (mgL^{-1})	20.5	15015	6316.55 ± 24167.13	Dry season
8	Total hardness (mgL^{-1})	18	6875	2035.82 ± 1485.42	Dry season
9	pH	6.7	8.42	7.40 ± 0.28	Dry season
10	Conductivity (µS/cm)	110	40850	13208.59 ± 10418.71	Dry season
11	Salinity (‰)	0.06	35.1	14.43 ± 18.10	Dry season
12	Alkalinity (mgL^{-1})	15.3	330	74.32 ± 74.25	Dry season
13	Acidity (mgL^{-1})	3.8	44	11.80 ± 7.48	Dry season
14	Dissolved oxygen (mgL^{-1})	4	5.6	4.67 ± 0.23	Dry season
15	Biological oxygen demand (mgL^{-1})	2	22	7.15 ± 3.52	Wet season
16	Chemical oxygen demand (mgL^{-1})	8	89	30.21 ± 21.08	Wet season
17	Nitrate – nitrogen (mgL^{-1})	3.3	59.8	10.54 ± 8.37	Wet season
18	Phosphate – phosphorus (mgL^{-1})	0.01	1.68	0.26 ± 0.29	Wet season
19	Sulphate (mgL^{-1})	20.8	1140	279.71 ± 232.16	Wet season
20	Silica (mgL^{-1})	0.9	6.0	2.63 ± 0.91	Dry season
21	Calcium (mgL^{-1})	10	720.1	188.49 ± 130.05	Dry season
22	Magnesium (mgL^{-1})	1.4	900	333.36 ± 264.92	Dry season
23	Copper (mgL^{-1})	0.001	0.079	0.003 ± 0.001	Wet season
24	Iron (mgL^{-1})	0.06	1.08	0.29 ± 0.25	Wet season
25	Zinc (mgL^{-1})	0.001	0.015	0.002 ± 0.002	Wet season
26	Chlorophyll *a* (µg/L)	4.2	55	19.63 ± 7.90	Dry season

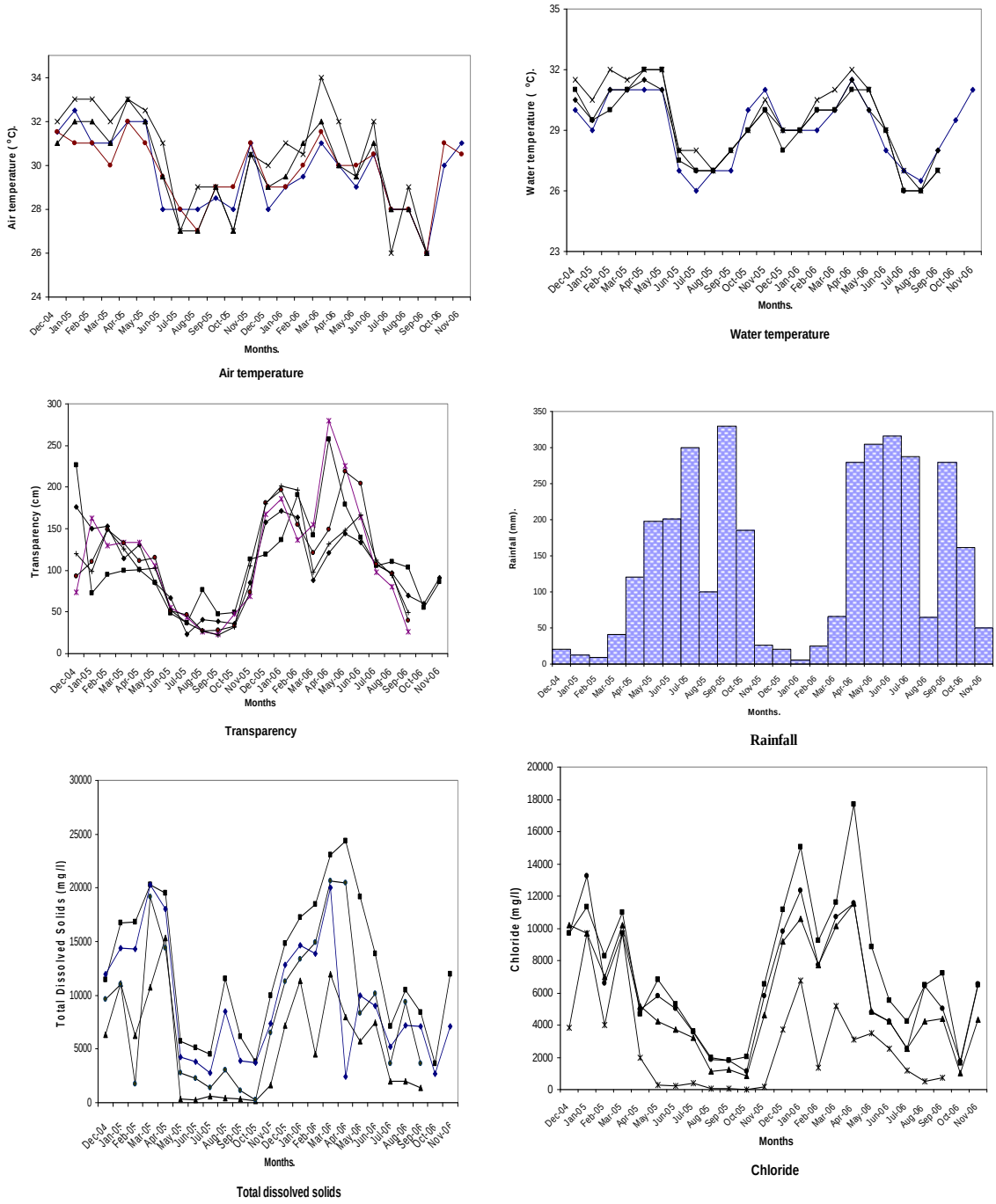

Fig. 2: Seasonal variation in some environmental factors and chlorophyll *a* at the Iyagbe lagoon from Oct., 2004 to Sept., 2006.

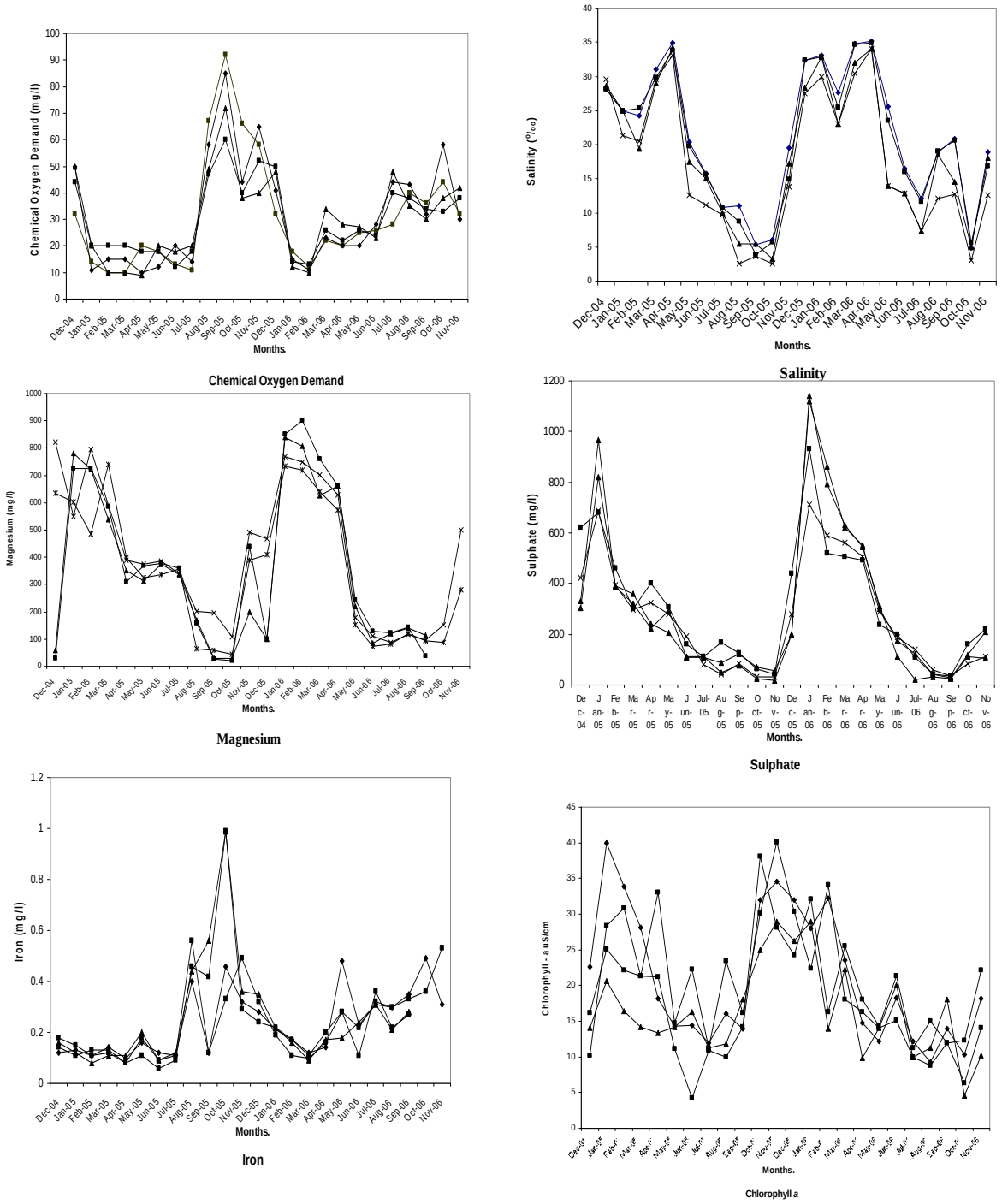

Fig. 2: Seasonal variation in some environmental factors and chlorophyll *a* at the Iyagbe lagoon from Oct., 2004 to Sept., 2006.

Fig 3: Pearson correlation coefficient between chlorophyll *a* and environmental factors.

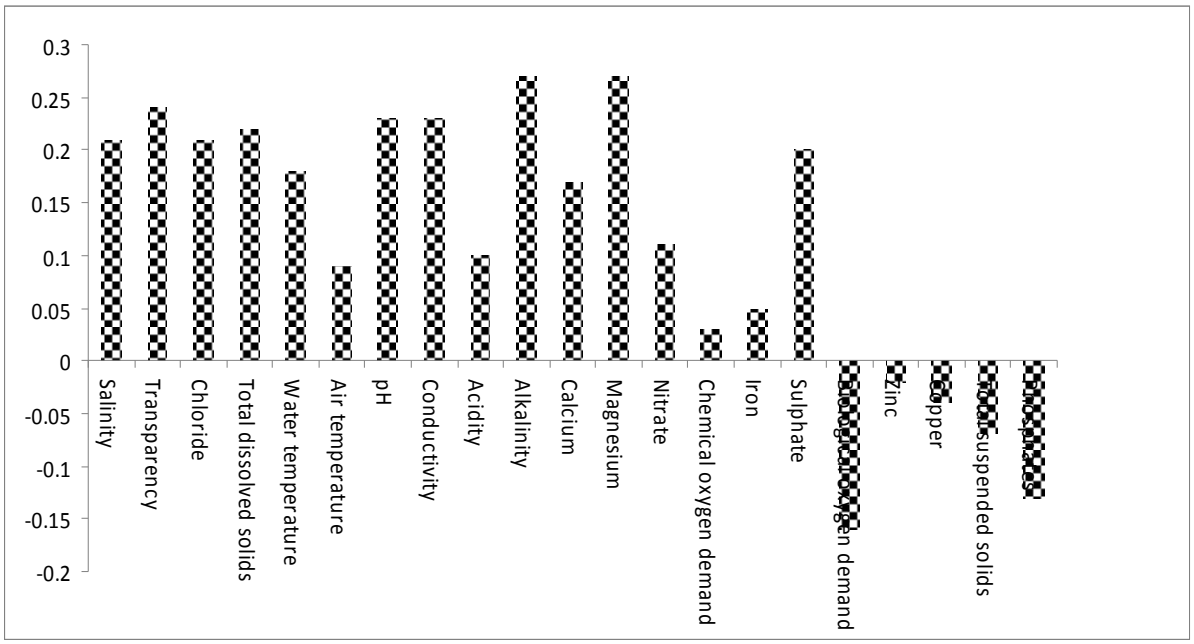

Table 4: Seasonal variation in Chlorophyll *a* values at the different stations in the Iyagbe lagoon, (Dec., 2004 – Nov., 2006).

	2004	2005														2006								
	Dec.	Jan.	Feb.	Mar.	Apr.	May.	Jun.	Jul.	Aug.	Sept.	Oct.	Nov.	Dec.	Jan.	Feb.	Mar.	Apr.	May.	Jun.	Jul.	Aug.	Sept.	Oct.	Nov.
Calabash Island	22.6	40	33.9	28.1	18.2	14.3	14.4	12	16	14	32	34.6	32	28	32.2	23.6	14.8	12.2	18.3	12.2	9.3	14	10.3	18.2
Tincan Island	10.2	28.4	30.8	21.3	33.1	14.8	22.3	11.3	23.4	16.2	30.1	40.1	30.3	22.4	34.1	18	16.3	14.1	15.1	10	8.8	12	12.3	22.1
Ibafon	14.1	22.3	33.4	20.8	30	20.1	18.3	14.9	20.1	14.3	32.1	33.2	26	15.2	30.8	20.1	20.2	18.8	15.3	10.8	12.1	18	14.2	11
Imore	11.3	30.1	33.1	16.9	28.1	16.3	11.4	12.2	18.2	18.1	24	36	20.1	22	16	14.2	21.6	16.2	20	25	16.3	20	16.8	8.6
Ito-Ogba	19.2	22.4	28.6	14.8	20.1	14.1	16.3	16.4	12.6	11.3	33.2	30.8	22	18.9	14.2	22.3	25	20.1	32.3	22.6	28.1	13	14.2	11.3
Abule Oshun	18	21.3	15.1	18.3	20.6	15.2	19.2	14.4	10.7	18.3	34.1	26.1	20.3	30.2	21.3	26.1	28.1	21.6	30.6	18.4	15.2	16	11.1	10.3
Idiagbon	11.3	20.8	15.9	21.2	14.4	14.8	18.3	12.3	12.3	21.3	30.2	24.2	24.6	26.3	20.6	23.2	22.3	24.1	22.8	19.3	14.3	21	6.6	9.6
Iyagbe	12.1	21.2	20.3	15	21.3	16.3	16.2	14.2	14.1	10.2	39	50.1	22.9	24	13	28.4	33.2	23.8	22.4	10.2	12.1	16	4.9	8.3
Agbaja	14.8	22.3	16.2	18.1	16.8	14.1	14.8	18.6	10	16.3	33.3	22.6	33.6	33.4	14.2	20.1	29.3	20.6	28	16.8	16.3	11	18.2	9.4
Ikare	10.3	24.4	18.1	16.3	17.1	21.2	11.3	10.1	16	12.1	34	55	38.1	26	23	29.2	25.3	26.5	24.3	14.1	18.8	20	10	8.6
Ilashe	16.2	25.1	22.1	21.3	21.2	11.1	4.2	10.9	10	14.2	38.1	28.1	24.2	32.1	16.3	25.6	18.1	14.3	21.3	11.2	15	12	6.3	14.1
Idi-Mangoro	14.1	20.6	16.4	14.2	13.4	14.2	16.3	11.3	11.8	18.1	25	29	26.3	29	14	22.3	9.8	14.1	20	10	11.3	18	4.6	10.2

Table 5: Pearson correlation co-efficient matrix of environmental characteristics at the Iyagbe lagoon, Lagos (December, 2004 – November, 2006)

	Air temperature	Water temperature	Transparency	T.D.S.	T.S.S.	Chloride	Total hardness	pH	Conductivity	Salinity	Alkalinity	Acidity	D.O.	B.O.D.	C.O.D.	Nitrate	Phosphate	Sulphate	Silica	Calcium	Magnesium	Copper	Iron	Zinc	Chlorophyll *a*
Air temperature	1																								
Water temperature	0.77	1																							
Transparency	0.34	0.40	1																						
T.D.S.	0.35	0.39	0.54	1																					
T.S.S.	-0.18	-0.22	0.38	0.22	1																				
Chloride	0.06	0.10	0.20	0.17	-0.08	1																			
Total hardness	0.39	0.41	0.55	0.62	-0.19	0.20	1																		
pH	0.27	0.32	0.43	0.46	-0.19	0.16	0.60	1																	
Conductivity	0.40	0.44	0.57	0.96	-0.25	0.17	0.64	0.49	1																
Salinity	0.38	0.45	0.57	0.88	-0.29	0.17	0.73	0.48	0.89	1															
Alkalinity	0.34	0.26	0.41	0.28	-0.16	0.14	0.54	0.71	0.33	0.28	1														
Acidity	0.13	0.10	0.42	0.33	-0.24	0.13	0.38	0.48	0.33	0.32	0.64	1													
D. O.	-0.13	-0.07	0.19	0.18	-0.26	0.22	0.08	0.10	0.17	0.20	0.06	0.18	1												
B.O.D.	-0.39	-0.45	-0.38	-0.36	0.37	-0.14	-0.46	-0.25	-0.40	-0.45	-0.31	-0.36	-0.05	1											
C.O.D.	-0.25	-0.26	-0.18	-0.26	0.45	-0.07	-0.15	-0.09	-0.29	-0.27	-0.16	-0.26	-0.20	0.57	1										
Nitrate	-0.01	-0.04	0.25	0.18	0.20	0.22	0.27	0.33	0.15	0.18	0.34	0.45	0.14	-0.07	0.11	1									
Phosphate	-0.25	-0.24	-0.32	-0.28	0.50	-0.08	-0.31	-0.13	-0.32	-0.37	-0.26	-0.29	-0.07	0.54	0.36	0.00	1								
Sulphate	0.46	0.37	0.50	0.53	-0.18	0.15	0.60	0.56	0.55	0.57	0.67	0.58	0.16	-0.40	-0.23	0.49	-0.30	1							
Silica	-0.18	-0.14	0.12	-0.01	-0.36	-0.04	-0.19	-0.16	0.02	0.04	-0.17	0.03	0.12	0.02	-0.08	-0.24	-0.16	-0.17	1						
Calcium	0.41	0.43	0.33	0.49	-0.15	0.11	0.64	0.38	0.52	0.56	0.27	0.14	0.18	-0.35	-0.16	0.07	-0.24	0.35	-0.09	1					
Magnesium	0.45	0.43	0.46	0.64	-0.18	0.21	0.77	0.60	0.67	0.66	0.60	0.52	0.14	-0.51	-0.30	0.32	-0.34	0.70	-0.16	0.52	1				
Copper	-0.23	-0.29	-0.20	0.08	0.59	-0.04	-0.10	0.01	-0.11	-0.17	-0.04	-0.12	-0.04	0.38	0.34	0.20	0.53	-0.08	-0.31	-0.10	-0.12	1			
Iron	-0.21	-0.16	-0.35	0.44	0.11	-0.10	-0.38	-0.21	-0.47	-0.48	-0.28	-0.31	-0.08	0.43	0.22	-0.12	0.37	-0.44	-0.26	-0.33	-0.44	0.21	1		
Zinc	-0.11	-0.19	-0.27	-0.11	0.16	-0.07	-0.13	0.01	-0.14	-0.15	-0.03	-0.16	-0.02	0.46	0.24	-0.03	0.37	-0.06	-0.25	-0.09	-0.14	0.43	0.27	1	
Chlorophyll *a*	0.09	0.18	0.24	0.22	-0.07	0.12	0.33	0.23	0.23	0.21	0.27	0.10	0.09	-0.16	0.03	0.11	-0.13	0.20	-0.18	0.17	0.27	-0.04	0.05	-0.02	1

Discussion

The characteristics of environmental factors from this study shows clearly that the Iyagbe lagoon experiences environmental gradients likened to a tropical estuarine aquatic environments from year to year (Hill and Webb, 1958; Webb, 1960; Sandison and Hill, 1966; Kjerfve, 1994; Kirk and Lauder, 2000). Furthermore environmental factors of the lagoon exhibited seasonal changes that were closely related to the distributive pattern of rainfall of the region. For instance during the wet season, reduced levels for air and water temperatures, transparency, salinity, pH, total dissolved solids, conductivity, chloride, total hardness, sulphate, calcium, magnesium, acidity, total dissolved solids and alkalinity were recorded. Conversely, in the dry season the values for these parameters increased. Reduced rain events and its associated input of floodwaters from rivers, creeks, adjoining wetlands and the effect of tidal seawater incursion probably lead to this trend of environmental gradients. Reduced phytoplankton densities as reflected in chlorophyll *a* values in the wet season may be linked to the low water clarity which reduces the amount of light getting to planktonic algal component for photosynthesis. Higher chlorophyll *a* values recorded in the dry season is a pointer to improved water clarity at this time which probably allowed greater light penetration. According to Suzuki *et al*. (2002), low chlorophyll *a* values reflecting limited phytoplankton growth in an investigation of a Mexican lagoon were associated to dark water which reduced light penetration into the lagoon considerably.

Pearson correlation co-efficient showed positive correlation between chlorophyll *a* values, salinity, total dissolved solids, alkalinity, pH, conductivity, total hardness and chloride values among others. The flushing of planktonic algal forms towards the sea during the rains by flood waters and hence dilution, could also account for the low chlorophyll *a* values (phytoplankton densities) recorded at such times. The range of chlorophyll *a* values for the Iyagbe lagoon was between 12 and 55µg/l i.e between the mesotrophic and eutrophic productivity status (Suzuki *et al*., 2002, APHA, 1998). Furthermore, Ogamba *et al*., (2004) reported a chlorophyll *a* range of 0.15 – 37.4µg/l for the wet season and 0.10 and 40.28µg/l for the dry season in the Elechi creek in the Niger delta. Kadiri (1993) also reported a range of 4.20 – 35.20 mgm^{-3} for chlorophyll *a* for the Ikpoba reservoir in Benin.

Kadiri (1993) reported on the seasonal changes in the chlorophyll *a* situation of a shallow reservoir in Benin, Nigeria. Higher cloud cover situations attributed to the rainy season have been noted to impair chlorophyll *a* estimates (Kadiri, 1993) and phytoplankton biomass (Nwankwo, 1988) in some parts of the country. On the other hand, increases in insolation usually noted in the dry season likely encourage higher productivity, as recorded for this study. Furthermore, Onyema *et al*. (2003, 2007), are of the view that higher insolation, increased hydrological stability and marine situation are important encouraging factors for primary production in the Lagos lagoon. According to Kadiri (1993) seasonal fluctuation in abundance of phytoplankton is influenced by changes in the physical and chemical properties of the water which themselves can be dependent on rainfall. Similarly, sainfall and salinity are known to regulate the occurrence and distribution of biota in the Lagos lagoon and its associated creeks (Nwankwo and Onyema, 2003; Nwankwo, 2004).

Besides the ample availability of nutrients in this region, values for chlorophyll *a* were comparatively low especially in the wet season which likely indicated limited phytoplankton production. Similarly, Dissolved oxygen levels throughout the period of study were comparatively higher in the dry season than the wet season. It is possible that higher primary productivity necessarily resulted in higher chlorophyll *a* value and revealed a similar trend in dissolved oxygen values, since oxygen is a by-product of photosynthesis. It is possible to infere that chlorophyll *a* values from this study were largely determined by the trend and continuum of environmental characteristics of the lagoon which varies tidally and seasonally.

Author:
I.C. ONYEMA Ph.D.
Dept. of Marine Sciences
Faculty of Science
University of Lagos, Akoka.
Lagos, Nigeria.
iconyema@yahoo.com.au, iconyema@gmail.com
+2348023446934, +2348060442323

9/2/2008

References.

American Public Health Association. (1998): Standard Methods for the Examination of Water and Waste Water. 20th ed. APHA New York. 1270pp.

Akinsoji, A., John, A. and Adekanye, M. (2002): Aquatic macrophytes of three selected sites in Lagos, Southwest Nigeria. Journal of Science, Technology Research and Development. 2(1): 9 – 15.

Brown, C.A. (1998): Distribution and population dynamics of an estuarine population of *Aloidis trigona* Hinds (Bivalvia). Acta. Hydrobiol. 40(4): 227 – 237.

Brown, C.A. and Oyenekan, J.A. (1998). Temporal variability in the structure of benthic macrofauna communities of the Lagos lagoon and harbour, Nigeria. Pol. Arch. Hydrobiol. 45(1): 45 – 54.

Chukwu, L. O. and Nwankwo, D. I. (2004): The impact of land based pollution on the hydro-chemistry and macrobenthic community of a tropical West African Creek. The Ekologia. 2 (1-2): 1 – 9.

F.A.O. (1969): Fisheries Survey in the Western and Mid-Western Regions of Nigeria. FAO/Sf: 74/NIR 6. 142pp.

Kjerfve, B. (Ed.) 1994: Coastal lagoon processes. Elsevier Oceanography Series 60. Elsevier, Amsterdam. 577pp.

Kirk, R.M. and Lauder, G.A. (2000): Significant coastal lagoon systems in the South Island, New Zealand. Coastal processes and lagoon mouth closure. *Science for conservation*.146**:** 47 p.

Kadiri, M.O. (1999): Phytoplankton distribution in some coastal waters of Nigeria. *Nigeria Journal of Botany*.**12** (1): 51 – 62.

Lee, R.E. (1999): Phycology. Cambridge University Press, New York. 614pp.

Nwankwo, D.I. (1984): Seasonal changes of phytoplankton of Lagos lagoon and the adjacent sea in relation to environmental factors. Ph.D. Thesis, University of Lagos. 447pp.

Nwankwo, D.I. (2004b). The Microalgae: Our indispensable allies in aquatic monitoring and biodiversity sustainability. University of Lagos Press. Inaugural lecture seris. 44pp.

Ogamba, E.N. Chindah, A.C., Ekweozor, I.K.E. and Onwuteaka, J.N. (2004): Water quality of phytoplankton distribution in Elechi creek complex of the Niger delta. Journal of Nigerian Environmental Society. 2(2): 121 – 130.

Ogbeibu, A.E. (2005): *Biostatistics*: A practical approach to reseach and data handling. Mindex Publishing Company limited, Benin city, Nigeria.264pp.

Onyema, I.C. (2008a): Phytoplankton biomass and diversity at the Iyagbe lagoon Lagos, Nigeria. University of Lagos, Akoka. Department of Marine Sciences. 266pp

Onyema, I.C. (2008b): A checklist of phytoplankton species of the Iyagbe lagoon, Lagos. Journal of Fisheries and Aquatic Sciences. **3**(3): 167 – 175.

Onyema, I.C. and Nwankwo, D.I. (2006): The epipelic assemblage of a polluted estuarine creek in Lagos, Nigeria. Pollution Research. **25** (3): 459 – 468.

Onyema, I.C., Otudeko, O.G. and Nwankwo, D.I. (2003): The distribution and composition of plankton around a sewage disposal site at Iddo, Nigeria. Journal of Scientific Research Development.**7:** 11-26.

Onyema, 1.C., Okpara, C.U., Ogbebor, C.I. Otudeko, O. and Nwankwo, D.I. (2007): Comparative studies of the water chemistry characteristics and temporal plankton variations at two polluted sites along the Lagos lagoon, Nigeria. Ecology, Environment and Conservation. 13: 1 – 12.

Sandison, E.E. (1966). The effect of salinity fluctuation on the life of *Balanus pallidus strusburi* (Darwin) in Lagos Habour, Nigeria. Journal of Animal Ecology. 35: 365 – 378.

Sandison, E.E. and Hill, M.B. (1966): The distribution of *Balanus pallidus* Strusburi (Darwin), Gryphaea gasar (Adanson) Dautzenbergi, *Mercierella enigmatica* farvel and *Hydroides uncinata* (Philippi) in relation to salinity in Lagos Harbour and adjacent creek. Journal of Animal Ecology. **38**: 235-258.

Suzuki, M.S., Figueiredo, R.O., Castro, S.C., Silva, C.F., Pereira, E.A., Silva, J.A. and Aragon, G.T. (2002): Sand bar opening in a castal lagoon (Iquipari) in the Northern region of Rio De Janeiro state: Hydrological and hydrochemical changes. Braz. J. Biol., 62 (1): 51 – 62.

Sverdrup, K. a., Duxbury, A. B., and Duxbury, A. C. (2006): Fundamentals of Oceanography 5th ed. New York: McGraw Hill Companies, Inc. 342. pp.

Webb, J.E. (1958a): The Ecology of Lagos lagoon. 1: The lagoons of the Guinea Coast. Philosophical Transaction Royal Society London. Ser B: 241-283.

Webb, J.E. (1958b): The life history of *Branchiostoma nigeriense* Webb. Philosophical Transaction Royal Society London. Ser B:335-354

Webb, J.E. (1960): Biology in the tropics. Nature. London. 188(4151): 617 - 619.

Webb, J.E. and Hill, M.B. (1958): On the Reactions of *Branchiostoma nigerence* Webb to its environment. Philosophical Transactions of the Royal Society of London. Ser B. 241: 355-391.

11/25/2008

Diversity and Distribution of Medicinal Plant Species in the Central Himalaya, India

Geeta Kharkwal

Department of Botany
Kumaun University
DSB Campus, Kumaun University, Uttaranchal, Nainital-263002, India
E-mail: **gkh_02@yahoo.co.in**; **geetakh@gmail.com**

Abstract: In this study, we examined diversity and distribution of medicinal plant species richness between 200-5800 m asl altitudes considering altitudinal gradients (200m asl altitudinal differences) in the Indian central Himalaya off which 126 were trees, 129 shrubs and 548 herbs. The total number of species, genera and families observed for herbs were maximum followed by tree and shrub species. In terms of species distribution Fabaceae and Rutaceae were found to be the most dominant family in tree species; Verbenaceae and Fabaceae in shrub species whereas in case of herb species, Asteraceae was found to be the dominant family. The total number of species including all growth forms was maximum near low altitude to mid altitude due to overlapping of climatic conditions, but further increase in altitude it decreased consistently, probably due to decrease in atmospheric temperature with increase in altitudes. [Academia Arena, 2009;1(1):32-42]. ISSN 1553-992X.

Key words: Plant species, diversity, distribution, altitude, central Himalaya

Introduction

Diversity, the variety and variability of plant and animal species are the most striking feature of life, which reflects the complexity, uniqueness, and intactness of natural ecosystems (Mohammad *et. al.*, 2000). An appropriate biodiversity management strategy should take into account the distribution patterns of species (Perring and Lovett 1999). Conservation of ecosystem and maintenance of biodiversity in central Himalaya is matter of both national and international concern.

Central Himalaya is one of the biodiversity rich states of India in terms of vegetation and flora varied altitude, topography, status of soil and climatic conditions which favors high species richness and support different forest types. Deciduous and evergreen tropical forests, subtropical, semi evergreen and sub tropical pine forest are the major forest type of this state (Champion & Seth, 1968). The wide geographical and climatic diversity provides a repository of valuable medicinal and wild edible plants of the region.

The use of the plant species of the Himalaya as medicine is known since the long time and about 1750 medicinal plants is reported from Indian Himalaya by Samant *et al.*, (1998). The unique diversity of medicinal plants in the region is manifested by the presence of a number of native (31%), endemic (15.5%) and threatened elements (14%) of total Red Data Book plant species of Indian Himalaya Region (Samant *et al.*, 1998). Plants provide food and other life supporting commodities and very important for survival of human beings and other organisms, besides they protect our environment and maintain nature. Tropical forests are major reservoir of plant diversity. Those forests inhabit a large number of trees, shrubs, herbs, climbers, faunal, wealth and a wealth of non-timber forest products including medicinal and wild edible plants. The increased demand of medicinal plants in drug and pharmaceutical industries have caused the over exploitation of many species. Many of these are close to extinction due to over harvesting or un-skilled harvesting. Some important species that need immediate attention for conservation in India are *Aconitum, Angelica, Artemisia, Atropa, Berberis, Dectylorhiza, Thalictrum, Hedychium* etc. To maintain the ecosystem equilibrium, awareness of the sustainable utilization of these species is important and their conservation in sustainable environment is urgently needed, keeping in view the demand among the hill communities and their drugs in the global market (Samant and Dhar, 1997; Dubay *et al.*, 2004). Wide geographical and climatic diversity provides a repository of valuable medicinal and wild edible plants of this region. Therefore the present study is an effort to identify important medicinal plants in this region based on primary and secondary resources.

The objectives of the present study were (i) to find out species richness in relation to different altitudinal range (ii) to analyze the pattern plant species variation between 200 m altitudinal gradient (iii) to examine the variation in nature of plant forms in respect to altitude.

Material and Methods

The field survey was conducted in different forest sites surrounding the Nainital catchments of Kumaun region in the Central Himalaya and the information provided by the secondary resources (Samant *et al.*, 1998) and available literature (Chopra *et al.*, 1956). The study area is located between 79°23' and 79°42' E longitude and 29°20' and 29°30' N latitude between 1500m to 2600m elevations in central Himalaya. Five sites were selected in the wide elevation range along the gradient of disturbances. Several field trips were undertaken for collection of plants during different years.

The climate is monsoon temperate and annual rainfall of the area is 2668 mm/year. The mean maximum temperature varies from 13.9 (Feb) to 23.7°C (April) and the mean minimum from 4.9 (Feb) to 16.5°C (July). The monsoon strikes in this area in the middle of June to the middle of September, which sometimes extends to late September and first week of October. The bedrock belongs to the Krol formation consists predominantly of carbonate, limestone, marl and slates in the lower part and dolomites in the upper part (Valdia, 1980).

For moisture content, 50g of fresh soil was dried in an oven at 80°C temperature till constant weight (Misra, 1968). For determination of soil pH, soil extract was assessed by digital pH meter using 1:5 proportions of soil and water. Soil organic carbon was determined using the wet oxidation method (Jackson, 1958). Percentage of organic matter was obtained by multiplying the % of organic carbon by a factor of 1.724. This factor is based upon the assumption that the organic matter of soil contains 58% carbon (Misra, 1968). Nitrogen content of soil was determined by Kjel Auto Vs-KTP Nitrogen Analyzer based on a micro-Kjeldahl technique (Misra, 1968).

The vegetation analysis of each forest site was carried out by using 10, 10m × 10m quadrats placed randomly for tree layer. The number and size of the quadrats were determined by Running Mean Method (Kershaw, 1973) and species area curve (Misra, 1968). Shrubs were sampled by using 10, 5m × 5m quadrats randomly. For the study of herbaceous vegetation, fifteen quadrats (1m × 1m) were placed on the above selected area in each of the forest/stands (hill-base, hill-slope and hill-top). Herbaceous vegetation was studied through tiller analysis. Each tiller of grasses was considered as an individual plant (Singh, 1967). In the case of creeping plant any unit of the plant having functional roots was considered as one plant. Vegetational data were analyzed following Curtis & McIntosh (1950), Species evenness (Margalef 1968), dominance (Simpson, 1949) and diversity (Shannon-Weaver, 1963) for the primary data.

Results and Discussion

Extensive survey of the locality of Central Himalayan region of Nainital area was made for the proposed study. A total of 166 species belonging to 61 family were recorded across the study sites, of which 16 were trees, 37 were shrubs and 113 were herbs (Table 1).

Percentage of sand in soil ranged from 50% to 65%. It was maximum in highly disturbed sites and reduced with decreasing disturbances. The value of silt and clay in different sites were 17.9-30% and 11-28.8% respectively. Moisture content of soil ranged from 29% to 65% and soil pH varied from 5.3 to 8.0. It was lower in the low elevation high-disturbed sites and higher in the high elevation less disturbed sites. There was no significant difference in the organic matter in high and less disturbed sites. It was comparatively higher in the oak forests towards higher elevations. The percentage value of carbon, nitrogen and organic matter in different sites were 1.2-3.4, 0.1-0.3 and 4.0-5.9, respectively. Percentage nitrogen also increased with increase in total organic matter.

Sandy loam soil is preponderance in lower elevation and clay loam in higher elevation (above 2200m asl). The pH of the soil was slightly acidic (6.65) to neutral (6.5-7), but in higher altitudes (above 2800-3000m asl) to medium (5.5-6) was strongly acidic. Organic matter content ranged from less than 1% to 4%. The soil moisture content varied from 21-43% at -3 bar water potential and 7.6-14.8% at -15bar water potential (Singh & Singh, 1987).

There was a positive relationship between shrubs and herbs diversity, and both increased with increasing disturbances. The tree, shrub and herb density were (5.1-9.5 ind/100m^2, 1.1-7.2 ind/25m^2 and 9.3- 34.7 ind/m^2 respectively. The diversity values for tree, shrub and herb species were ranged between 0.2-1.6, 1.9-3.3 and 3.2-4.0, respectively. ANOVA tests for tree, shrub and herb species (between species richness and diversity) showed significant variation at 5% level. Significant positive relations were found between moisture and density of shrubs ($P < 0.01$), and also moisture and density of herbs ($P < 0.05$). Equitability values for tree, shrub and herb species were 1.1-4.4, 12.7-19.4 and 16.7-28.8, respectively. The concentration of dominance in tree, shrub and herb species was 0.6-0.9, 0.2-0.6 and 0.08-0.6, respectively.

Based on secondary resources, a total of 777 species were found out of which a total of 126 tree species was encountered, belonging to 49 families and 52 genera. Fabaceae and Rutaceae were the most dominant family (with nine species) followed by Moraceae (with eight species), Rubiaceae (with seven species), Caesalpiniaceae (with six species), Meliaceae and Rosaceae (with five species), Anacardiaceae, Bignoniaceae, Combretaceae,

Lauraceae (with four species), Apocynaceae, Elaegnaceae, Fagaceae, Mimosaceae, Oleaceae, Pinaceae, Pistaciaceae, Sapindaceae (with three species), Burseraceae, Capparaceae, Euphorbiaceae, Mytricaceae, Pittosporaceae, Rhamnaceae, Tiliaceae (with two species), whereas the remaining 22 families were represented by one species each (Table 2).

The study showed that tree species distributed between <200-3600m asl altitude. At 200m asl altitudinal differences species ranged between 4 and 115 species, being minimum at 3400-3600 m asl and maximum at 1000-1200m asl and it declined thereafter with increasing altitude (Fig 1). A number of tree species found in the Himalaya showed varying patterns of distribution. The extension of climatic gradient enabled several species to realize their fullest range of elevational adaptability. Distributional ranges of several species were segregated along the widened altitudinal ranges (Singh & Singh, 1992).

A total of 129 shrub species was reported belonging 40 family 87 genera in which Verbenaceae and Fabaceae was the dominant family (nine species) followed by Asclepiadaceae (eight species), Apocynaceae, Berberidaceae, Caesalpiniaceae, Rosaceae (seven species), Euphorbiaceae (six species), Asparagaceae, Vitaceae (five species), Convolvulaceae, Loranthaceae, Periplocaceae, Rhamnaceae, Rutaceae, Urticaceae (three species), Celastraceae, Ericaceae, Myrsinaceae, Oleaceae, Polygonaceae, Rubiaceae, Solanaceae, Tiliaceae (two species) and 11 family represented by single species (Table 2).

Species richness of shrubs varied from <200 to 5600m asl altitudinal range. The distribution pattern of shrub species varied from 1(5400-5600m asl) to 73 (800-1200m asl) species. From 200-1200m asl, species richness increased sharply with altitude, thereafter species richness declined towards higher altitudes (Fig. 1).

Similarly, in case of herb species, a total of 548 belonging to 85 family were encountered. Asteraceae was the dominant family (with fifty-four species), followed by Lamiaceae (with thirty seven species), Poaceae (with twenty-nine species), Fabaceae, Orchidaceae(with twenty-seven species), Ranunculaceae (with twenty-two species), Apiaceae, Gentianaceae (with nineteen species), Solanaceae, Zingiberaceae Periplocaceae (with fifteen species), Scrophulariaceae, Euphorbiaceae (with thirteen species), Rubiaceae (with twelve species), Cucurbitaceae (with eleven species), Brassicaceae (with ten species), Convolvulaceae, Linaceae, Malvaceae, (with nine species), Alliaceae, Borginaceae (with eight species), Fumariaceae, Iridaceae (with six species), Acanthaceae, Geraniaceae, Violaceae, Rosaceae, Verbenaceae, Menispermaceae, Araceae (with five species), Amaranthaceae, Commelinaceae, Dioscoreaceae, Crassulaceae, Valerianaceae, Papaveraceae, (with four species), Caryophyllaceae, Chenopodiaceae, Geraniaceae, Mimosaceae, Papaveraceae, Polygonaceae (with three species), Achyranthaceae, Asclepiadaceae, Balsminaceae, Aristolochiaceae, Cannabaceae, Peperomiaceae, Leeaceae, Linaceae, Hypericaceae, Onagraceae, Hypodixaceae, Nyctaginaceae, Plumbaginaceae, Paranassiaceae, Piperaceae, Primulaceae, (with two species) whereas the remaining 26 families were represented by one species each (Table 2).

Herbs were the largest contributor of plant richness among the others forms and were distributed between <200-5800m asl. Herb richness ranged from 1 (5600-5800 m asl) and 202 (1400-1600m asl). The herb richness declined slightly at an elevation of 2800-3000m asl; after that it increased slightly upto 3800m asl and subsequently it declines.

It is well fact that the altitude represents a complex gradient along which many environmental variables change concomitantly. However, in general, it has been suggested that an increase of 270m asl altitudes corresponds to a fall of 1ºC in mean atmospheric pressure upto 1500m asl, above which the fall is more rapid (Osmaston, 1927). Pangtey *et al*. (1991) argued the effect of monsoon is not substantially weakened at higher altitudes and also the amount of rainfall is not much different from that of the lower altitudinal range of central Himalaya.

There were pronounced effect of elevation on different edhapic factors (elevation vs. soil moisture content, elevation vs. soil pH) and total plant species richness and a positive relation between soil moisture and plant species richness of the area but there was no relationship found between soil pH and plant species richness (Kharkwal et al., 2005). On the other hand, the distribution of plant species depends mainly on the altitude and climatic variables like temperature, rainfall, which act as the sole determinant for the species richness in this region.

The pattern of proportions of family to genera, family to species and genera to species were found to be similar for primary and secondary resources (Table 3). Margalef's index for herb species in chir-pine was maximum. Shannon-Weaver index for species diversity showed a higher value for Kharsu oak forest (Table 4). Simpson index was higher for Tilonj-oak and Chir-pine than other forests indicating that few species were dominant in that forest type (Table 4). The Simpson index was higher for Tilonj-oak and Chir-pine forest as compared to other forest indicating lower stability of these forests. Whittaker value varied for all forest types.

The various parts of plant species are used for different purposes i.e. food for humans medicine, fuel, timber and multipurpose. For example, species of *Quercus* provide excellent fuel and timber, seeds of *Myrica esulenta*, rhizome of *Valeriana wallichii* and *Hedychium spicatum* etc are traded and are source of income

generation in the area (Samant and Dhar, 1997). The results of the present study open new prospect of plant materials used in traditional medicine which will promote forest conservation and ecological research through surveys, development and implementation of land use plans by proper planting, afforestation, reforestation and forest rehabilitation. Such medicinal plants could also be incorporated into primary health care, as people generally feel safer with indigenous cures and also the costs of medicine would be much lesser than modern drugs.

The author is grateful to Head, Department of Botany, Kumaun University, Nainital for providing research facilities and Department of Science & Technology, New Delhi (Ref. No. SR/FT/L-31/2006) for financial assistance.

Table 1. A list of plants encountered in the study sites.

Species	Family	Habit
Acer oblongum Wall. ex DC.	Aceraceae	T
Achyranthes aspera	Amaranthaceae	H
Achyranthes bidentata Blume	Amaranthaceae	H
Aesculus indica (Colebr. ex Camb.) Hook.	Hippocastanaceae	T
Ageratum houstonianum Mill.	Asteraceae	H
Agrimonia pilosa Ledeb.	Rosaceae	H
Ainsliaea aptera DC.	Asteraceae	H
Ainsliaea latifolia (D. Don) Sch.-Bip.	Asteraceae	H
Ajuga parviflora Benth.	Lamiaceae	H
Anaphalis busua (Buch-Ham. ex D. Don) DC.	Asteraceae	H
Anaphalis cinnamonea Clarke	Asteraceae	H
Anaphalis contorta (D. Don) Hook. fil.	Asteraceae	H
Anemone vitifolia Buch.-Ham. ex DC.	Ranunculaceae	H
Arisaema tortuosum (Wall.) Schott	Araceae	H
*Artemisia nilagarica (*C.B. Clarke) Pamp.	Asteraceae	S
Arthraxon prionodes (Steud.) Dandy	Poaceae	H
Arundinaria falcate Nees	Poaceae	S
Aster asperculus (DC.) Hook. fil.	Asteraceae	H
Aster thomsonii Clarke	Asteraceae	H
Athyrium foliolosum Wall. ex Smith	Athyriaceae	H
Athyrium rupicola (Hope) C. Chr.	Athyriaceae	H
Begonia picta Smith	Begnoniaceae	H
Berberis asiatica Roxb. ex D. Don	Berberidaceae	S
Bidens biternata L.	Asteraceae	H
Bidens pilosa L.	Asteraceae	H
Biota orientalis (L.) Endl.	Cupressaceae	T
Boenninghausenia albiflora Reich. ex Meisn.	Rutaceae	S
Bupleurum tenue Buch.-Ham. ex D. Don	Apiaceae	H
Campanula colorata Wall.	Campanulaceae	H
Carex cruciata Wahlenb.	Cyperaceae	H
Carex nubigena Tilloch &Taylor	Cyperaceae	H
Carpesium cernuum L.	Asteraceae	H
Carum anathifolium Benth.	Apiaceae	H
Cassia floribunda Cav.	Caelapiniaceae	S
Cassia laevigata Willd.	Caesalpiniaceae	S
Cassia mimosoides L.	Caesalpiniaceae	H
Cedrus deodara (Roxb. ex D. Don) G. Don	Pinaceae	T
Celtis tetrasperma Roxb.	Ulmaceae	S
Centella asiatica (L.) Urban	Apiaceae	H
Circaea alpina L.	Onagraceae	H
Circaea lutea L.	Onagraceae	H
Clinopodium umbrosum (M. Bieb.) Koch	Lamiaceae	H
Colquehonia coccinea Wall.	Lamiacaea	S
Commelina benghalensis L.	Commelinaceae	H
Conyza japonica Thunb. Lessing ex DC.	Asteraceae	H

46.	*Conyza stricta* Willd.	Asteraceae	H
47.	*Coriaria nepalensis* Wall.	Coriariaceae	S
48.	*Cornus oblonga* Wall.	Cornaceae	T
49.	*Cotoneaster microphylla* Wall. ex Lindl.	Rosaceae	S
50.	*Craniotome furcata* (Link) Kunze	Lamiaceae	H
51.	*Crotalaria sessibiflora* L.	Fabaceae	H
52.	*Cupressus torulosa* D. Don	Cupressaceae	T
53.	*Cynoglossum glochidiatum* Wall. ex Benth.	Boraginaceae	H
54.	*Cynoglossum lanceolatum* Forsk.	Boraginaceae	H
55.	*Cyperus niveus* Retz.	Cyperaceae	H
56.	*Daphne cannabina* Wall.	Thymelaeaceae	S
57.	*Debregeasia longifolia* (Burm. fil.) Wedd.	Urticaceae	S
58.	*Debregeasia salicifolia* (D. Don) Rendle	Urticaceae	S
59.	*Desmodium multiflorus DC.*	Fabaceae	H
60.	*Deutzia staminea* R.Br.	Saxifragaceae	S
61.	*Dicliptera bupleuroides* Nees	Acanthaceae	H
62.	*Dipsacus mites* D. Don	Dipsacaceae	H
63.	*Epilobium royleanum* Haussk.	Onagraceae	H
64.	*Epipactis latifoila* (L.) Alloini	Orchidaceae	H
65.	*Erigeron bonariensis* L.	Asteraceae	H
66.	*Erigeron annua* (L.) Pers.	Asteraceae	H
67.	*Erigeron karvinskianus* DC.	Asteraceae	H
68.	*Eupatorium adenophorum* Spreng.	Asteraceae	S
69.	*Flemingia bracteata* (Roxb.) Wight	Fabaceae	H
70.	*Flemingia involucrate* Benth.	Fabaceae	S
71.	*Fragaria indica* Andrews	Rosaceae	H
72.	*Fraxinus micrantha* Lingelsheim	Oleaceae	T
73.	*Galinsoga ciliata* (Rafines.-Sch.) Blake	Asteraceae	H
74.	*Galium aparina* L.	Rubiaceae	H
75.	*Galium rotundifolium* L.	Rubiaceae	H
76.	*Geranium nepalense* Sweet	Geraniaceae	H
77.	*Geranium wallichianum* D. Don ex Sweet	Geraniaceae	H
78.	*Gerbera gossypina* (Royle) G.Beauv.	Asteraceae	H
79.	*Girardiana heterophylla* (Vahl) Decne.	Urticaceae	S
80.	*Goodyera repens* (L.) R.Br.	Orchidaceae	H
81.	*Habernaria latilabris* (Lindl.) Hook. fil.	Orchidaceae	H
82.	*Hedychium spicatum* Buch.-Ham. ex J.E.Smith	Zingiberaceae	H
83.	*Hypericum oblongifolium* Choisy	Hypericaceae	S
84.	*Ilex dipyrena* Wall.	Equifoliaceae	T
85.	*Indigofera heterantha* Wall. ex Brandis	Fabaceae	S
86.	*Jasminum humile* L.	Oleaceae	S
87.	*Justicia simplex* D. Don	Acanthaceae	H
88.	*Lantana camara* L.	Verbenaceae	S
89.	*Lepidium virginianum* L.	Brassicaceae	H
90.	*Leucas lanata* Benth.	Lamiaceae	H
91.	*Lindenbergia indica* (L.) Vatke	Scrophulariaceae	H
92.	*Litsea umbrosa* Nees	Lauraceae	T
93.	*Lonicera quinquelocularis* Hardw.	Caprifoliaceae	S
94.	*Lychnis fimbricata* Wall. ex Benth.	Caryophyllaceae	H
95.	*Lyonia ovalifolia* (Wall.) Drude	Ericaceae	T
96.	*Meizotropis pellita* (Hook.fil. ex Prain) Sanjappa	Fabaceae	S
97.	*Melissa fllava* Benth.	Lamiaceae	H
98.	*Micromeria biflora* (Buch.-Ham.ex D. Don) Benth.	Lamiaceae	H
99.	*Myrica esculenta* Buch.-Ham. ex D. Don	Myricaceae	T
100.	*Myrsine Africana* L.	Myrsinaceae	S
101.	*Neanotis calycina* (Wall. ex Hook.fil.) Lewis	Rubiaceae	H

102.Nervilea crispate (Blume) Schltr.	Orchidaceae	H
103.Onchychium cryptogrammoides C.Chr.	Cryptogrmmaceae	H
104.Oplismenus compositus (L.) P.Beauv.	Poaceae	H
105.Origanum vulgare L.	Lamiaceae	H
106.Oryzopsis aequiglumis Duthie ex Hook.fil.	Poaceae	H
107.Oxalis corniculata L.	Oxalidaceae	H
108.Oxalis latifolia BHK	Oxalidaceae	H
109.Paris polyphylla J.E.Smith	Liliaceae	H
110.Pilea umbrosa Wedd.	Urticaceae	H
111.Pilea scripta (Buch.-Ham.ex D. Don) Wedd.	Urticaceae	H
112.Pimpinella acuminate (Edgew.) Clarke	Apiaceae	H
113.Pimpinella diversifolia DC.	Apiaceae	H
114.Pinus roxburghii Sarg.	Pinaceae	T
115.Platystemma violoides Wall.	Gesneriaceae	H
116.Plectranthus striatus Benth.	Lamiaceae	H
117.Plectranthus japonicus (Burm.fil.) Koidz.	Lamiaceae	H
118.Polycarpaea corymbosa (L.) Lam.	Caryophyllaceae	H
119.Polygonum hydropiper L.	Polygonaceae	H
120.Polygonum amplexicaule D. Don	Polygonaceae	H
121.Polygonum nepalense Meisn.	Polygonaceae	H
122.Potentilla nepalensis Hook.	Rosaceae	H
123.Pouzolzia hirta (Blume) Hassk.	Urticaceae	H
124.Prinsepia utilis Royle	Rosaceae	S
125.Pteris cretica L.	Pteridaceae	H
126.Pyracanthus crenulata (D. Don) M.Roem.	Rosaceae	S
127.Quercus floribunda Lindl. ex Rehder	Fagaceae	T
128.Quercus leucotrichophora A. Camus	Fagaceae	T
129.Quercus semecarpifolia J.E. Smith	Fagaceae	T
130.Randia tetrasperma (Wall.) Hook.fil.	Rubiaceae	S
131.Rhamnus virgata Roxb.	Rhamnaceae	S
132.Rhododendron arboretum Smith	Ericaceae	T
133.Rosa moschata Mill. ex Herrm.	Rosaceae	S
134.Roscoea purpurea J. E. Smith	Zingiberaceae	H
135.Rubus ellipticus Smith	Rosaceae	S
136.Rubus lasiocarpus Smith	Rosaceae	S
137.Rumex hastatus D. Don	Polygonaceae	H
138.Sanicula elata Buch.-Ham. ex D. Don	Apiaceae	H
139.Sarcococa hookeiana Baill	Buxaceae	S
140.Satyrium nepalense D. Don	Orchidaceae	H
141.Scutellaria angulosa Benth.	Lamiaceae	H
142.Sedum sinuatum Royle ex Edgew.	Crassulaceae	H
143.Selinum wallichianum (DC.) Raizada & Saxena	Apiaceae	H
144.Setaria glauca (L.) P. Beauv.	Poaceae	H
145.Setaria homonyma (Steud.) Choiv.	Poaceae	H
146.Siegesbeckia orientalis L.	Asteraceae	H
147.Smilax vaginata Decne.	Smilacaceae	S
148.Solidago virg-aurea L.	Asteraceae	H
149.Stachys sericea Wall. ex Benth.	Lamiaceae	H
150.Swertia pulchella Buch.-Ham. ex D. Don	Gentianaceae	H
151.Swertia ciliata Burtt.	Gentianaceae	H
152.Synotis rufinervis (DC.) C. Jeffrey & Y.L.Chen	Asteraceae	H
153.Teucrium royleanum Wall. ex Benth.	Lamiaceae	H
154.Thalictrum foliolosum DC.	Ranunculaceae	H
155.Themeda anathera (Nees ex Steud.) Hack.	Poaceae	H
156.Torenia cordiflora Roxb.	Scrophulariaceae	H
157.Torilis japonicus (Houtt.) DC.	Apiaceae	H

158.Urena lobata L.	Malvaceae	H
159.Utrica dioica L.	Urticaceae	S
160.*Valeriana wallichii* DC.	Valerianaceae	H
161.Viburnum continifolium D. Don	Caprifoliaceae	S
162.Viburnum coriaceum Blume	Caprifoliaceae	S
163.Viola canescens Wall.	Violaceae	H
164.Viola pilosa Blume	Violaceae	H
165.Wikstroemia canescens Meisn.	Thymelaeaceace	S
166.Wulfenia amherstiana Benth.	Scrophulariaceae	H

Table 2. Family-wise contribution to genera and species

Species	Tree		Shrub		Herb	
	Genus	Species	Genus	Species	Genus	Species
Acanthaceae	-	-	1	1	1	5
Achyranthaceae	-	-	-	-	1	2
Agavaceae	-	-	1	1	-	-
Alangiaceae	1	1	-	-	-	-
Alliaceae	-	-	-	-	1	8
Amaranthaceae	-	-	-	-	2	4
Amaryllidaceae	-	-	-	-	1	1
Anacardiaceae	4	4	1	1	-	-
Annonaceae	3	3	-	-	-	-
Apiaceae	-	-	-	-	16	19
Apocynaceae	1	1	7	7	-	-
Araceae	-	-	-	-	4	5
Araliaceae	1	1	1	1	-	-
Arecaceae	3	3	-	-	-	-
Aristolochiaceae	-	-	-	-	1	1
Asclepiadaeae	-	-	6	8	2	2
Asparagaceae	-	-	3	5	-	-
Asteraceae	-	-	-	-	43	54
Athyriaceae	-	-	-	-	-	-
Balsminaceae	-	-	-	-	1	2
Berberdiaceae	-	-	2	7	-	-
Betulaceae	1	1	-	-	-	-
Bignoniaceae	3	4	-	-	-	-
Bombaceae	1	1	-	-	-	-
Borginaceae	-	-	-	-	7	8
Brassicaceae	-	-	-	-	8	10
Burseraeae	2	2	-	-	-	-
Caesalpiniaceae	3	6	3	7	1	1
Campanulaceae	-	-	-	-	-	-
Cannbaceae	-	-	-	-	2	2
Capparaceae	1	2	1	2	-	-
Caprifoliaceae	1	1	-	-	-	-
Cariaceae	-	-	-	-	1	1
Caryophyllaceae	-	-	-	-	3	3
Caryophyllaceae	-	-	-	-	3	3
Celastraceae	1	1	2	2	-	-
Chenopodiaceae	-	-	-	-	2	3
Clemaceae	-	-	-	-	1	1
Combretaceae	1	4	1	1	-	-
Commelinaceae	-	-	-	-	3	4
Convolvulaceae	-	-	2	3	7	9
Costaceae	-	-	-	-	1	1

Crassulaceae	-	-	-	-	2	4
Cryptogrammaceae	-	-	-	-	-	-
Cucurbitaceae	-	-	-	-	3	11
Cyperaceae	-	-	-	-	1	1
Dioscoreaceae	-	-	-	-	1	4
Dipsacaceae	-	-	-	-	-	-
Dipterocarpaceae	1	1	-	-	-	-
Droseraceae	-	-	-	-	1	1
Elaeagnaceae	3	3	1	1	-	-
Ephederaceae	-	-	1	1	-	-
Ericaceae	1	1	1	2	1	1
Euphorbiaceae	2	2	5	6	10	13
Fabaceae	7	9	6	9	16	27
Fagaceae	3	3	-	-	-	-
Fumariaceae	-	-	-	-	2	6
Gentianaceae	-	-	-	-	9	19
Geraniaceae	-	-	-	-	2	5
Hydrangeaceae	-	-	2	2	-	-
Hypericaceae	-	-	-	-	1	2
Hypoxidaceae	-	-	-	-	1	2
Iridaceae	-	-	-	-	3	6
Julandaceae	-	-	-	-	1	1
Lamiaceae	-	-	2	2	29	37
Lauraceae	4	4	-	-	-	-
Leeaceae	-	-	-	-	1	2
Liliaceae	-	-	-	-	12	16
Linaceae	-	-	-	-	2	2
Loranthaceae	-	-	2	3	-	-
Lythraceae	-	-	1	1	-	-
Malvaceae	1	1	3	6	8	9
Meliaceae	5	5	-	-	-	-
Menispermaceae	-	-	-	-	3	5
Mimosaceae	2	3	1	1	2	3
Molluginaceae	-	-	-	-	1	1
Moraceae	3	8	-	-	-	-
Morinaceae	-	-	-	-	1	1
Musaceae	-	-	-	-	1	1
Myricaceae	1	1	-	-	-	-
Myrsinaceae	-	-	2	2	-	-
Myrtaceae	2	2	-	-	-	-
Nelumbonaceae	-	-	-	-	1	1
Nyctaginaceae	-	-	-	-	2	2
Nymphaceae	-	-	-	-	1	1
Ochnaceae	1	1	-	-	-	-
Oleaceae	2	3	2	2	-	-
Onagraceae	-	-	-	-	2	2
Orchidaceae	-	-	-	-	12	27
Oxalidaceae	-	-	-	-	2	3
Paeoniaceae	-	-	-	-	1	1
Pandanaceae	1	1	-	-	-	-
Papaveraceae	-	-	-	-	3	4
Paranassiaceae	-	-	-	-	1	2
Pedaliaceae	-	-	-	-	1	1
Pedaliaceae	-	-	-	-	1	1
Peperomiaceae	-	-	-	-	1	2
Periplocaceae	-	-	3	3	5	15

Phytolaccaceae	-	-	-	-	1	1
Pinaceae	3	3	-	-	-	-
Piperaceae	-	-	-	-	1	6
Pistaciaceae	2	3	-	-	-	-
Pittosporaceae	1	2	-	-	-	-
Plumbaginaceae	-	-	-	-	1	2
Poaceae	-	-	-	-	24	29
Podophyllaceae	-	-	-	-	1	1
Polygonaceae	-	-	2	2	1	3
Portlaceae	-	-	-	-	1	1
Primulaceae	-	-	-	-	2	2
Punicaceae	1	1	-	-	-	-
Ranunculaceae	-	-	-	-	10	22
Rhamnaceae	1	2	2	3	-	-
Rosaceae	3	5	6	7	3	5
Rubiaceae	6	7	2	2	7	12
Rutaceae	7	9	3	3	1	1
Sapindaceae	3	3	1	1	1	1
Saxifragaceae	-	-	-	-	2	4
Scrophulariaceae	-	-	-	-	12	17
Simaroubaceae	1	1	-	-	-	-
Smilaceae	-	-	1	2	-	-
Solanaceae	-	-	2	2	7	15
Steruliaceae	1	1	-	-	-	-
Symplocaceae	1	1	-	-	-	-
Tamaricaceae	-	-	1	1	-	-
Taxaceae	1	1	-	-	-	-
Tiliaceae	1	2	2	2	-	-
Trilliaceae	-	-	-	-	1	1
Typhaceae	-	-	-	-	1	1
Ulmaceae	1	1	-	-	-	-
Urticaceae	-	-	2	3	3	5
Valerianaceae	-	-	-	-	2	3
Verbenaceae	1	1	6	9	3	5
Violaceae	-	-	-	-	2	5
Vitaceae	-	-	3	5	-	-
Zingiberaceae	-	-	-	-	6	15

Table 3. Ratios of species, genus and family

Ratio	**Primary resources**			**Secondary resources**		
	Tree	**Shrub**	**Herb**	**Tree**	**Shrub**	**Herb**
Genus: Species	1.14	1.09	1.30	2.42	1.48	1.56
Family: Species	1.23	1.44	3.05	2.57	3.23	6.45
Family: Genus	1.08	1.32	2.35	1.06	2.18	4.14

Table 4. Diversity indices of different forest sites

Forest	**Layer**	**Margalef**	**Shannon-Weaver**	**Simpson**	**Whittaker**
Chir-pine	Tree	1.85	0.22	1.83	1.5
	Shrub	16.22	2.29	0.62	2.18

	Herb	28.77	3.44	0.45	1.89
Chir-pine	Tree	1.12	0.63	0.97	1.5
	Shrub	19.44	3.27	0.62	5.26
	Herb	16.67	3.92	0.06	3.62
Banj oak	Tree	3.18	1.32	0.89	2.5
	Shrub	12.57	2.25	0.27	3.09
	Herb	22.43	3.66	0.34	2.06
Tilonj oak	Tree	3.36	0.53	3.36	1.67
	Shrub	14.41	1.99	0.32	2.5
	Herb	26.37	3.27	0.44	1.71
Kharsu oak	Tree	4.44	1.56	0.56	2.09
	Shrub	15.24	2.97	0.17	2.14
	Herb	18.87	4.00	0.08	2.12

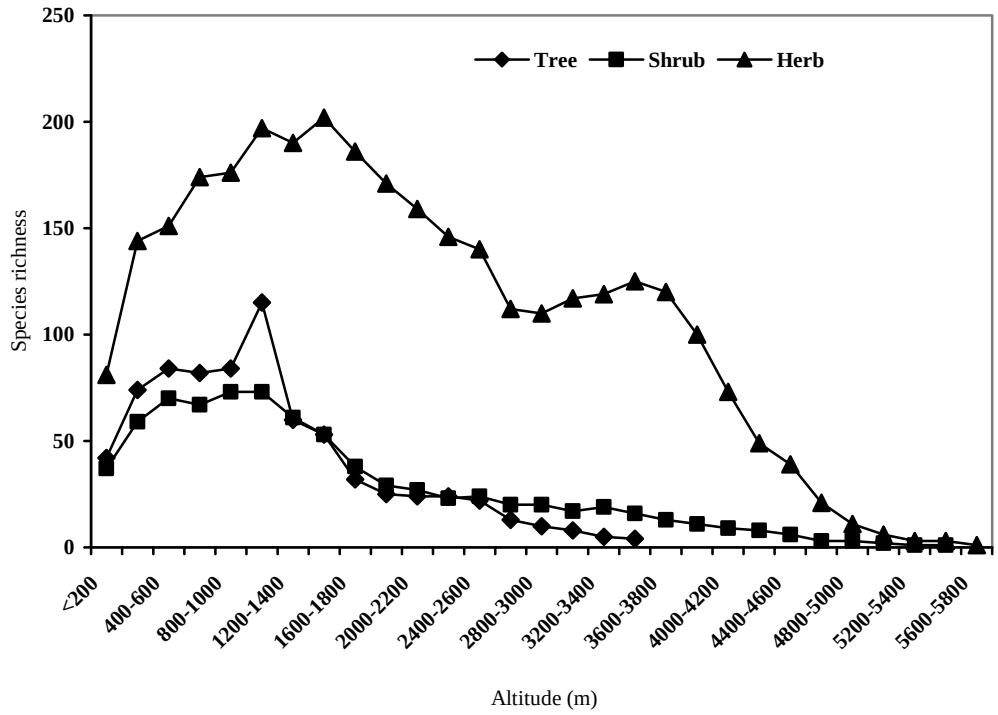

Figure 1. Total plant species richness in relation to altitude

Author:
Geeta Kharkwal
C/o Sumitra Verma
Charton lodge

Department of Botany
Kumaun University
Nainital-263002
Uttaranchal

E-mail: gkh_02@yahoo.co.in; geetakh@gmail.com

23/07/2008

References

Champion H.G. and Seth S.K., A revised survey of the forest types of India, Govt. of India, New Delhi, India, 1968.

Chopra R.N., Nayar S.L. and Chopra I.C., Glossary of Indian Medicinal Plants, Publications and Information Directorate (CSIR), New Delhi, 1956.

Curtis J.T. and McIntosh R.P., The interrelations of certain analytic and synthetic phytosociological characters. *Ecology***,** 1950**, 31:** 438-455.

Samant S.S. and U. Dhar, Diversity, Endemism and Economic Potential of Wild Edible Plants of Indian Himalaya. *Intern. J. Sustain. Dev. & World Ecology*, 1997, **4**: 179-191.

Dubey N.K., Kumar R. and Tripahti P., Global promotion of herbal medicine: India's opportunity, *Cure Med*, 2004, **86:** 37-41.

Kershaw K.P., Quantitative and dynamic plantecolofy. Edward Arnold Ltd., London, UK, 1973.

Jackson M.L., Soil *Chemical Analysis*. Prentice Hall Inc., New Jersey, USA, 1958.

Margalef D.R., *Perspectives in ecological theory*, University of Chicago Press, Chicago Press, 1968, pp112.

Misra R., Ecology Work Book Oxford and IBH Publishing Company, New Delhi, 1968, pp244.

Mohamed A. Ayyad; Amal M. Fakhry and Abdel-Raouf A. Moustafa, Plant biodiversity in the Saint Catherine area of the Sinai Peninsula, Egypt. *Biodiversity and Conservation***,** 2000**, 9:**265-281.

Osmaston, A.E., A forest Flora for Kumaun, Govt. Press, United Provinces, Allahabad, 1927, pp605.

Pangtey, Y.P.S., Rawal, R.S., Bankoti, N.S. and Samant, S.S., *Int. J. Biometeorol*, 1991, **34:**122-127.

Perring C. and Lovett J. C., Policies for biodiversity conservation: The case of Sub-Saharan Africa. *International Affairs***,** 1999**, 75**:281-305.

Samant S.S., Dhar U. and Palni L.M.S., *Medicinal plants of Indian Himalaya: diversity distribution and potential Value*. Nainital: Gyanodaya Prakashan, 1998.

Shannon C.E. and Wienner W., The mathematical theory of communication. University Illionis Press, Urbana, 1963.

Simpson E.H., Measurement of Diversity. *Nature***,** 1949, **163:** 688.

Singh J.S., Seasonal variation in composition, plant biomass and net primary productivity in the grass land of Varanasi. Ph.D. thesis, Banaras Hindu University, Varanasi, India, 1967, pp318.

Singh J.S. and Singh S.P., Forest vegetation of the Himalaya. *Botanical Review***, 52,** 80-1987.

Singh J.S. and Singh S. P., Forest of Himalaya: Structure, Functioning and Impact of man. Gyanodaya Prakashan, Nainital, India, 1992.

Valdia K.S., Geology of Kumaun lesser Himalaya, Wadia Institute of Himalaya Geology, Dehradun, India, 1980, pp291.

The Reason Why Planets And Moons Move In The Same Direction

Wang Taihai

Wenzhou Entry-Exit Inspection and Quarantine Bureau of the People's Republic of China
Address: Xingao Road, Aojiang town, Pingyang, Zhejiang, China 325401
Tel: +86 577 63193511, 63628702
Mobile: 13587886133
Fax: +86 577 63628702, 63638831
Email: ccibaj@wz.zj.cn; wth@wz.ziq.gov.cn

Abstract: The main features of our solar system are that all the planets revolve around the sun in the same direction, as do most of their moons, and all the planets lie more or less in the same plane of the sun's own rotation. For centuries scientists have tried to find a theory for the solar system origin that can explain these features. Any theory that could not explain these features was usually rejected. But through mechanical analysis, the author of this article found that these main features are not the result of our solar system's origin as most theories hypothesized but that of mechanics of their movement . The author found that if a planet does not revolve in the plane of the sun's own rotation and circle the sun counterclockwise, it will not be stable and its course will be deflected. The moving pattern of our solar system determines these main features. Only in this moving pattern can the solar system survive. [Academia Arena, 2009;1(1):43-46]. ISSN 1553-992X.

Keywords: the Sun, the Origin of the Solar System, the Coriolis Force

Up to now, theories for the origin of our solar system have tried to explain its main features that all the planets revolve around the sun in the same direction, as do most of their moons, and all the planets lie more or less in the same plane of the sun's equator. Most theories can explain these features well but can't adequately explain some other chemical or physical phenomena. In this article I will prove that these features are not the result of our solar system's origin but that of mechanics of their movement.

Through mechanical analysis, we will find that from whatever direction an alien celestial body intrudes upon our solar system, if it is captured by the sun or by a planet it will keep changing its orbit till it circles in the same direction and in the same plane as the already existing planets and moons do.

To simplify the discussion, let's take a look what will happen if the moon is not circling around the earth the way it does now. (Let's call the direction in which all the planets circle around the sun counterclockwise, with the opposite moving direction clockwise.)

Suppose the moon is orbiting the earth clockwise to start with, but because the earth/moon system is moving around the sun counterclockwise, the vertically moving moon will be deflected by the Coriolis force([1]) and its orbit around the earth will tilt rightward, eventually becoming a counterclockwise revolution. The Coriolis force will continue deflecting the moon until its orbit overlaps the plane of the sun's equator. Ultimately the moon will circle the earth counterclockwise in the plane of the earth's orbit as it almost does now.

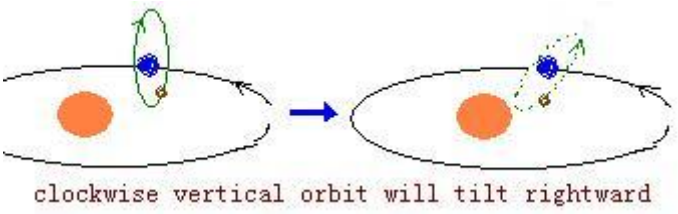

Now, let's suppose the moon's orbit around the earth is vertical to the plane of the earth's orbit and the direction is counterclockwise.

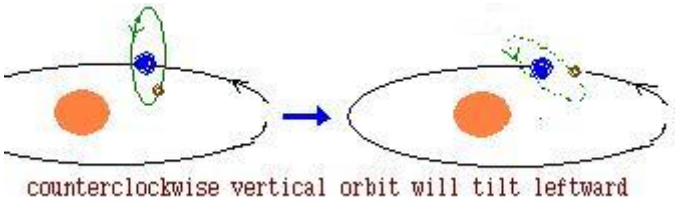

As illustrated above, the moon will be deflected by the Coriolis force and its orbit around the earth will tilt leftward to become counterclockwise around the earth eventually, too. The Coriolis force will continue deflecting the moon until its orbit overlaps the plane of the sun's equator completely. Ultimately the moon will also circle the earth counterclockwise in the plane of the earth's orbit.

Then, what if the moon was captured but clockwise by the earth right in the plane of the sun's equator to start with? By mechanical analysis, we can see that in this situation either the moon will collide with the earth or its orbit be distorted to become counterclockwise.

We know that when the moon moves around the earth, it is also moving around the sun. Between the moon and the earth, their masses, gravitational force, distance and the moon's relative orbital velocity to the earth must meet the Newton's law of universal gravitation and the circular motion principles. In addition, between the moon and the sun, their masses and motion parameters must also meet the Newton's law of universal gravitation and the circular motion principles. The relative orbit velocity of the moon can be calculated with the following formula.

$$V = \sqrt{\frac{F \cdot R}{m}}$$

Where:
V -the relative orbital velocity of the moon
F -the resultant force that dominates the moon's motion
R -the distance between the moon and the sun or the earth
m -the mass of the moon.

To simplify the problem, let us take four representative points A,B,M and N in the moon's orbit for analysis. When the moon is at point M or N, its relative orbit velocity to the sun is the same as that of the earth. As the moon moves clockwise further to point A, its relative orbit tangential velocity to the sun increases to the highest, but the forces from the sun and the earth are in opposite directions so that the resultant force (F) on the moon is at a minimum. Now the moon is at a minimum distance to the sun (R), too. According the equation above, the moon should have a minimum relative orbital velocity to the sun (V). But the actual value is at maximum.

When we take point B for analysis, we will also find the inconsistence where the moon should have a highest relative velocity to the sun but the actual value is the lowest.

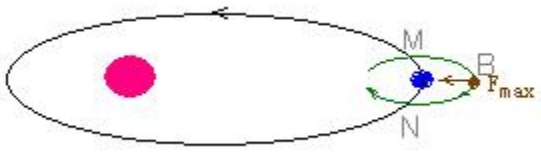

From the above analysis, we can see if a moon runs but clockwise around a planet, its orbit would not be stable. By further analysis we can see its orbit will be elongated to a narrow strip by and by and the collision possibility between the moon and its planet is very high or is inevitable.

However a moon comes to be captured by a planet, the moon can only move stably around the planet counterclockwise, the same as the way our moon is moving around the earth.

The above analysis accounts not only for the orbits of the moons around their planets but also accounts for the planets' orbit and the periodic comets around their suns. The principle is the same. The sun is moving around the Milky Way Galaxy center at a very high relative velocity. Any captured planet or periodic comet that doesn't move within the plane of the sun's equator will be deflected by the Coriolis force and be made to run counterclockwise around the sun within its equator plane. So the main features that the planets all revolve around the sun in the same direction, as most of their moons do, and the planets all lie more or less in the same plane of the sun's own rotation are not the result of the formation of the solar system, but is the result of the dynamics of our solar system.

Notes:

(1) Coriolis force is a sidewise force exerted on a body when it moves in a rotating reference frame. It is a fictitious force because it is a by-product of measuring coordinates with respect to a rotating coordinate system as opposed to an actual push or pull.

PS

1. Some are suspicious of the Coriolis Force effect, and argued with me on Coriolis Force fiercely. So I reexplain my point in another way. Take the second illustration for example.

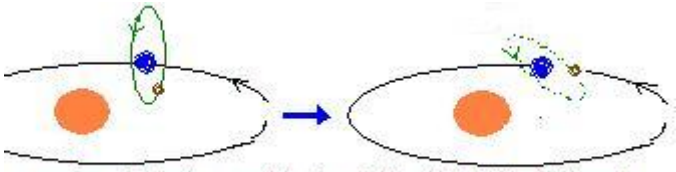

Let's see what will happen if the moon circles the earth freely in a counterclockwise polar orbit.

When the moon is right over the earth's north pole, its velocity (V) relative to the sun is the same as that of the earth because they are at the same orbital distance to the sun. Now the moon circles in, its centripetal force (F) to the sun is reduced. Why, because part of it is balanced off by the earth on the opposite side. On the other hand, its distance to the sun (R) is shortened now. Now let's use the formula

$$V = \sqrt{\frac{F \cdot R}{m}}$$

The F and the R are both reduced, but its velocity is the same as the earth's. So once the moon moves in between the Sun and the Earth, the moon will have redundant velocity and will go faster than required by the F and R.

A track and field athlete knows this principle well. The lead runner always occupies the innermost tack while turning so he can keep himself ahead of the others.

Now the moon is in the inner track and with the same relative velocity to the sun, it will surpass the earth. Thus moon's orbit changes.

When the moon is ahead of the earth, universal gravitation force between the moon and the earth, and that of between the moon and the sun will apply a resultant force that will slow the moon down; Only when the speed of the moon is reduced by this among can the V, F and R in the above formula be satisfied.

2. I make a summary of what my article already provided, what my article is expected to provide, and what I can further provide. I just don't want to disappoint all the visitors here.

-It provides a new idea(the Reason Why planets and Moons Move in the Same Direction) on an old topic.

-It provides a laconic deduction.

-It provides a qualitative analysis.

-It is expected to provide detailed deduction on the origin of the solar system, including how the sun, the planets and their moons formed, what were they before they became spheres...

-It is expected to present the reasoning mathematically.

quantitative analysis is expected.

-My specialty is not math, physics, or cosmology. And I am not in research. So it's not easy for me to present quantitative analysis if I get no help from competent scholars. Aware of my weakness, I deliberately chose this title for my article. I think my article can be considered as a complete thesis for the title I use(the Reason Why planets and Moons Move in the Same Direction) .

-If you ask me how the birth of suns, their planets and moons come about, it's out of the topic that I want to discuss. As Darwin told us the reason why polar bears are white, but should you censure him for not answering the question why there are white polar bears on earth? Those are two different topics.

-In my reasoning, I must simplify all the complicated systems so that I can reason it with my brain, or I will have to recourse to the advanced theories or complicated formulas which are beyond my competence.

-So, what I have provided and that I would provide are all basically qualitative analysis, just as Copernicus did when he discovered our solar system is solar-centric, but gave no equation to show how that is achieved.

I do hope my work can be further carried on by competent scholars in quantitative ways.

The Contact information of the Author:

Mr. Wang Taihai
Wenzhou Entry-Exit Inspection and Quarantine Bureau of the People's Republic of China
Address: Xingao Road, Aojiang town, Pingyang, Zhejiang, China 325401
Tel: +86 577 63193511, 63628702
Mobile: 13587886133
Fax: +86 577 63628702, 63638831
Email: ccibaj@wz.zj.cn; wth@wz.ziq.gov.cn

Date: 2005-7-18

Distribution and Sources of Organochlorine Pesticides (OCPs) in Karst Cave, Guilin, China

Annette Sylvie Muhayimana [1*], Qi Shihua [1]*, Wang Yinghui [1], Kong Xiangsheng [1], Odhiambo Joshua Owago [1], Zhang Junpeng [1]

(1) Department of Environmental Engineering, Faculty of Environmental Studies,
Key Laboratory of Bio and Environmental Geology of Ministry of Education, China University of Geosciences, Wuhan, Hubei 430074, China

Abstract: Despite the numerous researches done on Organochlorine pesticides (OCPs) in China and in the world, information regarding emissions and concentrations of OCPs in Karst caves is extremely limited. Karst areas have much higher ecological vulnerability and are so easy to be contaminated. This paper presents results of a monitoring program conducted in Dayan cave, Guilin, China that was designed to characterize levels, trends and sources of pesticides in soil (sediment) samples. Thirteen soil samples were collected and OCPs were analysed. Inside the cave a total concentration of OCPs (∑OCPs) detected was 29.659 ng /g with a mean value of 3.295 ng /g and ∑OCPs detected outside the cave was 74.108 ng /g with a mean value of 18.527ng/g. ∑OCPs outside the cave was higher than ∑OCPs outside the cave. The concentration of Chlordane in OCPs was highest among all the OCPs detected with range of 0.12─13.253ng/g and mean value of 3.93 ng /g. The next compound with high level of concentration was Heptachlor which ranged from Non-detected (ND) to 2.465 ng/g with a mean value of 1.4 ng/g. The pollution of OCPs in soil comparing with other countries and other areas in China was light. The analysis of Dichlorodiphenyltrichloroethane (DDT) and Hexachlorocyclohexane (HCH) isomers showed that there was fresh input of Dicofol and Lindane in the study area. By calculating the ratios of Dichlorodiphenyldichloroethane (DDD) to Dichlorodiphenyldichloroethylene (DDE), it was found that the degradation of DDT outside the cave was aerobic and the degradation of DDT inside the cave was anaerobic. [Academia Arena, 2009;1(1):47-56. ISSN 1553-992X].

Key words: Organochlorine pesticides, Karst cave, Soil, Guilin, China.

1. Introduction

Organochlorine pesticides are a group of persistent organic pollutants (POPs) which are to be eliminated or reduced on their release into the environment in many countries. Because of their persistence in the environment, and biological accumulation through the food web, OCPs can cause environmental damage, and affect human health (Colborn et al, 1996) .Due to their volatility and persistence in the air; OCPs are subjected to long-range atmospheric transport (LRAT). Therefore, OCPs released in the tropical and subtropical environments could be dispersed rapidly through air and water, and tend to be redistributed on a global scale (Tanabe, 1991) .The origin and fate of OCPs in soils with different land use have been extensively studied in many countries. Although the usage of OCPs was phased out for decades, the elevated concentrations were still observed in many agricultural soils (Harris et al., 2000) and the relationship between sites of greatest application and current residue levels was found strong (Shivaramaiah et al., 2002). The release of OCPs from soils continues to be a source of OCPs pollution to the environment (Meijer et al., 2001).

China is a large producer and consumer of Pesticides in the world (Rongbing et al., 2006). Large amount of OCPs were used in past decades to sustain over population in China. HCH and DDT were widely used in China from 1952-1983. Although their use had been discontinued in China since 1983, their persistence has left residual amounts in the soil in many areas (Zhao Ling and Ma Yongjun, 2001). At present the use of DDT is still allowed to control mosquitoes, particularly in the malarial transmission zones in China (Zhang et al., 2005). Accordingly, China still produces a small amount of DDT and China is also allowed to export DDT to other countries for the same purpose. This paper presents the current status of OCPs residues in Dayan cave (Karst cave).

2. Materials and Methods

2.1 Study Area

Region of research was in Guilin located in Guangxi Zhuang Autonomous Region in southeast China.Guangxi province (Southeast of China). The Geographical coordinates are 25° 40' 25" North, 108° 44' 0" East and has an altitude of 150m. It is bounded to the north-east by Hunan province, to the south-east by Hezhou town and it is next to Guangdong province. It has a surface area of 27, 800 square kilometers and a population of 4.76 million.

Dayan is an intermediate upper layer cave of Guilin Maomoatou cave system, located in the middle part of Guangming Mountain at right side of Taohua River in the north-west of Guilin. Guangming Mountain is a large peak cluster in Fenglin Plain, with an area of 0.92km^2, the highest peak altitude of 404.4m and the plain altitude of 151 m.The outcrop is a thick limestone layer of the Devonian system with a high intensity of Karst process. Dayan is a noncommercial karst cave located northeast to Ludiyan cave. The map of Guangxi showing Guilin and plane diagram of Dayan cave are shown in Fig 1 and Fig 2 respectively.

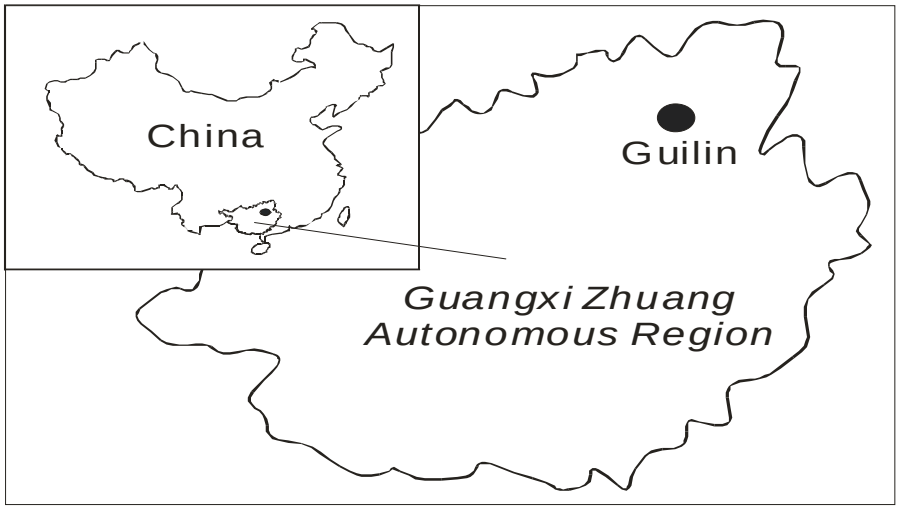

Fig 1: Map of Guangxi province showing Guilin

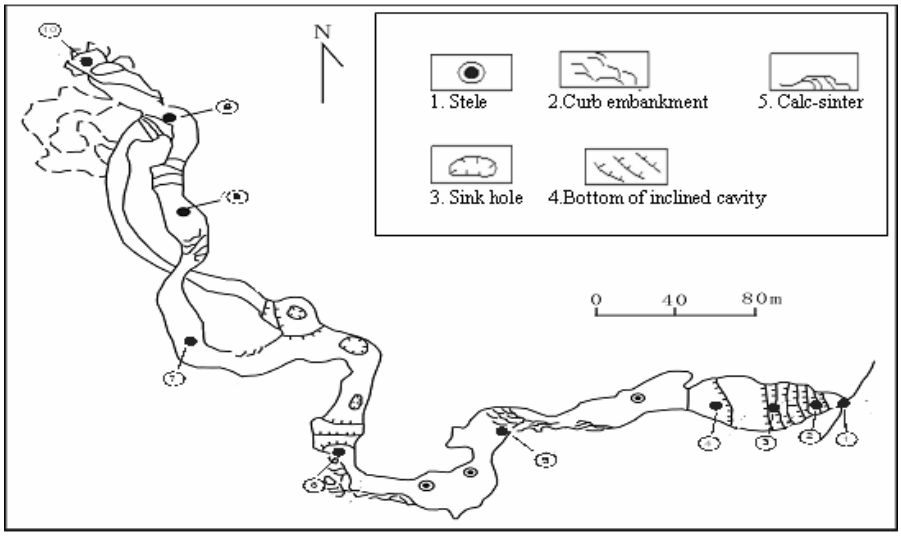

Fig 2: Map of Dayan Cave showing sampling locations (1 to 10) are sampling locations

2.2 Soil sampling

Ten sampling locations were chosen inside the cave that followed the horizontal section from the east gate as shown in Fig 2. Sampling location 1 was at the east gate (outside the cave) and the serial number was from 1 to10. Three samples (1', 2', and 3') were also taken outside the east gate. Nine samples were obtained inside the cave (2 to10) and 4 samples outside the cave (1, 1', 2', and 3'). Sampling was done with the use of a hand shovel. The weight of each sample collected was 500g. After the collection of samples, they were kept frozen prior to the commencement of the laboratory analysis.

2.3 Analysis

2.3.1 Experimental procedures

Before analyising the samples (before experiment) all glass wares were acid washed and cleansed with distilled water before they were dried in the oven at 200^{o}C for about four hours. Reagents used for the experiment included: dichloromethane (DCM), hexane, acetone, sodium sulfate, alumina gel (100-200 mesh), silica gel (100-200 mesh), mesh hydrochloric acid and vitriol. Filter paper, aluminium foil, absorbent cotton and active copper were also used as materials.

Mixed standard sample of OCPs [2,4,5,6-tetrachloro-m-xylene (TCMX) and decachlorobiphenyl (PCB 209)] were used as surrogate standards and were added to all the samples before the extraction. The whole process of pretreatment was based on US EPA SW-8080A method as reference. 20 g of the sample were weighed with electronic balance and injected with the surrogate (using a syringe) before the sample was Soxhlet-extracted for 48 hours with redistilled Dichloromethane (DCM). Active copper slices were added to the conical flask containing DCM to eliminate the influence of sulphur contained in the sample. After 48 hrs in the soxhlet extractor, the extracted samples were added with Sodium sulphate ($NaSO_4$) to remove unwanted water. After that, the solvents were concentrated to about 5 ml and then passed though a mixture of silica gel and alumina gel (10/3, V/V) for purification and it was rinsed by a mixture of DCM and hexane (2/3,V/V). The solvent was then condensed with high purity Nitrogen. 4 ml of the hexamethyl-benzene and PCNB (5ppb) were added as internal standards to help in quantifying the amount of OCPs present in the samples. Finally samples were stored and kept in the refrigerator until next analysis (Analysis by HP 6890 GC).

2.3.2 Analysis by HP 6890 GC

HP 6890 GC (Gas Chromatography) was equipped with a ^{63}Ni electron capture detector and a 30 m x 0.32 mm i.d (0.25 *lm* film thickness) DB-5 fused silica capillary column. Nitrogen was added as a carrier gas at 1.2ml/min. the oven temperature was kept at 40^{o}C for 5 minutes and increased to 290^{o}C at a rate of 4^{o}C/min. Injector and detector temperatures were maintained at 250 and 300^{o}C respectively. 2 Microliters (µl) of each sample was injected for analysis.

2.3.3 Quality control and Quality assurance (QC/QA)

Quality control and Quality assurance was made by the use of the US EPA method in the process of the experiment. Method blanks (solvents), duplicate samples, and spiked blanks (standards spiked into solvent) were analyzed. In addition, surrogate standards were added to each of the samples to monitor procedural performance and matrix effects. The concentrations of OCPs were corrected for the recovery ratios for the surrogates. The recovery ratios for the surrogates in the samples conform to the reported ranges by US EPA. The recovery rates and standard deviation of OCPs during separation and testing are within the limiting value of the US EPA 610 method. Recovery rates of TCMX and PCB209 are 69±6% and 76±7% respectively.

3. Results and Discussions

3.1 Concentration and distribution of OCPs

A summary of concentrations of OCPs detected in soil samples of Dayan cave is shown in Table1. Inside the cave ∑OCPs detected was 29.659 ng /g with a mean value of 3.295 ng /g and ∑OCPs detected outside the cave was 74.108 ng /g with a mean value of 18.527ng/g. ∑OCPs outside the cave is higher than the total concentration outside the cave (Fig 3).

The levels of OCPs outside the cave compared to the levels inside indicated that despite the relatively closed environmental system of the cave and less human interference inside the cave, it still had OCPs contamination due to air transfer, rain water filtration and other processes, but the degree of contamination was not high.

Table 1. Levels of OCPs in soil samples of Dayan Cave

	OCPs overall level range Min—Max(mean value）	OCPs level range inside the cave Min—Max(mean value) （2 to 10 samples）	OCPs level range outside the cave Min—Max(mean value) （1，1′，2′，3′ samples）
α-HCH	0.014—0.170 (0.087)	0.014—0.126(0.043)	0.095—0.170(0.130)
β-HCH	0.026—0.219 (0.102)	0.026—0.219(0.087)	0.100—0.138(0.117)
γ-HCH	0.015—0.285 (0.092)	0.015-0.180(0.044)	0.075—0.285(0.140)
δ-HCH	0.009—0.072 (0.034)	0.009—0.045(0.024)	0.020—0.072(0.044)
TC	0.021—6.119 (1.841)	0.021—1.674(0.279)	3.226—6.119(3.403)
CC	0.085—7.134 (2.221)	0.101—3.111(0.849)	3.899—7.134(4.198)
Hep	ND—2.465 (1.399)	ND—1.087(0.139)	1.871—2.465(1.632)
Hep-Epo	ND—1.908 (0.911)	ND—1.022(0.379)	1.000—1.908(1.185)
EndoI	ND—0.230 (0.067)	ND—0.040(0.021)	0.103—0.230(0.122)
EndoII	ND—0.161 (0.046)	ND—0.057(0.021)	0.026—0.161(0.080)
Endosulfate	0.030—0.500 (0.175)	0.030—0.180(0.086)	0.200—0.500(0.294)
p,p'-DDE	0.011—0.342 (0.108)	0.011—0.109(0.041)	0.115—0.342(0.174)
p,p'-DDD	ND—0.121 (0.079)	ND—0.077(0.038)	0.011—0.121(0.059)
o,p'-DDT	0.049—0.467 (0.212)	0.049—0.226(0.113)	0.302—0.467(0.310)
p,p'-DDT	ND—0.090 (0.031)	ND—0.039(0.011)	0.046—0.090(0.050)
ΣDDTs[b]	0.094—0.875 (0.371)	0.094—0.384(0.162)	0.532—0.875(0.434)
ΣHCHs[a]	0.100—0.665(0.269)	0.100—0.453(0.197)	0.313—0.665 (0.430)
ΣOCPs[c]	1.159—23.625(10.911)	1.159—11.180(3.295)	13.250—23.625(18.527)

ND=Non- detected

ΣHCHs[a]= α-HCH + *β*-HCH + *δ*-HCH + *γ*-HCH.

ΣDDTs[b]= *p, p'*-DDE + *p, p'*-DDD + *o, p'*-DDT + *p, p'*-DDT.

ΣOCPs[c] =ΣHCHs+ΣDDsT+Σother OCPs.

Σother OCPs = Heptachlor (Hep) + Heptachlor epoxide (Hep-Epo) + TC (Trans-Chlordane) + CC (Cis-Chlordane) +EndoI (*α*- Endosulfan) +EndoII (*β*-Endosulfan) +Endosulfate.

The concentration of Chlordane (TC+CC) in OCPs was highest among all the OCPs detected inside and outside the cave with a total concentration of 39.689ng/g and mean value of 9.92 ng /g inside the cave and a total concentration of 4.52 ng/g outside the cave with a mean value of 1.13 ng /g.

This is because South china have been using Chlordane to kill termites, so the high concentration of Chlordane observed may be predominantly due to the use of technical Chlordane as a termiticide in this area in previous years . In China, technical chlordane is still being extensively used against termites in buildings, with an estimated amount of over 200 tons year^{-1} in recent years (Xu et al., 2004).

The next compounds with highest levels of concentration were Heptachlor (Hep) and Heptachlor epoxide (Hep-Epo.) Heptachlor (Hep) was also used and produced in large quantity in China. From 1967 to 1969 the amount of Heptachlor produced was 17 tons, to kill the termites and other insects in the soil. It is shown in Fig 4 that the majors parts of OCPs (HCHs and DDTs) at the cave's innermost sampling locations 9 and 10 did not show the lowest values, but rather slightly greater than the values of sampling locations 7 and 8 at the middle of the cave. This suggests that there may be a fracture pore near the north mouth that allows some air to come in.

Fig 4 shows that the total concentration of DDTs (∑DDTs) in soil samples was higher than the total concentration of HCHs (ΣHCHs). This trend is consistent with the previous observations on the contamination of OCPs in soil in China (Zhou et al., 2001). A most likely explanation for the current low concentration of HCHs in soil is due to the difference in the physicochemical and biochemical properties, wherein HCHs have higher water solubility, vapor pressure and biodegradability, and lower lipophicility

and particle affinity compared to the DDTs (Rui et al., 2005). DDTs tend to remain in the particulate phase longer than HCHs. (Nhan et al., 2001).

In comparison with recent research reports, the concentrations of ∑DDTs and ∑HCHs measured in the study area were in the same low range with other pristine areas such as Tibet plateau where the concentration of ∑DDTs ranged from ND to 2.83 ng/g and ∑HCHs ranged from 0.18 to 5.38 ng/g (Fu et al., 2001), and European high altitude mountains that had ∑DDTs and ∑HCHs residual level in the range of 1.7-13 ng/g and 0.08-0.49 ng/g respectively (Grimalt et al., 2004).

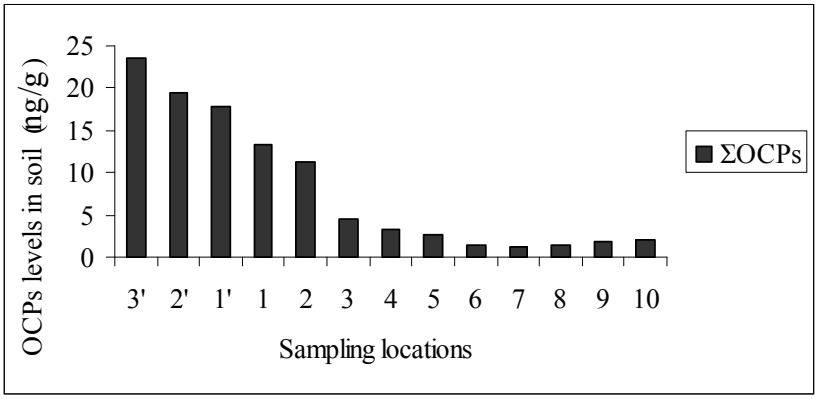

Fig 3: Distribution of ΣOCPs in soil of Dayan cave

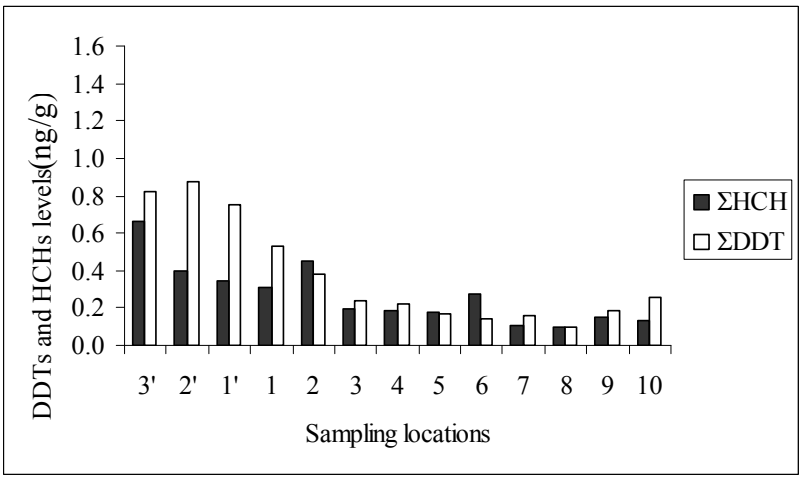

Fig 4: Distribution of ΣHCHs and ΣDDTs in soil of Dayan cave

The average concentration outside the cave and inside the cave of ∑DDTs and ∑HCHs was lower than the average concentration of ∑DDTs and ∑HCHs in Hong Kong soils which was 0.52 ng/g and 6.19ng/g respectively (Zhang et al, 2006), and they were much lower than the average concentrations of ∑DDTs (37.6 ng/g) and ∑HCHs (12.2 ng/g) found in soils of Pearl River Delta Region (Fu et al., 2003). Some other studies reported around China, had higher residual levels of OCPs such as Beijing (Zhu et al, 2005), Tianjin (Tao et al., 2005), Nanjing (An et al., 2005). In Europe, ΣDDTs and ΣHCHs levels were in the range of 4.3-2400 ng/g and 0.36-110 ng/g in Poland soils (Falandysz et al., 2001). In comparison with similar research the levels of OCPs in Guilin were low and the reason is because there are mainly rice farms in the vicinity of Guilin city in which small amounts of OCPs were used with the rotary method of planting rice. The existence of alternating wet and dry conditions was beneficial to the aerobic and anaerobic degradation of OCPs, leading to a reduced amount of soil OCPs.

3.1.1 Distribution and degradation of HCH isomers

It has been widely recognized that HCH is available in two formulations: technical HCH and lindane. Technical HCH contains isomers in the following percentages: α, 55–80%; β, 5–14%; γ, 8–15%; δ, 2–16%; ε, 3–5% (Qiu et al., 2004), and Lindane contains > 90% of γ-HCH. The ratio of α- to γ-HCH has been used to identify the possible HCH source. If the source of HCH comes from fresh input of technical HCH, the ratio of α - to γ -HCH is between 3 and 7 (Yang et al., 2008). However, a lindane source will reduce the ratio to close or <1 (Willet et al., 1998). A higher ratio of α - to γ -HCH than 7 can be explained by long-range transport or re-cycling of technical HCH, because α -HCH has a longer atmospheric lifetime than γ isomer by about 25% (Willet et al., 1998). As shown in Fig 6, the ratios of α-HCH/γ-HCH in all soil sampling locations were lower than 3. Accordingly, the contamination of HCHs in this region probably came from local use of lindane and also indicated Lindane inputs in the past several years.

By analyzing the individual HCH isomers (Fig 5), it was found that β-HCH had the highest level of concentration among all the samples and it accounted from 20.03-79.13 %, especially in sample 3 to 7 where it accounted from 23-79% of the total HCHs detected. The β-HCH was higher because of its persistence in soil. The persistence of β-HCH in soils is mainly due to the higher K_{ow} (log K_{ow} =3.78) and lower vapor pressure value ($3.6x10^{-7}$ mmHg, 20°C) (Zhang et al., 2006). These will make β-HCH easier to be absorbed to the soil organic matter and less evaporative loss from soils (Mackay et al., 1997). Furthermore, the spatial arrangement of Chlorine atoms in the molecular structure of β-HCH was supposed to be more resistant to microbial degradation in soils (Middeldorp et al., 1996).

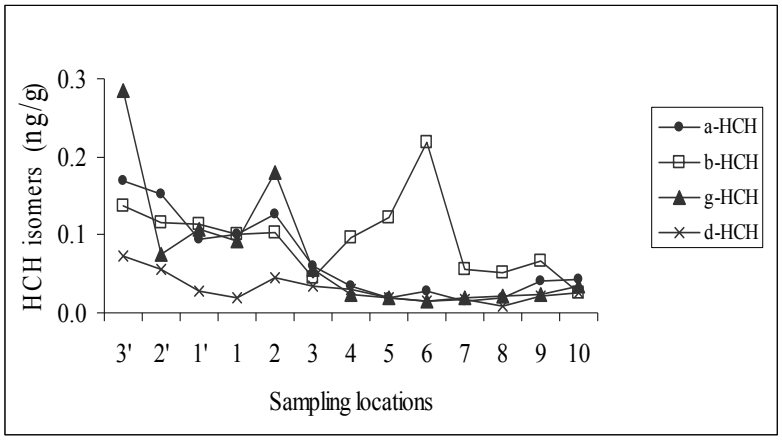

Fig 5: HCH isomers in soil of Dayan cave

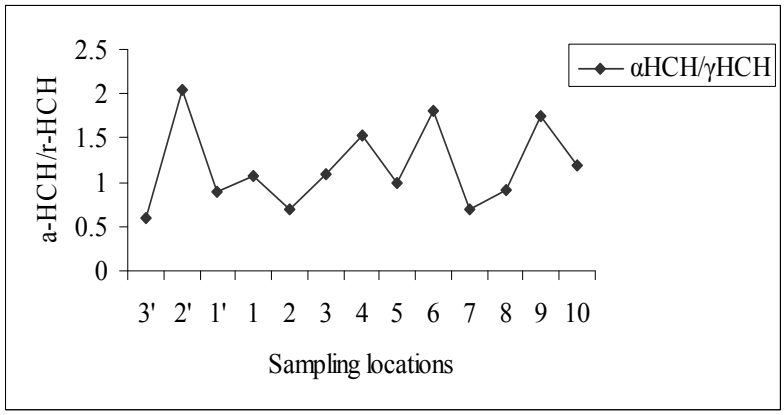

Fig 6: Ratios of α-HCH to γ-HCH in soil of Dayan cave

3.1.2 Distribution and degradation of DDT isomers

Commercial DDT generally contains 75% *p,p'*-DDT, 15% *o,p'*-DDT, 5% *p,p'*-DDE, <0.5% *p,p*'-DDD, <0.5 *o,p'*-DDE and <0.5% of unidentified compounds (WHO, 1979), but in Dicofol, the concentration of *o,p'*-DDT is more than *p,p*'-DDT (Qiu et al., 2005). DDTs isomers have a long persistence in the environment and their levels of concentrations in this study are shown in Fig.7. DDT can be biodegraded under aerobic conditions to DDE and under anaerobic conditions to DDD (Bossi et al., 1992). The ratio of DDD/DDE greater than 1 indicates that the soil was dominated by DDD, the product of anaerobic degradation of DDT, and the ratio lesser than 1 indicates that the soil was dominated by DDE, the product of aerobic degradation of DDT (Zhou et al., 2006). DDE and DDD Changes in the ratio of DDE and DDD to ΣDDTs has been regarded as an indication of either no or decreasing inputs to the environment. The ratio of (DDE+DDD)/ΣDDTs greater than 0.5 can be thought to be subjected to a long term weathering (Dong et al, 2002) and More *o*, *p*′-DDT than *p*, *p*′-DDT in the environment can demonstrate the Dicofol type DDT usage (Qiu et al., 2004).

The ratios of (DDE+DDD)/ ΣDDTs are shown in Fig.9. The ratios were in the range of 0.26-0.61 with most values being less than 0.5 (mean value is 0.4) and in Fig.7 it is shown that the concentration of *o,p'*-DDT was more than the concentration of *p,p'*-DDT as in Dicofol, this suggests that there was fresh input of Dicofol in the study area. Also, most values of DDD/DDE ratios as shown in Fig. 8 were greater than 1 inside the cave and ranged from 0.092 to 7 with an average value of 2.31, and the ratios of DDD/DDE outside the cave ranged from 0.052 to 0.53 with an average value of 0.35.

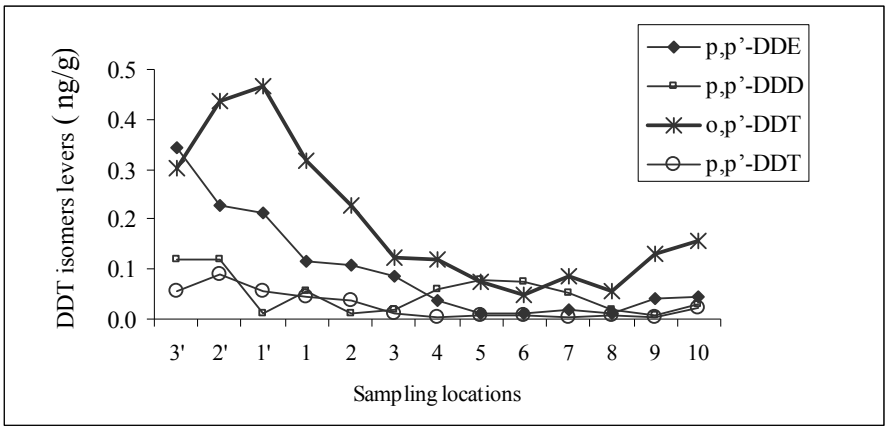

Fig 7: Distribution of DDT isomers in soil of Dayan Cave

The results obtained clearly indicated that DDT in soil inside and outside of the Dayan cave may be derived from Dicofol and DDT was retained under anaerobic conditions inside the cave and under aerobic condition outside the cave.
The use of Dicofol in China is mainly in the southern and eastern provinces, mostly on litchi, longan, citrus crops and cotton (Yang et al., 2008).

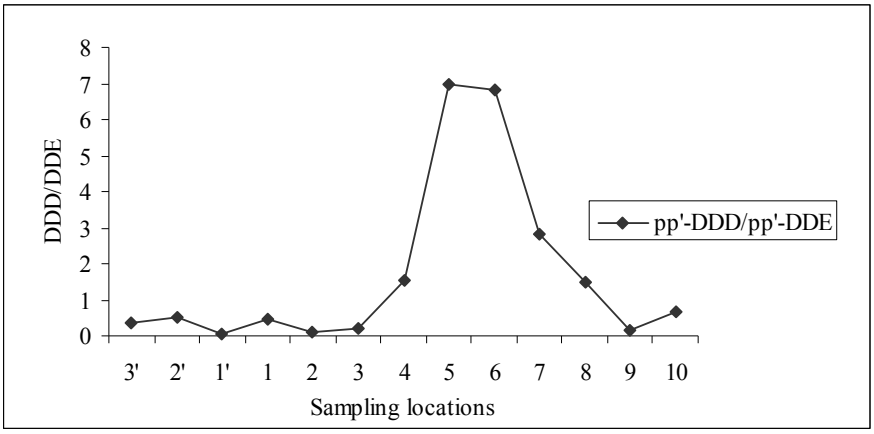

Fig 8: Ratios of DDD/DDE in soil of Dayan Cave

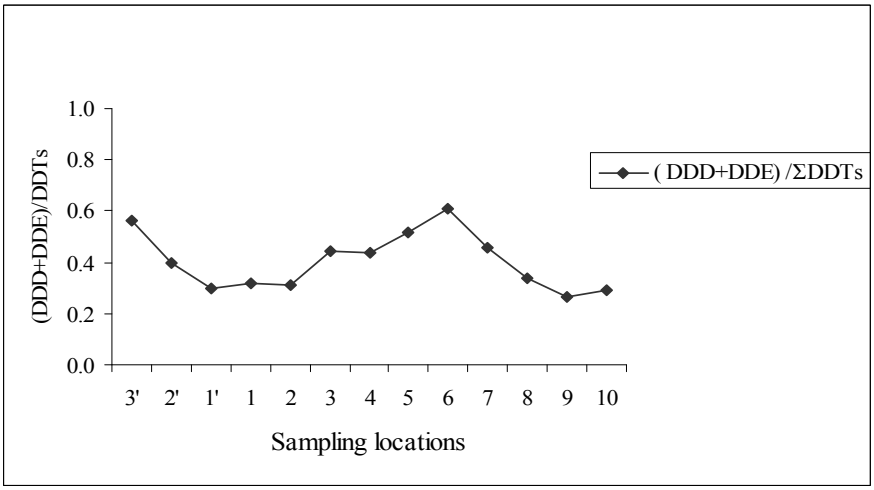

Fig 9: Ratios of (DDD + DDE)/ ΣDDTs in soil of Dayan cave

4. Conclusion

The use of HCHs and DDTs in China has been banned for 20 years and this sanction resulted in a tremendous decrease of OCPs concentrations in soils of Dayan cave. The residual levels of OCPs in soils outside Dayan cave were less than corresponding national values and among all the OCPs detected the concentration of chlordane and heptachlor were highest because they have been used in the study area.

ΣDDTs and ΣHCHs in soil inside the cave were low in comparison with worldwide background mountains and polar regions. As conclusion the pollution of OCPs in the soils inside and outside Dayan cave was light. The analysis of isomers of DDTs and HCHs showed that there is fresh use of Dicofol and Lindane respectively in the study area. DDT degradation outside the cave was aerobic while inside the cave the degradation of DDT was anaerobic.

Acknowledgement

The authors wish to pay tribute to the referenced authors .This study discusses their work, but the views expressed are those of authors and do not represent those of the referenced authors.

Corresponding to:
Annette Sylvie Muhayimana
Department of Environmental Engineering
Faculty of Environmental Studies,
Key Laboratory of Bio and Environmental Geology of Ministry of Education,
China University of Geosciences, Wuhan, Hubei 430074, China
E-mail: teteli2001@yahoo.com

Qi Shihua
Department of Environmental Engineering
Faculty of Environmental Studies,
Key Laboratory of Bio and Environmental Geology of Ministry of Education,
China University of Geosciences, Wuhan, Hubei 430074, China
E-mail: shihuaqi@cug.edu.cn

References

1. An, Q., Dong, Y.H., Wang, H., 2005. Residues and distribution character of organochlorine pesticides in soils in Nanjing area. Acta Scientiae Circumstantiae, 25, 470-474.
2. Bossi, R., Laesen, B., Premazze, G., 1992. Polychlorinated biphenyl congeners and other chlorinated hydrocarbons in bottom sediment cores of lake Garden (Italy), Sci. Total Environ., 121, 77–93.
3. Colborn, T., Dumanoski, D., Myers, J.P., 1996. Our Stolen Future. Dutton, New York, USA.
4. Doong, R.A., Peng, C.K., Sun, Y.C., Liao, P.L., 2002.Composition and distribution of organochlorine pesticide residues in surface sediments from the Wu-Shi River estuary, Taiwan. Mar. Pollut. Bull., 45, 246–253.
5. Falandysz, J., Brudnowska, B., Kawano M., 2001. Polychlorinated Bi-phenyls and Organochlorine Pesticides in Soils from the Southern Part of Poland. Arch. Environ Contam. Toxicol., 40:173-178
6. Fu, J.M., Mai, B.X., Sheng , G.Y., Zhang, G., Wang, X.M., Peng, P.A., Xiao, X.M., Ran, R., Cheng, F.Z., Peng, C.Z., Wang, Z.S., Tang, U.W., 2003. Persistent organic pollutants in environment of the Pearl River Delta, China: an overview. Chemosphere, 52, 1411-1422.
7. Fu, S., Chu, S.G., Xu, X.B., 2001. Organochlorine pesticide residue in soils from Tibet, China. Bull. Environ. Contam. Toxicol., 66, 171–177
8. Grimalt, J .O., Drooge, B .L., Ribes, A., Vilanova, R. M., Fernandez, P., Appleby, P., 2004. Persistent organochlorine compounds in soils and sediments of European high altitude mountain lakes. Chemosphere, 54 (10): 1549
9. Harris, M.L., Wilson, L.K., Elliott, J.E., Bishop, C.A., Tomlin, A.D., Henning, K.V., 2000. Transfer of DDT and metabolites from fruit orchard soils to American Robins (Turdus migratorius) twenty years after agricultural use of DDT in Canada. Arch. Environ. Contam. Toxicol., 39, 205–220.
10. Mackay, D., Shiu, W.Y., Ma, K.C., 1997. Illustrated Handbook of Physical-Chemical properties of Environmental Fate of Organic Chemicals, vol.V. Lewis Publishers, Boca Raton, FL.

11. Meijer, S.N., Halsall, C.J., Harner, T., Peters, A.J., Ockenden, W.A., Johnston, A.E., Jones, K.C., 2001. Organochlorine pesticides residues in archived UK soil. Environ. Sci. Technol., 35, 1989–1995.
12. Middeldorp, P.J.M., Jaspers, M., Zehnder, A.J.B., Schraa, G., 1996. Biotransformation of α-, β-, γ-, and *δ*- hexachlorocyclohexane under methanogenic conditions. Environ. Sci.Technol., 30, 2345-2349.
13. Negoita , T .G., Covaci ,A., Gheorghe, A., Schepens, P. , 2003.Distribution of polychlorinated biphenyls (PCBs) and organochlorine pesticides in soils from the East Antarctic coast. Journal of Environmental Monitoring, 5 (2):281-286.
14. Nhan, D.D., Carvalho, F.P., Am N.M., Tuan, N.Q., Yen, N.T.H., Villeneuve, J.P., 2001. Chlorinated pesticides and PCBs in sediments and molluscs from fresh water canals in the Hanoi region. Environ. Pollut., 112, 311-20.
15. Qiu, X.H., Zhu, T., Li, J., Pan, H.S., Li, Q.L., Miao, G.F., Gong, J.C., 2004. Organochlorine pesticides in the air around the Taihu Lake, China. Environ. Sci. Technol., 38, 1368-1374.
16. Qiu, X.H., Zhu, T., Yao, B., Hu, S.W., 2005. Contribution of Dicofol to current DDT pollution in China. Environ. Sci. Technol., 39, 4385-4390.
17. Rui, Q.Y., Gui, B.J., Qun, F.Z., Chun, G.Y, Jian, J.B.S., 2005. Occurrence and distribution of Organochlorine pesticides in Sediments collected from East China Sea. Environmental international, 31,799-804.
18. Shivaramaiah, H.M., Odeh, I.O.A., Kennedy, I.R., Skerritt, J.H., 2002. Mapping the distribution of DDT residues as DDE in the soils of the irrigated regions of Northern New South Wales, Australia using ELISA and GIS. J. Agric. Food Chem., 50, 5360–5367
19. Tanabe, S., 1991. Fate of toxic-chemicals in the tropics. Marine Pollution Bulletin, 22, 259–260.
20. Tao, S., Xu, F.L., Wang, J., Liu, W.X., Gong, Z.M., Fang, J.Y., Zhu, L.Z., Y.M. Luo, Y.M., 2005.Organochlorine pesticides in agriculture soil and vegetables from Tianjin, China. Environ. Sci. Technol., 39, 2494–2499.
21. Willett, K.L., Ulrich, E.M., Hites, S.A., 1998. Differential toxicity and environmental fates of Hexachlorocyclohexane isomers. Environ. Sci. Technol., 32(15): 2197-207
22. World Health Organization (WHO), 1979. DDTs and its derivations. WHO, New York.
23. Xu, D., Deng, L., Chai, Z., Mao, X., 2004. Organohalogenated compounds in pine needles from Beijing city, China. Chemosphere, 57, 1343–1353.
24. Yang, Y., Li, D., Mu, D., 2008. Levels seasonal Variations and sources of OCPs in ambient air of Guangzhou, China. Atmospheric Environment, 42, 677-687.
25. Zhang, H.B., Luo, Y.M., Zhao, Q.Z., Wong, M.H., Zhang, G.L., 2006. Residues of Organochlorine pesticides in Hong Kong soils. Chemosphere, 63, 633-641.
26. Zhang, H., Lu, Y., Dawson, R.W., Shi, Y., Wang, T., 2005. Classification and ordination of DDT and HCH in soil samples from the Guanting Reservoir, China. Chemosphere, 60, 762-769.
27. Zhao, L., Ma, Y., 2001. Effect of organic residues on soil environment. Soils, 33, 309-311.
28. Zhou, J.L., Maskaoui, K., Qiu, Y.W., Hong, H.S., Wang, Z.D., 2001.Polychlorinated biphenyl congeners and Organochlorine insecticides in the water column and sediments of Daya Bay, China. Environ Pollut., 113: 373-84
29. Zhou, R., Zhu, L., Yang, K., Chen, Y., 2006. Distribution of OCP's in surface water and Sediments from Qiantang River, East China. Department of Environmental Science, Zhejiang University.
30. Zhu, Y., Liu, H., L., Xi, Z., Cheng, H., Xu, X., 2005.Organochloline pesticides (DDTs and HCHs) in soils from outskirts of Beijing, China. Chemosphere, 60, 700-778.

Stem Cell and Renal Disease

Hongbao Ma *, ***, Shen Cherng **, Yan Yang ***

* Bioengineering Department, Zhengzhou University, Zhengzhou, Henan 450001, China, mahongbao@zzu.edu.cn, 01186-137-8342-5354

** Department of Electrical Engineering, Chengshiu University, Niaosong, Taiwan 833, China, cherngs@csu.edu.tw; 011886-7731-0606 ext 3423

*** Brookdale University Hospital and Medical Center, Brooklyn, NY 11212, USA, youngjenny2008@yahoo.com, 347-321-7172

Abstract: The renal disease is a common problem in human society. End-stage renal disease is a big heath problem in the United States and in all places of the world. Embryonic stem cells, pluripotent derivatives of the inner cell mass of the blastocyst, are the most primitive cell type likely to find application in cell therapy. Their potential to generate any cell type of the embryo makes them to be the most attractive stem cell therapy. It is possible to introduce stem cells into a damaged adult kidney to aid in repair and regeneration. Transdifferentiation offers the possibility of avoiding complications from immunogenicity of introduced cells by obtaining the more easily accessible stem cells of another tissue type from the patient undergoing treatment, expanding them in vitro, and reintroducing them as a therapeutic agent. Adult stem cells may possess a considerable degree of plasticity in the differentiation. Immunoisolation of heterologous cells by encapsulation creates opportunities for their safe use as a component of implanted or ex vivo devices. [Academia Arena, 2009;1(1):57-61]. ISSN 1553-992X.

Keywords: stem cell; renal; kidney; disease; treatment

1. Introduction

Stem cell is the origin of an orgnism's life. Stem cells have the potential to develop into many different types of cells in life bodies, that are exciting to scientists because of their potential to develop into many different cells, tissues and organs (Ma, 2005). End-stage renal disease (ESRD) is a big heath problem in the United States and it costs more than $30 billion each year on ESRD therapy in this country (Arnold, 2000; Mai et al., 2006; Ross et al., 2006). The patients suffering from acute renal failure (ARF) are even worse. ARF develops predominantly due to the injury and necrosis of renal proximal tubule cells (RPTCs) as a result of ischemic or toxic insult. The cause of death subsequent to ARF is generally the development of systemic inflammatory response syndrome. The disease state arising from renal failure is the result of many factors. It is important to reveal the kidney's role in reclamation of metabolic substrates, synthesis of glutathione, free-radical scavenging enzymes, gluconeogenesis, ammoniagenesis, hormones, growth factors, and the production and regulation of multiple cytokines critical to inflammation and immunological. There is considerable drive to develop improved therapies for renal failure (Mehta et al., 2007). It is estimated that there are over 2 million patients in USA who suffer from end-stage renal disease. About 60,000 patients in the United States are currently on the waiting list for a kidney transplant, and some patients have waited for several years before an appropriate donor can be found. Despite the advances in kidney transplantation, the shortage of donor organs limits treatment for the ESRD patients and requires many patients to remain on dialysis for extended periods of life time. The alternate methods has resulted in rapid progression of new approaches, such as therapeutic cloning and stem cell therapy (Berzoff et al., 2008; Sirmon, 1990).

Some of the most notable recent findings are as follows: (1) the 'stemness' profile may be determined by approximately 250 genes; (2) organ-specific stem-cell growth and differentiation are stimulated during the reparative phase following transient injury; (3) two bone marrow stem-cell types show a remarkable degree of differentiation potential; (4) some organs contain resident marrow-derived stem cells, and their differentiation potential may only be expressed during repair; (5) the metanephric mesenchyme contains pluripotent and self-renewing stem cells; (6) marrow-derived cells invade the kidney and differentiate into mesangial and tubular epithelial cells, and these processes are increased following renal injury; and (7) epithelial-to-mesenchymal transition generates renal fibroblasts (Oliver, 2004).

Cell therapy is dependent on cell and tissue culture methodologies to expand specific cells to replace important differentiated functions lost or deranged in various disease states. Cell-based therapeutics is the question of cell sourcing, and advance of stem cell research is powerful on the resolving of this problem. Stem cell is at present a great deal of speculation over the extent to which stem cell populations traditionally considered distinct may in fact be interchangeable. Stem cells can be self-renewal to differentiate into specialized cell types and they are classified as totipotent, pluripotent and multipotent. Progenitor cells are more lineage-restricted than stem cells but retain the proliferative capacity lacking in terminally differentiated cells (Lin et al., 1996).

Embryonic stem (ES) cells, pluripotent derivatives of the inner cell mass of the blastocyst, are the most primitive cell type likely to find application in cell therapy. Their potential to generate any cell type of the embryo makes them to be the most attractive stem cell therapy. However, the political and ethical debates surrounding the use of human ES cells make the application of stem cells complicated. These factors have combined to intensify the focus on. Neural stem cells (NSCs) are self-renewing, multipotent cells that generate the neuronal and glial cells of the nervous system. In mammals, contrary to long-held belief, neurogenesis occurs in the adult brain, and NSCs reside in the adult central nervous system (Taupin, 2006; Winkler, 2003).

It is possible to introduce stem cells into a damaged adult kidney to aid in repair and regeneration. Transdifferentiation offers the possibility of avoiding complications from immunogenicity of introduced cells by obtaining the more easily accessible stem cells of another tissue type from the patient undergoing treatment, expanding them in vitro, and reintroducing them as a therapeutic agent. Adult stem cells may possess a considerable degree of plasticity in the differentiation. However, the differentiation of stem cells is normally unresolved. Pluripotent cells can be derived from fibroblasts by ectopic expression of defined transcription factors. A fundamental unresolved question is whether terminally differentiated cells can be reprogrammed to pluripotency (Hanna et al., 2008).

Developing nephrons are derived from renal stem cells and transplantation of fetal kidneys may be thought of as a therapeutic stem cell application. There are two bioengineering programs with the aim of producing a device providing full renal replacement therapy in the short to medium term. Both employ biomaterial scaffold structures to overcome the as yet insurmountable difficulties inherent in marshalling cells into organized three-dimensional structures capable of coordinated filtration, resorption/meta-/catabolism/secretion, collection, and disposal of waste. Initial experiments involved adult rabbit renal cortex harvested and fractionated into glomeruli, distal, and proximal tubules, expanded separately in vitro, and seeded onto biodegradable polyglycolic acid sheets for subcutaneous implantation into syngenic hosts. The potential impact of advances in stem cell technology on all the prospective cell-based therapeutic approaches for the treatment of renal failure discussed above is enormous. The kidney has a dramatic capacity to regenerate after injury. Whether stem cells are the source of the epithelial progenitors replacing injured and dying tubular epithelium is an area of intense investigation. Many surviving renal epithelial cells after injury become dedifferentiated and take on mesenchymal characteristics. These cells proliferate to restore the integrity of the denuded basement membrane, and subsequently redifferentiate into a functional epithelium. An alternative possibility is that a minority of surviving intratubular cells possess stem cell properties and selectively proliferate after damage to neighboring cells. Some evidence exists to support this hypothesis but it has not yet been rigorously evaluated (Vigneau et al., 2007).

In recent years, it has been shown that functional stem cells exist in the adult bone marrow, and they can contribute to renal remodelling or reconstitution of injured renal glomeruli, especially mesangial cells, and hMSC found in renal glomeruli differentiated into mesangial cells in vivo after glomerular injury occurred (Wong et al., 2008).

2. Isolation of Kidney Stem Cells

It is difficult to find a definitive marker for kidney stem cells that makes it difficult to isolate and define kidney stem cells. However, kidney stem cells have been isolated from other organs using 4 different ways. For the first method, when the DNA of the cells is labeled with a marker such as bromodeoxyuridine, the cells retain the label for a long period of time. This label retention is used to identify and isolate stem cells. The second method references the side-population (SP) cells that extrude Hoechst dye through the activity of multidrug resistance proteins, which are part of the ATP-binding cassette transporter superfamily. The third method isolates kidney stem cells referencing specific cell surface markers that have been used to identify stem cells in other organs or the metanephric kidney. The markers used to isolate kidney stem cells include Oct-4, Nanog, CD24, CD133 and stem cell antigen-1

(Sca-1). The fourth method uses culture conditions that select stem cells in other organ systems (http://content.karger.com/produktedb/produkte.asp?typ=fulltext&file=000117311#SA4).

As Zheng et al described in 2008, any unique characteristic can be used to isolate a pure population of stem cell is still lacking. There is few specific biomarker found for epidermal stem cells alone, but epidermal stem cells and transient-amplifying cells share some biomarkers (Bickenbach, 2003) (Zheng, et al, 2008).

3. Culture of Renal Stem Cell

Shimony et al characterized a new model of renal, stromal and mesenchymal stem cell (MSC) matrix deprivation, based on slow rotation cell culture conditions (ROCK). This model induces anoikis using a low shear stress, laminar flow. The mechanism of cell death was determined via FACS (fluorescence-activated cell sorting) analysis for annexin V and propidium iodide uptake and via DNA laddering. Their results showed while only renal epithelial cells progressively died in STCK, the ROCK model could induce apoptosis in stromal and transformed cells; cell survival decreased in ROCK versus STCK to 40%, 52%, 62% and 7% in human fibroblast, rat MSC, renal cell carcinoma (RCC) and human melanoma cell lines, respectively. Furthermore, while ROCK induced primarily apoptosis in renal epithelial cells, necrosis was more prevalent in transformed and cancer cells [necrosis/apoptosis ratio of 72.7% in CaKi-1 RCC cells versus 4.3% in MDCK (Madin-Darby canine kidney) cells]. The ROCK-mediated shift to necrosis in RCC cells was further accentuated 3.4-fold by H(2)O(2)-mediated oxidative stress while in adherent HK-2 renal epithelial cells, oxidative stress enhanced apoptosis. ROCK conditions could also unveil a similar pattern in the LZ100 rat MSC line where in ROCK 44% less apoptosis was observed versus STCK and 45% less apoptosis versus monolayer conditions. Apoptosis in response to oxidative stress was also attenuated in the rat MSC line in ROCK, thereby highlighting rat MSC transformation. They concluded that the ROCK matrix-deficiency cell culture model may provide a valuable insight into the mechanism of renal and MSC cell death in response to matrix deprivation (Shimony et al., 2008)

Celprogen Company has human kidney stem cell derived from human adult and fetal kidney consented tissue. The following is the information and technique of the kidney stem cells:

(1) Positive markers: CD34, Nestin & CD133

(2) Morphology and proliferation: Mixed population of cells with approximately 70% attached cells and the other 30% in suspension; need to change cell culture media every day after 48 hours of initial cell culture or when the media starts changing color to slight yellow for pink. Fast growing cell culture. Change media with Celprogen's Human Kidney Stem Cell Complete Growth Media with the appropriate Human Stem Cell Extracellular matrix and tissue culture media for differentiation, expansion or maintaining stem cells in their un-differentiated stage. Temperature 370C in 5% CO2 humidified incubator.

(3) Subculturing:

A. Thaw the vial with gentle agitation in a 370C water bath or a dry 370C shaking incubator. For water bath thawing
B. keep the O-ring out of the water, thawing time 2-3 minutes.
C. Remove the thawed vial and wipe with 70% ethanol. Then transfer to the tissue culture hood.
D. Transfer the vial contents to a 15 ml sterile centrifuge tube, and gently add 7ml of pre-warmed Human Kidney Stem Cell Complete Media to the centrifuge tube. Use an additional 0.5 ml of Human Kidney Stem Cell complete media to rinse the vial and transfer the liquid to the centrifuge tube repeat this once more to ensure you have all the cells transferred to the 15 ml centrifuge tube. Add 1 ml of Human Kidney Stem Complete Media to bring the final volume to 10 ml in the 15 ml centrifuge tube.
E. Centrifuge the cells at 100 g for 5 minutes. Remove the supernatant and resuspend the cell pellet in 500 ul of Human Kidney Stem Cell Complete Growth Media.
F. Add the 500 ul of cells to T75 flask pre-coated with Human Kidney Stem Cell Extracellular matrix with 15 ml of Human Stem Cell Complete Growth Medium.
G. Incubate the cells in the T75 flask in a 370C in 5% CO2 humidified incubator. Perform 100% Media Change every 24 to 48 hours.
H. Medium renewal every day, and recommended sub-culturing ratio: 1:3.

(4) Freezing Medium: Human Stem Cell Complete growth Medium supplemented with 90% Fetal Bovine Serum with 10% DMSO.

(5) Storage temperature: liquid nitrogen vapor phase (San Pedro, CA 90731, USA, http://www.celprogen.com; http://ftp.celprogen.com/Technical_Resources/36100-27%20Human%20Kidney%20Stem%20cell%20data%20sheet.pdf.

In mice with cisplatin-induced acute kidney injury, administration of bone marrow-derived mesenchymal stem cells (MSC) restores renal tubular structure and improves renal function (Imberti et al., 2007).

4. Application of Kidney Stem Cells

Stem cell has powerful potential application purpose in science, medicine and industry, but it is also potentially danger for its enexpected plasticity. The evidence for bone marrow-derived stem cell contributions to renal repair has been challenged. The research and application for adult renal stem cells are also debated. The use of embryonic tissue in research continues to provide valuable insights but will be the subject of intense societal scrutiny and debate before it reaches the stage of clinical application. Embryonic stem cells, with their ability to generate all of kind of cell in living body, are great chance for our human civilization but have ethical and political hurdles for human use (Brodie and Humes, 2005). Stem cell research has attracted great attention because it could be used for the regeneration of damaged organs that are untreatable by conventional medical techniques, and stem cells (such as endothelial stem cells and neural stem cells) have been discovered to be practical useful in clinical applications. The potential for stem cell gene therapy has increased and many therapeutic applications have already been done. Chronic renal failure is a candidate for stem cell gene therapy. In the application of renal stem cell in medical treatment, mesenchymal stem cells could be transplanted, and in contrast, hematopoietic stem cells may be used for gene delivery for diseases, which need foreign cytokines and growth factors, such as glomerulonephritis. The stem cell gene therapy for chronic renal failure and the potential of the novel strategy and the major practical challenges of its clinical application are big targets for the stem cell researches (Yokoo et al., 2003). Ectopic expression of the human telomerase reverse transcriptase gene in human mesenchymal stem cells can reconstitute their telomerase activity and extend their replicative life-spans (Li, et al, 2007).

Discussion

Kidney is derived from the ureteric bud and metanephrogenic mesenchyme, and these two progenitor cells differentiate into more than 26 different cell types in adult kidney. The ureteric bud contains the precursor of the epithelial cells of the collecting duct and the renal mesenchyme contains precursors of all the epithelia of the rest of the nephron, endothelial cell precursors and stroma cells, but the relatedness among these cells is unclear. A single metanephric mesenchymal cell can generate all the epithelial cells of the nephron, indicating that the kidney contains epithelial stem cells. These stem cells also are present in the adult kidney. Embryonic renal epithelial stem cells can generate other cell types (Al-Awqati and Oliver, 2002). The key important target in kidney stem cell research and application is to get kidney stem cells from other types of the cells, and it is also important to find the better way to change kidney stem cells to other cell types.

As the nature will, to live eternally is an extracting dream in all the human history. Stem cell is the original of life and all cells come from stem cells. Germline stem cell (GSC) is the cell in the earliest of the cell stage. It is possible to inject the GSC into adult human body to get the eternal life. This article is to try to describe the stem cell and to explore the possibility of the eternal life with the stem cell strategy The production of functional male gametes is dependent on the continuous activity of germline stem cells. The availability of a transplantation assay system to unequivocally identify male germline stem cells has allowed their in vitro culture, cryopreservation, and genetic modification. Moreover, the system has enabled the identification of conditions and factors involved in stem cell self-renewal, the foundation of spermatogenesis, and the production of spermatozoa. The increased knowledge about these cells is also of great potential practical value, for example, for the possible cryopreservation of stem cells from boys undergoing treatment for cancer to safeguard their germ line (Ma, et al, 2007).

Correspondence to:
Hongbao Ma
Bioengineering Department
Zhengzhou University
Zhengzhou, Henan 450001, China

mahongbao@zzu.edu.cn; hongbao@gmail.com
01186-137-8342-5354

References

Al-Awqati Q, Oliver JA. 2002. Stem cells in the kidney. Kidney Int 61(2):387-395.
Arnold WP. 2000. Improvement in hemodialysis vascular access outcomes in a dedicated access center. Semin Dial 13(6):359-363.
Berzoff J, Swantkowski J, Cohen LM. 2008. Developing a renal supportive care team from the voices of patients, families, and palliative care staff. Palliat Support Care 6(2):133-139.
Bickenbach JK. 2003. The continuing saga of epidermal stem cells. J Invest Dermatol 121(5):xv-xvi.
Brodie JC, Humes HD. 2005. Stem cell approaches for the treatment of renal failure. Pharmacol Rev 57(3):299-313.
Hanna J, Markoulaki S, Schorderet P, Carey BW, Beard C, Wernig M, Creyghton MP, Steine EJ, Cassady JP, Foreman R, Lengner CJ, Dausman JA, Jaenisch R. 2008. Direct reprogramming of terminally differentiated mature B lymphocytes to pluripotency. Cell 133(2):250-264.
Imberti B, Morigi M, Tomasoni S, Rota C, Corna D, Longaretti L, Rottoli D, Valsecchi F, Benigni A, Wang J, Abbate M, Zoja C, Remuzzi G. 2007. Insulin-like growth factor-1 sustains stem cell mediated renal repair. J Am Soc Nephrol 18(11):2921-2928.
Li K, Zhu H, Han X, Xing Y. Ectopic hTERT gene expression in human bone marrow mesenchymal stem cell. Life Science Journal. 2007;4(4):21–24.
Lin CS, Lim SK, D'Agati V, Costantini F. 1996. Differential effects of an erythropoietin receptor gene disruption on primitive and definitive erythropoiesis. Genes Dev 10(2):154-164.
Ma H, Cherng S. Eternal Life and Stem Cell. Nature and Science. 2007;5(1):81-96.
Ma H, Chen G. Stem cell. The Journal of American Science 2005;1(2):90-92.
Mai ML, Ahsan N, Gonwa T. 2006. The long-term management of pancreas transplantation. Transplantation 82(8):991-1003.
Mehta RL, Kellum JA, Shah SV, Molitoris BA, Ronco C, Warnock DG, Levin A. 2007. Acute Kidney Injury Network: report of an initiative to improve outcomes in acute kidney injury. Crit Care 11(2):R31.
Oliver JA. 2004. Adult renal stem cells and renal repair. Curr Opin Nephrol Hypertens 13(1):17-22.
Ross EA, Alza RE, Jadeja NN. 2006. Hospital resource utilization that occurs with, rather than because of, kidney failure in patients with end-stage renal disease. Clin J Am Soc Nephrol 1(6):1234-1240.
Shimony N, Avrahami I, Gorodetsky R, Elkin G, Tzukert K, Zangi L, Levdansky L, Krasny L, Haviv YS. 2008. A 3D rotary renal and mesenchymal stem cell culture model unveils cell death mechanisms induced by matrix deficiency and low shear stress. Nephrol Dial Transplant 23(6):2071-2080.
Sirmon MD. 1990. Renal disease in noninsulin-dependent diabetes mellitus. Am J Med Sci 300(6):388-395.
Taupin P. 2006. The therapeutic potential of adult neural stem cells. Curr Opin Mol Ther 8(3):225-231.
Vigneau C, Polgar K, Striker G, Elliott J, Hyink D, Weber O, Fehling HJ, Keller G, Burrow C, Wilson P. 2007. Mouse embryonic stem cell-derived embryoid bodies generate progenitors that integrate long term into renal proximal tubules in vivo. J Am Soc Nephrol 18(6):1709-1720.
Winkler J. 2003. [Adult neural stem cells: therapeutic potential in neurology]. Med Klin (Munich) 98 Suppl 2:27-31.
Wong CY, Cheong SK, Mok PL, Leong CF. 2008. Differentiation of human mesenchymal stem cells into mesangial cells in post-glomerular injury murine model. Pathology 40(1):52-57.
Yokoo T, Sakurai K, Ohashi T, Kawamura T. 2003. Stem cell gene therapy for chronic renal failure. Curr Gene Ther 3(5):387-394.
Zheng N, Wang L, Wu J, Li H, Wang Y, Zhang Q. Rapid enrichment of stem cell population by filter screening and biomarker-immunoassay from human epidermis. Life Science Journal. 2008; 5(4):33–37.

Relationship between Continuity and Momentum Equation in Two Dimensional Flow

Idowu, I. A, Olayiwola, M.O and Gbolagade A.W
Department of Mathematical Sciences
Olabisi Onabanjo University
Ago-Iwoye,Nigeria
ejabola@yahoo.com

Abstract

In this paper a quantitative discussion on a theory describing the relationship between the continuity and momentum equation in two dimensional flow together with the momentum equation in vectorial form: $\rho \, dq/dt = -\nabla p + \rho g + \mu \nabla^2 q$, on expanding $\nabla * (\nabla . q)$ in cylindrical polar coordinates, the end result proved to be Euler equation. [Academia Arena, 2009;1(1):62-72]. ISSN 1553-992X.

Keyword: Continuity equation, Momentum equation, Cylindrical coordinates, polar coordinate.

Classification: Fluid Mechanics

1.0 Introduction:

A more detailed view of the fluxes across the parcel can be obtained within a reasonable space of text of we restrict our attention to two dimensions. We can then write the equations for the component and look closely at the change in these components.

We consider planar view of a parcel unit depth. Assume ρ is constant across the parcel, so we can write for the mass of the parcel, $\delta\mu = \rho\delta v = \rho\delta x\delta y\delta z$. In the two-dimensional flow, each component of velocity can vary in both x and y directions. We can approximate those velocity changes across our incremental parcel by a Taylor expansion. In this case we will consider the base values of qualities such as pressure and velocity to be the value of the center of the parcel and expand around these values. Note that value of the corner, $x = y = z = 0$, could also be assured as base values. Since the parcel is infinitesimal with respect to mean flow scales. The magnitudes of these values are uniform across the parcel in the limit $\delta v \to 0$. We are writing the incremental change at the point, we need not be zero. Again we look at the total change in the density and the scope of the parcel as it instantaneously occupies the point (x, y). We can derive the continuity equation in a slightly different manner,

by considering a specific infinitesimal parcel in a Largrangian sense. The derivation will illustrate the close connection between Largrangian and Eulerian perspectives and we will send up with the familiar Eulerian expression. Starting with the Langrangian perspectives we consider a very small parcel such that $\delta\nu \to 0$, with no sinks or sources. We then follow the particular parcel that experiences volume and density changes with respects to five only field varcash will vary infinitesimal across the small dimensions of the parcel. Then the statement for the constant mass of fluids parcel, then the statement, for the constant mass of this parcel $\rho\delta\nu$ is completely expressed in the five derivatives, $D((\rho\delta\nu)/\partial t) = 0$. However, when the parcel moves through the fluid, to volume must distorts and changes due to the changing forces in the thus field. The derivative which separated into density and volume changes by using the chain rule for differentiation. In the end, the derivative can be converted to the Eulerian expression.

2.0 Mathematical Analysis

The differences between the various derivatives can be explained in a more formal manner as follows:

Let consider a fluid particle moving with a load velocity;

$$q = i\upsilon + j\nu + \kappa\omega \qquad 1$$

and let the change of the property $b = b(x, y, z, t)$ of the particle be investigated. The change in b with time and position may be expressed as

$$db = \left(\frac{\partial b}{\partial t}\right)\partial t + \left(\frac{\partial b}{\partial x}\right)\partial x + \left(\frac{\partial b}{\partial y}\right)\partial y + \left(\frac{\partial b}{\partial z}\right)\partial z \qquad 2$$

The rate of change of s in time $\partial b / \partial t$ equation become

$$\frac{\nabla b}{\nabla t} = \frac{\partial b}{\partial t} + U\frac{\partial s}{\partial x} + V\frac{\partial b}{\partial y} + W\frac{\partial b}{\partial z}\} \qquad 3$$

$$\frac{\nabla b}{\nabla t} = \frac{\partial b}{\partial t} + z \cdot \partial b \qquad 4$$

With (3) we can direct operation of ∂b in new coordinates.

$$\frac{\nabla b}{\nabla t} = \frac{\partial b}{\partial t} + q_r \frac{\partial b}{\partial r} + q_{\vartheta} \frac{\partial b}{r \partial \theta} + q_z \frac{\partial b}{\partial z},$$

5

$$\frac{\nabla b}{\nabla t} = \frac{\partial b}{\partial t} + q_r \frac{\partial b}{\partial r} + q_{\vartheta} \frac{\partial b}{r \partial \theta} q_{\theta} \frac{\partial b}{r \sin \theta \partial \theta}$$

Which the law of conservation of mass has already been presented in a form applicable to a control volume may be rewritten as:

$$(1) = \int_v \frac{\partial R}{\partial t} \partial v + \int_s \partial q \cdot nds$$

6

Application of the divergence

(2) theorem to the surface integral

$$\int_s pq \cdot nds = \int_v \Delta \cdot (pq) dv \cdot$$

7

Apply 6 into

$$\int_v \left[\frac{\partial p}{\partial t} = \Delta \cdot (pq) \right] dv = 0$$

8

Hence, $\frac{\partial p}{\partial t} + \Delta(pq) = 0$

9

The equation (9.0) is known as the equation f continuity. It is the differential form of the law of conservation of mass written in form of the flow field.

Equation (9.0) is now rewritten in detail in the three most continuity used coordinate systems.

In Cartesian coordinates

$$\frac{\partial p}{\partial t} + \frac{\partial (pu)}{\partial x} + \frac{\partial (pw)}{\partial y} + \frac{\partial (pw)}{\partial z} = 0$$

10

In cylindrical coordinates

$$\frac{\partial p}{\partial t} + \frac{d}{r} \frac{\partial (rpqr)}{\partial r} + \frac{1}{r} \frac{\partial (pq\theta)}{\partial \theta} + \frac{\partial (pqz)}{\partial z} = 0$$

11

In spherical coordinates

$$\frac{\partial p}{\partial t}+\frac{1}{r^2}\frac{\partial(r^2 pq)}{\partial r}+\frac{1}{r\sin\theta}\frac{\partial(pq\theta\sin\theta)}{\partial\theta}+\frac{1}{\sin\theta}\frac{\partial(pq\theta)}{\partial\theta}=0 \qquad 12$$

In some particular cases equation of continuity assumes simpler form given in Cartesian coordinates.

$$\left.\begin{array}{l}\Delta\cdot(pq)=0\\ or\\ \Delta\cdot q=0\end{array}\right\}. \qquad 13$$

Now, for momentum, Newton's second law of motion states that the rate of change of momentum of a thermodynamics system equals the sum total of the forces acting on the system.

$$\frac{D}{Dr}\int_v pqdv=\int_v gpdv+\int_s Tds \qquad 14$$

When g is a general body force per unit mass,

and T is the system boundary for *x*-component Equation 14 becomes

$$\frac{D}{Dt}\int_v pxdv=\int_v gxpdv+\int_s Tnxds \qquad 15$$

The Reynolds transport theorem may now be applied to the left-hand side of this equation

$$\frac{D}{Dt}\int_v pudv=\int_v \rho\left[\frac{du}{\partial t}+\frac{u\partial u}{\partial u}+\frac{v\partial u}{\partial y}+\frac{w\partial u}{\partial z}\right]dv \qquad 16$$

The stress term *Tu* inside the surface integral is now written in terms of its components to yield

$$\int_s T_{nn}ds=\int_s\left[T_{xxi}+T_{ynj}+T_{zx}k\right]\cdot nds=\int_v\left[\frac{\partial\tau_{xx}}{\partial u}+\frac{\partial\tau_{yx}}{\partial y}+\frac{\partial\pi t}{\partial_x}\right]dv \qquad 17$$

where the divergence theorem has been used again

By subtraction of equation 16 and 17 into equation 15 yields

$$\int_v\left\{\rho\left[\frac{\partial u}{\partial t}+\frac{u\partial u}{\partial u}+\frac{v\partial u}{\partial t}+\frac{w\partial u}{\partial t}-g_x\right]-\left[\frac{\partial T_{xx}}{\partial u}+\frac{\partial T_{yn}}{\partial y}+\frac{\partial T_{zx}}{\partial z}\right]\right\}\partial v=0 \qquad 18$$

Becomes

$$\rho\left[\frac{\partial u}{\partial t}+\frac{u\partial u}{\partial x}+\frac{v\partial u}{\partial y}+\frac{\omega\partial u}{\partial t}\right]=Pg_x+\frac{\partial T_{xx}}{\partial x}+\frac{\partial T_{yx}}{\partial y}+\frac{\partial T_{zx}}{\partial z} \qquad 19$$

Similarly for the y- and Z- Components

$$\rho\left[\frac{\partial u}{\partial t}+\frac{u\partial v}{\partial x}+\frac{v\partial u}{\partial y}+\frac{\omega\partial u}{\partial t}\right]P_{g_x}+\frac{\partial T_{xx}}{\partial x}+\frac{\partial T_{yx}}{\partial y}+\frac{\partial T_{zx}}{\partial z} \qquad 20$$

$$\rho\left[\frac{\partial u}{\partial t}+\frac{u\partial v}{\partial x}+\frac{v\partial u}{\partial y}+\frac{\omega\partial u}{\partial t}\right]=P_{g_x}+\frac{\partial T_{xx}}{\partial x}+\frac{\partial T_{yx}}{\partial y}+\frac{\partial T_{zx}}{\partial z} \qquad 21$$

The . ∇ g term vanishes for incompressible flows. Hence the thermodynamic presume may be define for an incompressible fluid as the average normal stress:

$$\rho=\frac{T_{xx}+T_{yy}+T_{zz}}{3} \qquad 22$$

It is customary to separate out the pressure terms from the total stress

$$.\mathrm{Tij}+-\mathrm{p}\partial ij+\tau ij \qquad 23$$

And $\tau_{ij}=\partial\mu\Sigma ij$ equation 23 is written in tensor form as

$$T=-p+\tau \qquad 24$$

$$P=\begin{vmatrix} p & 0 & 0 \\ 0 & p & 0 \\ 0 & 0 & p \end{vmatrix}$$

Equation 23 is used to modify the momentum equation by subtraction 8 from 20.

$$\rho=\left[\frac{\partial u}{\partial t}+U\frac{\partial u}{\partial x}+V\frac{\partial u}{\partial y}+W\frac{\partial u}{\partial t}\right]=-\frac{\partial\rho}{\partial x}+\rho_{gy}+\frac{\partial\tau_{xx}}{\partial x}+\frac{\partial\tau_{yx}}{\partial y}+\frac{\partial\tau_{zx}}{\partial z} \qquad 25$$

$$\rho\left[\frac{\partial u}{\partial t}+U\frac{\partial v}{\partial x}+V\frac{\partial v}{\partial y}+W\frac{\partial v}{\partial t}\int\right]=-\frac{\partial p}{\partial x}+\rho_{gy}+\frac{\partial\tau_{xy}}{\partial x}+\frac{\partial\tau_{yx}}{\partial y}+\frac{\partial\tau_{zx}}{\partial z} \qquad 26$$

$$\rho\left(\frac{\partial w}{\partial t}+U\frac{\partial w}{\partial x}+V\frac{\partial w}{\partial y}+W\frac{\partial w}{\partial t}\right)=-\frac{\partial p}{\partial y}+\rho_{gy}+\frac{\partial \tau_{xz}}{\partial x}+\frac{\partial \tau_{yz}}{\partial y}+\frac{\partial \tau_{zz}}{\partial z} \qquad 27$$

This may be put in symbolic compact form.

$$\rho\frac{\Delta q}{\Delta t}=-\nabla_p \rho g+\nabla.\tau \qquad 28$$

The expression for the stress and the rate of strain component in several coordinate system are now written down.

In Cartesian coordinates of q=iu + jv + kw

$$\varepsilon_{xy}=\frac{1}{2}\left(\frac{\partial u}{\partial y}+\frac{\partial v}{\partial x}\right),\varepsilon_{xy}=\frac{1}{2}\left(\frac{\partial v}{\partial z}+\frac{\partial w}{\partial y}\right),\varepsilon_{xy}=\frac{1}{2}\left(\frac{\partial u}{\partial z}+\frac{\partial w}{\partial x}\right),$$

$$\lambda_{xy}=\mu\left(\frac{\partial u}{\partial y}+\frac{\partial v}{\partial x}\right),\lambda_{xy}=\mu\left(\frac{\partial v}{\partial z}+\frac{\partial w}{\partial y}\right),\lambda_{xy}=\mu\left(\frac{\partial u}{\partial z}+\frac{\partial w}{\partial x}\right),$$

$$\varepsilon_{xx}=\frac{\partial u}{\partial x},\quad \varepsilon_{yy}=\frac{\partial v}{\partial y},\quad \varepsilon_{zz}=\frac{\partial w}{\partial r},$$

$$\lambda_{xx}=\partial\mu\frac{\partial u}{\partial x},\quad \lambda_{yy}=\partial\mu\frac{\partial r}{\partial y},\quad \lambda_{zz}=\partial\mu\frac{\partial w}{\partial z}, \qquad 29$$

In cylindrical coordinates $\mathrm{q}=\mathrm{e}_r q_r+e_9 q_9+e_z q_z$

$$\varepsilon_{R9}=\frac{1}{2}\left[\frac{1}{r}\frac{\partial qr}{\partial \vartheta}+r\frac{\partial}{\partial r}\left(\frac{q^{\vartheta}}{r}\right)\right],\quad \tau_{R9}=\mu\left[\frac{1}{r}\frac{\partial qr}{\partial 9}+r\frac{\partial}{\partial r}\left(q^{\vartheta}/r\right)\right]$$

$$\varepsilon_{r9}=\frac{1}{2}\left[\frac{\partial qr}{\partial \vartheta}+\frac{\partial}{\partial r}\right],\quad \tau_{rz}=\mu\left[\frac{\partial qr}{\partial z}+\frac{\partial z}{\partial r}\right]$$

$$\varepsilon_{9z}=\frac{1}{2}\left[\frac{\partial q\vartheta}{\partial \vartheta}+\frac{1}{r}\frac{\partial qz}{\partial \vartheta}\right],\quad \tau_{9z}=\mu\left[\frac{\partial q\vartheta}{\partial z}+\frac{1}{r}\frac{\partial qz}{\partial \vartheta}\right]$$

$$\varepsilon_{rr}=\frac{\partial qr}{\partial r}\qquad \varepsilon_{9ee}=\left(\frac{1}{r}\frac{\partial q\vartheta}{\partial \vartheta}+\frac{qr}{r}\right),\qquad \varepsilon_{zz}=\frac{\partial qz}{\partial z}$$

$$\tau_{rr}=2\mu\frac{\partial qr}{\partial r},\quad \tau_{99}=2\mu\left(\frac{1}{r}\frac{\partial q\vartheta}{\partial \vartheta}+\frac{qr}{r}\right),\ \tau_{zz}=2\mu\frac{\partial qz}{\partial z} \qquad 30$$

In spherical coordinates $\mathrm{q}=e_r q_r+e_9 q_9+e_\phi q_\phi$

$$ER\theta = \frac{1}{2}\left[\frac{1}{R}\partial qR/\partial\theta + R\left(\frac{\partial}{\partial R}\right)\right], \tau R\theta = \mu\left[\frac{1}{R}\partial qR/\partial\theta + R\left(\frac{\partial}{\partial R}\right)\right]$$

$$ER\varphi = \frac{1}{2}\left[\frac{1}{RSin\theta}\partial qR/\partial\theta + R\left(\frac{\partial}{\partial R}\right)\right], \tau R\theta = \mu\left[\frac{1}{RSin\theta} + R\,\partial q/\partial R\left(\frac{q^{\theta}}{\partial R}\right)\right]$$

$$E\theta\varphi = \frac{1}{2}\left[\frac{1}{RSin\theta}\partial qR/\partial\theta + \frac{Sin\theta}{R}\partial/\partial\theta\left(\frac{q\varphi}{Sin\theta}\right)\right], \tau R\theta = \mu\left[\frac{1}{RSin\theta}\partial q\theta/\partial\varphi + \frac{Sin\theta}{R}\partial/\partial R\left(\frac{q^{\theta}}{Sin\theta}\right)\right]$$

ERR= $\frac{\partial qR}{\partial R}$, $\quad \tau_{RR} = 2\mu\frac{\partial qR}{\partial R}$,

$$E\theta\theta = \left(\frac{1}{R}\frac{\partial qR}{\partial R} + \frac{qr}{R}\right), \qquad \tau\theta\varphi = 2\mu\left(\frac{1}{R}\frac{\partial qR}{\partial R} + \frac{qr}{R}\right)$$

$$E\varphi\varphi = \left(\frac{1}{RSin\varphi}\frac{\partial q\varphi}{\partial\varphi} + \frac{qR}{R}\frac{q\theta Cot\theta}{R}\right), \qquad \tau\varphi\varphi = 2\mu\left(\frac{1}{RSin\varphi}\frac{\partial q\varphi}{\partial\varphi} + \frac{qR}{R}\frac{q\theta Cot\theta}{R}\right) \quad 31$$

Equation 29-31 may be used to eliminate the stress components from the differential momentum equation 25-27

Becomes

$$\rho\left(\frac{\partial v}{\partial t} + u\frac{\partial v}{\partial x} + v\frac{\partial v}{\partial y} + w\frac{\partial v}{\partial z}\right) = \rho_{gx}\frac{\partial p}{\partial y} + \mu\left(\frac{\partial^2 v}{\partial x^2} + \frac{\partial^2 v}{\partial y^2} + \frac{\partial^2 v}{\partial z^2}\right)$$

$$\rho\left(\frac{\partial v}{\partial t} + u\frac{\partial v}{\partial x} + v\frac{\partial v}{\partial y} + w\frac{\partial v}{\partial z}\right) = \rho_{gw}\frac{\partial p}{\partial w} + \mu\left(\frac{\partial^2 v}{\partial x^2} + \frac{\partial^2 v}{\partial y^2} + \frac{\partial^2 v}{\partial z^2}\right)$$

$$\rho\left(\frac{\partial w}{\partial t} + u\frac{\partial w}{\partial x} + v\frac{\partial w}{\partial y} + w\frac{\partial w}{\partial z}\right) = \rho_{gw}\frac{\partial p}{\partial w} + \mu\left(\frac{\partial^2 w}{\partial x^2} + \frac{\partial^2 w}{\partial y^2} + \frac{\partial^2 w}{\partial z^2}\right) \quad 32$$

Equ. 32 constitute a system of three nonlinear second order partial differential equation. The proper boundary conditions for the velocity on a rigid boundary are: $q_n = q_t = 0$

Where q_n is the minimal component of the velocity relative to the solid boundaries and q_r is its tangential component. These conditions are also termed the non-peneuration ($q_n = 0$) and no-slip ($q_t = 0$) viscous boundary conditions.

Equation 3.2 becomes

$$\rho\frac{Dq}{Dt} = -\nabla\rho + \rho g - \mu\nabla x(\nabla xq) = -\nabla\rho + \rho g - \mu\nabla^2 q \quad 33$$

If ∇^2 is the Laplacian operator applied to the velocity vector in Cartesian coordinates. By expanding $\nabla \times (\nabla \times q)$ in cylindrical polar coordinates and using (13) we obtain

$$\rho\left(\frac{\partial qr}{\partial t} + q_r \frac{\partial qr}{\partial r} + q\theta \frac{\partial qr}{r\partial \theta} + q_z \frac{\partial qr}{\partial z} - \frac{q^2\theta}{r}\right)$$

$$= \rho_{gr} - \frac{\partial p}{\partial r} + \mu\left[\frac{\partial}{\partial r}\left(\frac{1}{r}\frac{\partial}{\partial r}\right)(rq_r)\right] + \frac{1}{r^2}\frac{\partial^2 q_r}{\partial z^2} - \frac{p}{r^2}\frac{\partial q\theta}{\partial \theta} \qquad 34$$

$$\rho\left(\frac{\partial q\theta}{\partial t} + q_r \frac{\partial q\theta}{\partial r} + q\theta \frac{\partial q\theta}{r\partial \theta} + q_z \frac{\partial q\theta}{\partial z} - \frac{qrq\theta}{r}\right)$$

$$= \rho_{g\theta} - \frac{\partial p}{r\partial \theta} + \mu\left[\frac{\partial}{\partial r}\left(\frac{1}{r}\frac{\partial}{\partial r}(rq\theta)\right) + \frac{1}{r^2}\frac{\partial^2 \theta q_r}{\partial z^2} + \frac{\partial^2 \theta q_r}{\partial z^2} + \frac{2}{r^2}\frac{\partial q\theta}{\partial \theta}\right] \qquad 35$$

$$\rho\left(\frac{\partial qz}{\partial t} + qr \frac{\partial qz}{\partial r} + q\theta \frac{\partial qz}{r\partial \theta} + q_z \frac{\partial qz}{\partial z}\right)$$

$$= \rho_{yz} - \frac{\partial p}{\partial y} + \mu\left[\frac{I}{r}\frac{\partial}{\partial r}\left(r\frac{\partial qz}{\partial r}\right) + \frac{1}{r^2}\frac{\partial^2 qz}{\partial \theta^2} + \frac{\partial^2 qz}{\partial z^2}\right] \qquad 36$$

By repeating the for spherical coordinate, we obtaqin,

$$= \rho_{y\varphi} - \frac{1}{RSin^2\theta}\frac{\partial p}{\varphi} + \mu\left[\frac{I}{R}\frac{\partial}{\partial R}\left(R\frac{\partial q\theta}{\partial R}\right) + \frac{1}{R^2 Sin\theta}\frac{\partial^2}{\partial \theta^2} + \left(Sin\theta \frac{\partial q\varphi}{\partial \theta}\right)\right]$$

$$+ \mu\left[\frac{I}{RSin^2\theta}\frac{\partial^2 q\varphi}{R^2 Sin^2\theta} + \frac{2}{R^2 Sin\theta}\frac{\partial qr}{\partial \varphi} + \frac{2Cos\theta}{R^2 Sin^2\theta}\frac{\partial q\varphi}{\partial \varphi}\right] \qquad 37$$

By substituting $\mu = 0$ in the navier-stokes equating which is called momentum equation (3.2) – (3.7) we obtain an equation

$$\rho\frac{Dq}{Dt} = \rho_g - \nabla\rho \qquad 38$$

This is called the Euler equation

3.0 Discussion

Solutions of the momentum equation result in velocity vectors q and pressure ρ which satisfy both the momentum equation and the continuity equation. Given such a combination, [q . ρ], we can check whether it

constitutes a solution by substitution into the equations. How to find such a solution is another matter and any general step leading toward this goal is useful. For two dimensional flows it is possible to eliminate the continuity equation from the system of equations by using only functions which satisfy the continuity equation. This elimination is a formal step toward a solution and functions which affect this elimination and the stream functions.

And if the flow is defined as two dimensional when its description in Cartesian coordinates shows no z-component of the velocity and no dependence on the z-coordinate. Such a flow can be described in the $z = 0$ plane, show a flow pattern identical to that in the $z = 0$ plane. The $z = 0$ plane is therefore called representative plane.

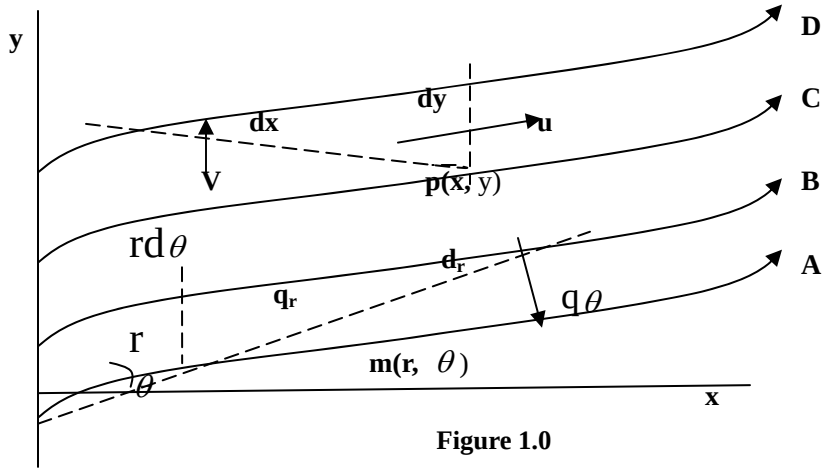

Figure 1.0

The figure 1.0 shows a representative plane for two-dimensional flow, with four streamlines denoted by the letters A, B, C, D. the whole pattern may be shifted

In the z-direction parallel to itself. Thus the streamlines also represent stream sheets, i.e barriers which are not crossed by the flow. The Mass flux entering at the left, between, say, streamlines A and B must therefore come out at the right side without change. Because the distance between the two streamlines accommodating this mass flux seems in the drawing to increase, the mass flux seems per unit Cross section $\rho..q$, must decrease from left to right. There is therefore some relation between the convergence and divergence of stream lines and the vector $\rho.q$. Furthermore, because stream sheets are not crossed by the flow, each sheet represents a certain mass flux per unit depth of stream sheet taking place below it i. flowing between it and some particular stream sheet representing zero flux.

This mass flux is called the stream function and it is denoted by φ

$$\partial\varphi = (\partial y)(up)$$

$$= (-\partial x)(vp)$$

From which follows

$$u\lambda = \frac{\partial x}{\partial y}, \quad v\rho = \frac{-\partial\varphi}{\partial x}$$

Using planne polar coordinate in the representative plane and letting.

$$\varphi B = \varphi A + d\varphi$$

$$d\varphi = (rdq(q_r\rho)$$

$$d\varphi = (dr)(-qq\rho)$$

From which follows

$$q_r\rho = \frac{1}{r}\frac{\partial\varphi}{\partial\theta}, \qquad q\theta\rho = \frac{-\partial\varphi}{\partial r}$$

REFERENCES

1. Atmospheric Turbulence and Air Pollution Modeling, Nieuwstadt, F. T. M. and Dop, H. eds., Reidel, 1982.
2. Gill. A, Atmosphere- Ocean Dynamics, International Geophysics Series, 30, Academic Press, 1982.
3. H. Schhchting, Boundary layer theory, "7th.ed. Mc graw. Hill, New York 1979.
4. Lamb, H. Hydrodynamics, dover, 1945. Classical Inviscid flow. Milne-Thompson, L.M. Theoretical Hydrodynamics Macmillan, 1938.
5. Meyer, R.E., ed. Transition and Turbulence, Academic Press, 1981
6. Panofsky, H. A. and Dutton, J.A. Atmospheric Turbulence; Models and Methods to Engineering Applications, Wiley, 1984.
7. Panton, R.L. incompressible Flow, Wiley, 19 84. an excellent treatment of classic flow topics: graduate level engineering fluid dynamics.
8. R B Bird W E Stewart and E.N Lightfoot, "Transport Phenomenon" Wiley, New York, 19 60
9. Sorbjan, Z. Structure of the Atmospheric Boundary Layer, Pretice-Hall, 1989.

10. Stull. R.B. An Introduction to Boundary Layer Meteorology, Kluwer, 1988.

11. W. F Huges, An Introduction to viscos flow, “Hemisphere, Washington, DC 19 79.

10/23/2008

对宇宙加速膨胀的最新解释: 这是由于在宇宙早期所发生的宇宙黑洞间的碰撞所造成的**

<<对黑洞和大爆炸的新概念—两者都无奇点[1][2]>> 一文的第 5 篇

张 洞 生
1957 年毕业于北京航空学院,即现在的北京航天航空大学
永久住址: 17 Pontiac Road, West Hartford, CT 06117-2129, U.S.A.
E-mail: ZhangDS12@hotmail.com

内容提要: 在 1998 年,由美国加里福里亚大学的劳仑斯伯克莱国家实验室的 Saul Perlmutter 教授和澳大利亚国立大学的 Brain Schmidt 所分别领导的两个小组通过对 Ia 型超新星爆炸的观测发现了我们宇宙的加速膨胀,他们指出那些遥远的星系正在加速地离开我们.[3] 现在,多数的相关的科学家们认为我们宇宙的加速膨胀是由于宇宙中存在具有排斥力和负能量的神秘的暗能量所造成的,其中一些科学家们正为获得以后的诺贝尔奖而努力寻找这种暗能量. 特别是, 我们宇宙诞生于 137 亿年前,那时暗能量並没有随宇宙诞生而出现,而暗能量却是在大约 90 亿年前蹦出来的.[3]究竟什么是暗能量呢? 现在还无人知道. 中国科技大学物理学教授李淼就幽默地说过: “有多少个暗能量的学者,就能想像出多少种暗能量”.[3] 那么, 我们宇宙的加速膨胀就只能用具有排斥力和负能量的神秘的暗能量来解释吗? 按照黑洞的原理和其本性, 任何一个黑洞的膨胀产生于吞噬外界的能量物质和与其它黑洞的碰撞,它所吞噬的能量物质愈多就膨胀得愈快.[参考后面的公式(6b)和(6c)].在本文中, 对我们宇宙的加速膨胀将用一个宇宙黑洞和另一个宇宙黑洞在其早期的碰撞来解释. 虽然本文中的论证可能相对地简单,但比现有的其它各种理论的论证更为合理. [Academia Arena, 2009;1(1):73-78]. ISSN 1553-992X.

关键词: 暗能量, 有排斥力的暗能量, 有负能的暗能量, 宇宙的加速膨胀, 宇宙黑洞, 宇宙黑洞的碰撞,多宇宙,超光速的空间膨胀,

**本文原文为英文，曾发表在“Nature and Science”杂志 的 2007 年 5〔3〕期上，其网址是http://www.sciencepub.org/nature/0503。现翻译成中文，略有修改。

I.我们宇宙的加速膨胀证明了多宇宙的真实存在.

新近的观测表明,所谓的 “暗能量”並不是随宇宙的诞生而出现,而是在宇宙的诞生后约 50 亿年才蹦出来的; 由于它的出现造成了宇宙的加速膨胀. 这就清楚地表明暗能量不是我们宇宙所固有的,而是来自我们宇宙的外界,即外面的宇宙.这就是多宇宙存在的强有力的证据. 况且, “近来,在我们的宇宙空间,发现了许多超重级黑洞.一个超重级黑洞的质量约等值于 10^9 太阳. 据此计算,其平均密度约等于 $0.0183 g/cm^3$.”—摘引自<对黑洞和大爆炸的新概念>[2]一文的第 15 节. 在这些超重级黑洞中,也会有许多恒星及其行星存在.而这种黑洞往往处于星系的核心地位,其外围有太多的能量物质可供吞噬使其不断长大. 几十亿年之后,就可能有智慧生物出现在其内的某些行星上.而他们将无法知道他们本黑洞外的世界. 这就是说,甚至在我们同一个宇宙内,不同的超重级黑洞内的智慧生物之间也无法互通信息. 因为**每一个黑洞就是一个完全独立的宇宙**. 幸好我们的太阳系不在银河中心的超重级黑洞内,否则,我们连整个银河都无法知道,更不会知道我们整个的宇宙了. 因此,我们宇宙中超重级黑洞之间的关系是和我们宇宙与其它宇宙之间的关系是一样的,因为**我们宇宙一直就是一个真实的超级巨型黑洞**.[1][2]上述在我们宇宙中的超重级黑洞可吞噬起外面能量物质或与其它的黑洞相碰撞. 同样的道理,我们这个黑洞宇宙也会吞噬我们宇宙外的能量物质或和其它宇宙发生碰撞.

II.暗能量是怎样提出来的。 任何对宇宙的加速膨胀解释的理论必须符合我们宇宙的平直性要求和当今较准确的观测值 ($\Omega = 1.02 \pm 0.02$),而只有本文的解释才符合此要求。有排斥力的暗能量和所有其它理论都可能成为找不到的幽灵，因为它们都不符合此要求，解释不了我们宇宙的平直性.

爱因斯坦的广义相对论场方程如下:

$G\mu\nu = 8\pi G\, T\mu\nu + \Lambda g\mu\nu$[4] (1)

$G\mu\nu$ 是描述时空几何特性的**爱**因斯坦张量. $T\mu\nu$ 是物质场的能量-动量张量. $\Lambda g\mu\nu$ 是宇宙学项,其中 Λ 被誉为宇宙学常数. $\Lambda g\mu\nu$ 具有排斥力,它是**爱**因斯坦为了保持我们宇宙中引力和斥力的平衡后来才加进去的.[4] 为了便于分析,$T\mu\nu$ 可分为下面三项:

$T\mu\nu = T^1\mu\nu + T^2\mu\nu + T^3\mu\nu$ (2)

按照当今的较准确的观测和理论计算, $T^1\mu\nu \approx 4\% T\mu\nu$,[3] $T^1\mu\nu$ 代表可见的有引力的普通物质, 如星星星际间物质等.根据对许多星系旋转速度分布的观测和理论计算, $T^2\mu\nu \approx 22\% T\mu\nu$,[3] i.e. $T^2\mu\nu \approx (5 \sim 6)\, T^1\mu\nu$. $T^2\mu\nu$ 代表有引力的不可见的暗物质. $T^3\mu\nu \approx 74\%\ T\mu\nu$,[3] 它就是 除 $(T^1\mu\nu + T^2\mu\nu)$之外的所谓的暗能量. 暗能量与 $(T^1\mu\nu + T^2\mu\nu)$ 一起的总量必需品能保持我们宇宙的平直性和 $(\Omega \rightarrow 1)$,即 $\Omega = \rho_r / \rho_o \approx 1$.因为 Guth 和 Linde 所提出的宇宙暴涨论的预言以及宇宙动力学均要求宇宙的平直性和 $\Omega = \rho_r / \rho_o \approx 1$,也就是要求宇宙的实际密度 ρ_r 必须极为接近其临界密 ρ_o. 近来,许多较准确的观测已证实 $\Omega = 1.02 \pm 0.02$[4] 而较好地符合理论的要求. 当然,这里所提到的暗能量是指具有**有引力暗能量.**

然而,为了解释新近对遥远的 Ia 型超新星爆发所发现的宇宙的加速膨胀,许多科学家提出了一些新理论.他们将 $(T^3\mu\nu + \Lambda g\mu\nu)$合并到一起成为 $\Lambda g\mu\nu$, 认为 $\Lambda g\mu\nu$ 是 $(T^3\mu\nu = 74\% T\mu\nu)$ 而具有排斥力的未知的和神秘的暗能量. 新理论最著名的代表是量子场论. 在该理论中,把 $(T^1\mu + T^2\mu\nu = 0)$ 当作真空状态,或者说是最低能量状态或量子场的基本态, [4] 也是微观宇宙的零点能. 而将宇宙中$(T^1\mu + T^2\mu\nu \neq 0)$的宏观能量物质即普通物质作为量子场的激发态. 对宇宙真空状态的观测到是非常符合于 $(T^1\mu\nu + T^2\mu\nu) = 0$, 于是, $\Lambda g\mu\nu$ 正好作为具有排斥力的 $T^3\mu\nu$ 的真空能. **不幸的是,按照量子场论所计算的 $\Lambda g\mu\nu$ 值比**

在真空中实际的观测值要大 10^{120} 倍. 由于这种原因,用量子场论来解爱因斯坦的广义相对论场方程就会遇到无法克服的困难. 很显然, 由量子场论所计算出来的如此庞大的真空能量值是无法保持宇宙的平直性和使张量 Gμν 在爱因斯坦的广义相对论场方程中与实际的观测值相符合. 量子场论似乎把真空能量当作 "无限的免费午餐". 在宇宙中任何一点究竟储藏有多少真空能量和能被取出来多少? 为什么从真空中出来的负能量不和宇宙中现有的正能量发生湮灭? 如何使 74% 的具有负能的暗能量 Λgμν 保持宇宙的真实的平直性? 用量子场论解决上述问题就难免不违反宇宙的根本规律—因果律.由此可见,任何新理论,包括量子场论在内,如要恰当的解释我们宇宙的加速膨胀就必不可违反宇宙的平直性,而且要使 **Ω** 比当今的准确的观测值 ($\Omega = 1.02 \pm 0.02$)[4]还要准确.

其实,一些科学家和一些观测並不支持有 "神秘暗能量" 或 "有排斥力的暗能量"的存在.

意大利国家核物理研究所的里奥托称: "宇宙的加速膨胀不需要神秘暗能量,它只不过是被忽略的大暴涨后的膨胀效应."[5]

欧洲航天局的 XMM 牛顿天文望远镜的科学家们观测到了炽热气体在古老星系团和年青星系团中的比例是一样的,他们认为只有宇宙中不存在暗能量才能解释这种现象.[6] 然而,现今 ($T^1\mu\nu + T^2\mu\nu$)的总量是太少了,不足以维持宇宙的平直性和使宇宙的实际密度 ρ_r 极为接近其临界密 ρo. 因此, $T^3\mu\nu / T\mu\nu \approx 74\%$是维持宇宙的平直性所必需的. 但是,这里的 $T^3\mu\nu$ 应当是那些未被观测到的和看不见的而有正能的暗能量.[3][4]

在 2007 年 1 月 8 日,一个美国科学研究小组宣布,经过几年的努力,他们首次绘出了我们宇宙暗物质的三维图.他们指出,在我们宇宙,大约有 1/6 是可见物质, 其余的 80%以上都是暗物质.[7] 他们实际上否定了暗能量的存在.

近代宇宙学通常将宇宙学项并入物质场的能量-动量张量,这就相当于引进一个能量密度的能量-动量分布: 即 $\rho\Lambda = \Lambda/8\pi G$, 或者 $p\Lambda = -\Lambda/8\pi G$.[4] 因而**近代宇宙学从引进 ρΛ 和 pΛ 已经实际上认为热能的排斥力是宇宙中引力的天然的对抗者**. 因此, 近代宇宙学是无需有排斥力的暗能量的.

III. 黑洞在吞噬外界物质或与其它黑洞碰撞后的膨胀规律

根据施瓦兹恰尔德对广义相对论的特殊解,任何真正的引力黑洞或者说施瓦兹恰尔德黑洞(RCBH),即无电荷无旋转和球对称黑洞存在的必要条件是:

$R_b = 2GM_b/C^2$, or $R_bC^2/2G = M_b$ [9][2] **(3)**

M_b-- 黑洞的质量, R_b--黑洞的施瓦兹恰尔德半径, C—光速, M_θ —太阳质量,C--引力常数,

A。当黑洞吞噬外界物质**时,**

$M_b = 4\pi\rho_b R_b^3/3$ (4)

从公式(3) 和 (4),

$3C^6 = 32\pi G^3\rho_b M_b^2$ (5)

$dR_b = (2G/C^2)dM_b$ (6)

$dR_b/dt = (2G/C^2)\, dM_b/dt$ (6a)

公式(3), (4), (5) 和 (6) 表明, 当 M_b 由于吞噬外界物质而增加 10 倍时, 其密度 ρ_b 会降低 100 倍, 而 R_b 增加 10 倍.

黑洞视界两对面的相对膨胀速度 V_b 是: $V_b = 2dR/dt$, 因此,

$V_b = (4G/C^2)\, dM_b/dt \leq 2C$ (6b)

在 $dR_b/dt = C$ 的条件下, 当 dt = 1 秒时, $dM_b/dt = 2\times10^{38}$g/sec, 这相当于每秒吞噬外界物质达到 10^5 太阳. 所以 $V_b = 2C$ 可能是一个黑洞每秒吞噬外界物质所能达到的最高速度.当无外界物质可吞噬时, $V_b = 0$.

黑洞视界的膨胀的加(或减)速度 a_b 是: $a_b = dV_b/dt$, 于是,

$a_b = (4G/C^2)d^2M_b/dt^2$ **(6c)**

公式(6c) 表明, **黑洞视界的加(或减)速膨胀 a_b 直接正比例于其每秒吞噬外界物质的增多或减少. 因此, 黑洞吞噬外界物质所造成的加(或减)速膨胀是其正常的活动的表现.** 从公式(3) 和 (6),

$R_b + dR_b = (2G/C^2)(M_b + dM_b)$ (6d)

B. 从公式(3), **如果两个黑洞M_{b1} 和 M_{b2} 碰撞以后**, R_{b1} 和 R_{b2} 分别是其施瓦兹恰尔德半径, 于是, $R_{b1}C^2/2G = M_{b1}$, $R_{b2}C^2/2G = M_{b2}$, 结果为:

$M_{b1} + M_{b2} = (R_{b1}+R_{b2})\, C^2/2G$ **(7)**

这样一来, 一个新的黑洞形成了,其质量是 $M_{bn} = M_{b1} + M_{b2}$, 其施瓦兹恰尔德半径是 $R_{bn} = (R_{b1}+R_{b2})$.

结论: 从公式 (6d) and (7)可见, 一旦一个黑洞形成了,不管它是增多或减少其质量,或甚至与其它黑洞相碰撞,它仍然是一个黑洞, 在它最后收缩成为 10^{-5}g 的最小黑洞(MGBH)而消失前,它将永远是一个黑洞.[1][2]

IV. 我们宇宙一直就是一个真实的宇宙黑洞 (UBH).

为了解释我们宇宙作为一个真实的宇宙黑洞 (UBH)的特性,两个较精确地有关我们宇宙的观测数据将采用如下. (a). 我们宇宙从大爆炸到现在的年龄 A_u 是: **$A_u = 13.7\times10^9$yrs**.[3] (b)**. 哈伯常数, $H_o = (0.73\pm0.05)\times100$kms^{-1}Mpc^{-1}** [4]. 如果上述两个数据较可靠的话,可得出如下结果. (a). 如果我们的银河系处在足够大的宇宙中,则我们宇宙现今的**可视半径 R_{uv}** 是: **$R_{uv} = C\times A_u = 1.3\times10^{28}$cm,** 就是说,可观测的最远的星云离我们大约 1.3×10^{28}cm, 这就是光在我们宇宙年龄 A_u 内的行程, 我们宇宙的可视视界为 $2R_{uv}$. (b). **我们宇宙的实测密度 ρ_r 为: $\rho_r = 3\, H_o^2/(8\pi G) \approx 10^{-29}$g/cm^3**.

A. 现在按照实测密度$\rho_r \approx 10^{-29}g/cm^3$, 我们宇宙黑洞 ($M_{ub}$) 可按黑洞公式计算出来. 设 M_{ub} 是我们宇宙黑洞的能量物质的总量, R_{ub} 是起施瓦兹恰尔德半径. 从公式(3) $R_{ub}C^2/2G = M_{ub}$, 和公式 (4) $M_{ub} = 4\pi\rho_r R_{ub}^3/3$, 和 $\rho_r \approx 10^{-29}g/cm^3$, 可算出, **我们宇宙黑洞的组成是: $M_{ub} = 8.5\times10^{55}g$, $R_{ub} = 1.265\times10^{28}cm$, $\rho_r \approx 10^{-29}g/cm^3$.**

B. 证实我们宇宙 (M_{ub})是真正的宇宙黑洞的确凿证据. 如果我们宇宙(M_{ub})是真正的宇宙黑洞, 它应当由宇宙大爆炸所产生的大量原始的最小黑洞MGBH (i.e. MGBHs its $M_b \approx 10^{-5}g$, $R_b \approx 1.5\times 10^{-33}cm$, $T_b \approx 0.65\times10^{32}K$, 参考 [1]) 所组成, 设 MGBH 的总数 N_{ub1} 是: $N_{ub1} = M_{ub}/MGBH = 8.5\times10^{55}/10^{-5} = 8.5\times10^{60}$. 同时, 从公式 (7) 可见, $N_{ub2} = R_{ub}/R_b = 1.265\times10^{28}cm/1.5\times10^{-33}cm = 8.43\times10^{60}$. **由于 $N_{ub1} = N_{ub2}$, 这就是确凿的证据表明我们宇宙是一个真正巨大的宇宙黑洞--UBH.**

C. 宇宙的平直性和 ($\Omega = \rho_r / \rho_o \approx 1$) 是宇宙黑洞的本性: 按照哈伯定律,在我们宇宙,距离任何一点P为R_p 的相对膨胀速度V_p为, H_o--哈伯常数,

$$V_p = H_o R_p \qquad (8)$$

从公式(3)和 (4), 在黑洞视界上,当 R_p 延伸到 R_{ub} 时, $V_p = C$, 于是,

$$H_o^2 = 8\pi G \rho_o /3 \qquad (9)$$

既然我们宇宙是一个真正的宇宙黑洞,它就必然是一个封闭的球体; 因此, ρ_o 就是我们宇宙黑洞的临界密度, 从公式 (3) 和 (4)可知,它是单值且仅由 M_{ub} 或 R_{ub} 所决定.[2] 然而,宇宙的实际密度 ρ_r 也是来自同一个观测的 H_o, i.e. $H_o^2 = 8\pi G \rho_r /3$. 其必然结果是: **ρ_r 应完全等于公式 (9) ρ_o**, 所以, **($\Omega = \rho_r/\rho_o = 1$) 是宇宙黑洞的本性. 反过来, $\Omega = \rho_r/\rho_o = 1$** 也可证明我们宇宙是一个真正的宇宙黑洞.

D. 由于 $R_{ub} < R_{uv}$ ($R_{ub} = 1.265\times10^{28}cm$, $R_{uv} = C\times A_u = 1.3\times10^{28}cm$), **人类可观测到的最远的边界只能是宇宙黑洞的视界半径R_{ub}, 而不是虚构的宇宙黑洞M_{uv} 的视界半径 R_{uv}.**

设 ρ_{ov} 被不同于黑洞理论的其它理论定义为宇宙的临界密度,严格的说,公式(3) 不能用之于决定 ρ_{ov}, 因为在我们宇宙黑洞之外的 M_{uv} 的真实状况是无法知道的. 然而, 近代宇宙学中, ρ_{ov} 实际上是一个假想值,而按照公式(3) 和(4)从虚构的 M_{uv} 和 R_{uv} 计算出来. 于是**, M_{uv}, R_{uv} and ρ_{ov} 被人为的形成了一个虚构的而大于我们的以确定的 R_{uv} 为视界半径的虚宇宙黑洞 (M_{uv}).** 虚宇宙黑洞的组成是: $R_{uv} = 1.3\times10^{28}cm$, $M_{uv} = 8.77\times10^{55}g$, $\rho_{ov} = 0.95\times10^{-29}g/cm^3$. 因此,所谓的 **$\Omega$ 就成为: $\Omega = \rho_r/\rho_{ov} = 10^{-29}g/0.95\times10^{-29} = 1.05$. 然而, 这里的 ρ_r/ρ_{ov} 实际既是两个宇宙黑洞的密度之比,而不是一个宇宙黑洞的实际密度与其临界密度之比.只是由于现今 $R_{ub} \approx R_{uv}$, $M_{ub} \approx M_{uv}$, $\Omega = \rho_r/\rho_{ov} \approx 1$, Ω 才被多数宇宙学者们用来作为判断宇宙未来命运的判别式:是封闭宇宙还是开放宇宙.既然我们宇宙如上所证明是一个真实的宇宙黑洞,它就是一个封闭宇宙,定义一个宇宙黑洞的 Ω 是没有意义的.**

因此, 我们现在可见的宇宙是我们的宇宙黑洞-- M_{ub}, 而不是虚宇宙黑洞-- M_{uv}.

如果我们宇宙黑洞(M_{ub})之外还有足够多的能量物质可供吞噬, 在 n 年之后, M_{ub} 将扩大到现在的虚宇宙黑洞 M_{uv}. $n = (R_{uv} - R_{ub})/C = (1.3\times10^{28}-1.265\times10^{28})/3\times10^{10} = 3.7\times10^8$yrs. 然而,到那时, 宇宙年龄 A_u 将不是现在的 13.7×10^9 年, 而是 $A_u + n = 14.07\times10^9$ 年.

E. 我们宇宙黑洞的视界($2R_{ub}=2.53\times10^{28}cm$) $\le$ ($2R_{uv} = 2C\times A_u = 2.6\times10^{28}cm$). 这表明宇宙黑洞的视界的相对膨胀速度从大爆炸到现在平均几乎等于 2C.

V. 我们宇宙的加速膨胀(AEOU) 是由于两大宇宙黑洞在其早期的碰撞所造成的.

从上述的论证可知**,** 既然我们现在的宇宙是宇宙黑洞 M_{ub}, 而不是虚宇宙黑洞 M_{uv}. 因此, 我们宇宙的加速膨胀 AEOU 就是我们宇宙黑洞 M_{ub} 的加速膨胀 AEOUBH.

我们宇宙的加速膨胀 (AEOU) 是通过对遥远的 Ia 型超新星爆炸的观测所发现的. AEOU 是发生在大爆炸的约 5×10^9 年之后而距今约 9×10^9 年.下面 AEOU 将被两个宇宙黑洞(UBHs)的碰撞来解释和论证.

假设在 **9×10^9 年以前, 我们的小宇宙黑洞 M_{ub1} 与另一个大宇宙黑洞 M_{ub2} 发生碰撞或掉入其内,会发生什么事呢?**

设 M_{ub1} 是小宇宙黑洞的总质量**,** R_{ub1} 是其施瓦兹恰尔德半径, N_{o1} 是组成 M_{ub1} 的 MGBHs ($M_b \approx 10^{-5}g$, $R_b \approx 1.5\times 10^{-33}cm$, $T_b \approx 0.65\times10^{32}K$) 总数.

设 M_{ub2} 是大宇宙黑洞的总质量, R_{ub2} 是其施瓦兹恰尔德半径.

对 M_{ub1} 和 M_{ub2} 碰撞后的分析如下.

A. 一旦小 M_{ub1} 与大 M_{ub2} 在约 9×10^9 年前发生碰撞**,** 从公式(7) 可知, $M_{ub1} + M_{ub2} = (R_{ub1} + R_{ub2}) C^2/2G$, 这就是说, M_{ub2} 由于俘获 M_{ub1} 必定增大其施瓦兹恰尔德半径到 ($R_{ub2} + R_{ub1}$). 于是, M_{ub2} 在Δt 时间内得到一个视界的膨胀速度V_{ub22}, $V_{ub22} = R_{ub1}/\Delta t$. 又假如$M_{ub2}$的视界在碰撞前未充分膨胀到$R_{ub2}$, M_{ub2} 就应有一个原始暴涨的膨胀余波速度V_{ub21}. 又假如M_{ub2} 外有能量物质可供吞噬,它就又有一 个膨胀速度 V_{ub23}. 因此, **M_{ub2} 的视界的总膨胀速度V_{ub2} 是: $V_{ub2} = (V_{ub21} + V_{ub22} + V_{ub23})$.**

B. 回头来看我们原始的M_{ub1}, 一旦原始的M_{ub1} 在约 9×10^9 年前与M_{ub2} 相碰撞, 它就能从M_{ub2} 吞噬能量物质, 从公式(7) 可知, M_{ub} 是从 M_{ub1} 发展出来的现有的宇宙黑洞, 于是, $M_{ub} = M_{ub1} + \Delta M_{ub12} + \Delta M_{ub13} = (R_{ub1} + \Delta R_{ub12} + \Delta R_{ub13}) C^2/2G = R_{ub}C^2/2G$. 假如 M_{ub1} 在碰撞前未充分膨胀到 R_{ub1}, M_{ub1} 就应有一个原始暴涨的膨胀余波速度 V_{ub11}.在通常情况下, M_{ub1} 只能从M_{ub2} 吞噬能量物质 ΔM_{ub12}, 这将导致 R_{ub1} 膨胀 ΔR_{ub12} 和得到膨胀速度$V_{ub12} = \Delta R_{ub12}/\Delta t$. 然而, **由于$M_{ub2}$ 有总膨胀速度 $V_{ub2} = (V_{ub21} + V_{ub22} + V_{ub23})$, M_{ub2} 能使 M_{ub1} 产生一个附加的空间膨胀ΔR_{ub13},** 而导致 M_{ub1} 吞噬更多的能量物质 ΔM_{ub13}. 因此, M_{ub1} 会得到一个附加的空间膨胀速度$V_{ub13} = \Delta R_{b13}/\Delta t$. 结果**,** M_{ub1} 的视界的总膨胀速度**V_{ub1} 是: $V_{ub1} = V_{ub11} + V_{ub12} + V_{ub13}$.**

结论: 由于小宇宙黑洞 M_{ub1} 与另一个大宇宙黑洞 M_{ub2} 相碰撞, 而 M_{ub1} 从 M_{ub2} 吞噬能量物质达 90 亿年之久. 由此可见, 小宇宙黑洞 M_{ub1} 加速膨胀的主要原因是 M_{ub2} 的总膨胀速度 V_{ub2} 使 M_{ub1} 产生的空间膨胀速度 V_{ub13}，其次原因是从大宇宙黑洞 M_{ub2} 不断地吞噬大量的能量物质而得到 V_{ub12}. 如果没有 9×10^9 年前发生的碰撞, 我们原始的 M_{ub1} 决不会长大,而反会因发射霍金辐射变得稍为小一点点. **由于现在的 $R_{bu} \approx C\times A_u$, 这表明我们宇宙黑洞视界平均的膨胀速度已几乎达到 2C.** 因此, 按照公式(7)的原理,原始宇宙黑洞 M_{ub1} 与现今宇宙黑洞 M_{ub} 之比是: $M_{ub1}/M_{ub} \approx (13.7\times10^9 - 9\times10^9)/13.7\times10^9 \approx 4.7\times10^9/13.7\times10^9 \approx 34.3\%$, 相应地, M_{ub1} 的原始 R_{ub1} 是: $R_{ub1}/R_{ub} \approx 34.3\%$; 从 9×10^9 年前直到现在 M_{ub1} 增加的质量 ΔM_{ub} 是: $\Delta M_{ub}/M_{ub} \approx 9\times10^9/(13.7\times10^9) \approx 65.7\%$, 而增加的 ΔR_{ub} 是: $\Delta R_{ub}/R_{ub} \approx 65.7\%$. 如是,

$$\mathbf{M_{ub1}/M_{ub} \approx 34.3\%,\quad R_{ub1}/R_{ub} \approx 34.3\%}$$
$$\mathbf{\Delta M_{ub}/M_{ub} \approx 65.7\%,\quad \Delta R_{ub}/R_{ub} \approx 65.7\%} \quad \mathbf{(10)}$$

VI. 两类黑洞的不同的演变过程和相同的最后命运,

A. 质量大于 $3M_\theta$的致密恒星塌缩成黑洞的演变过程简单扼要地叙述如

当一个质量大于 $3M_\theta$ 的致密超星星爆炸塌缩后,其余烬会成为一个黑洞,其所有的能量物质 M_b 将扩充到 R_b 内的空间.(注释: 大多数科学家们认为在任何黑洞中心均有一个奇点, [9] 但作者已确认黑洞中心绝不可能存在奇点. [1][2]). 根据霍金的黑洞理论,如果黑洞外部有能量物质,它将被黑洞最终完全地吞噬进去.同时,黑洞会扩展它的体积和 R_b, 降低其温度. 如果黑洞外已无任何能量物质, 黑洞只能发射霍金辐射而极其缓慢地收缩其体积,提高其温度, 以至最终收缩成为最小引力黑洞, 即 MGBH, (its $M_b \approx 10^{-5}$g,$R_b \approx 1.5\times10^{-33}$cm, $T_b \approx 0.65\times10^{32}$K, 参见 [1]). 一旦黑洞收缩成为 MGBH 就不再收缩,而是立即在最强烈的爆炸中解体和消失, 这是所有黑洞最后的共同命运, 因为在 MGBH 内由高温所产生的排斥力大大地超过了其总能量物质的引力. [10][1][2]

根据霍金的黑洞理论,任一个黑洞的寿命 τ_b (从黑洞 M_b 的形成到收缩成为 MGBH) 是:

$$\tau_b \approx 10^{-27} M_b^3 \text{ (s)} \quad [11][1][2] \qquad (11)$$

例如,一个质量≈ $3M_\theta$ 的致密恒星塌缩成黑洞,当其外界无能量物质时,其寿命 $\tau_b \approx 2\times10^{65}$ 年.

$$d\tau_b \approx 3\times10^{-27} M_b^2 dM \text{ (s)} \quad [12][2] \qquad (11a)$$

假设我们现今宇宙黑洞 $M_{ub} = 8.5\times10^{55}$g, 而且外界已无能量物质可供吞噬并开始发射霍金辐射.一年之后, 即 $d\tau_b = 1$ 年, 我宇宙黑洞所损失的质量约为: $dM \approx 3\times10^7\times10^{27}/[3\times(8.5\times10^{55})^2) \approx 10^{-74}$g/yr.

B. 我们宇宙黑洞(UBH) 的演变过程.

我们宇宙作为一个宇宙黑洞(UBH-- M_{ub})的演变过程是与上述由致密恒星塌缩成黑洞的演变过程大不相同的. 作者在以前的文章<<**对黑洞和大爆炸的新概念—两者都无奇点**>>[1][2] 中指出, 13.7×10^9 年前,我们宇宙诞生于极大量的 ($N_{ub1} = N_{ub2} = 8.5\times10^{60}$, see IV) 原始最小引力黑洞 MGBHs, (其 $M_b \approx 10^{-5}$g, $R_b \approx 1.5\times10^{-33}$cm, $T_b \approx 0.65\times10^{32}$K) 的合并所产生的大爆炸, 而后演变膨胀至现在的宇宙. [1]

我们宇宙作为一个宇宙黑洞 (UBH-- M_{ub}) 未来的命运和寿命取决于其外面是否仍然有能量物质可被吞噬.如果现在已无能量物质在外面, 我们宇宙黑洞就只能发射霍金辐射而极其缓慢地收缩其体积,提高其温度,经过极长的 τ_b 年后, M_{ub} 会最终收缩成为最小引力黑洞 (即 MGBH), 而立即在最强烈的爆炸中解体和消失. 如果现今的 $M_{ub} = 8.5\times10^{55}$g,则 $\tau_b > 10^{-27} M_{ub}^3 = 10^{-27}\times(8.5\times10^{55})^3 > 10^{133}$ 年.

然而我们宇宙黑洞现在还在膨胀. 这表明在宇宙黑洞外仍然有大量能量物质可供吞噬. 宇宙黑洞还要继续长大.直到所有外界能量物质被吞噬完后,宇宙黑洞就会停止膨胀,而后发射霍金辐射，极其缓慢地收缩其体积,提高其温度, 以至最终收缩成为最小引力黑洞后 (即 MGBH,其 $M_b \approx 10^{-5}$g)而在最强烈的爆炸中解体和消失.

虽然两种黑洞有不同的演变过程,但它们最终都会收缩成为最小引力黑洞后(即 MGBH,其 $M_b \approx 10^{-5}$g)而在最强烈的爆炸中解体和消失.这就是它们共同的命运.

VII. 在我们宇宙,所有的能量物质粒子都同时具有引力和热能所产生排斥力.各个粒子之间都有这两种力同时作用着,以维持在各种不同条件下的平衡.宇宙中无需有排斥力的暗能量,它们也可能真的不存在.

在我们宇宙中,现在所有的黑洞 BH 包括我们宇宙黑洞 UBH 都是具有极长寿命的稳定实体. 既然如此,每个黑洞内部的平衡和稳定是很重要的. 在宇宙中, 每个能量物质粒子都同时有质量所产生的引力和温度所产生的热排斥力,甚至中微子和光也不例外, (任何光都有其等效的质量 m_s, $m_s = h/C\lambda$, 对于热, $m_s = \kappa T/C^2$). 引力和热压力总是不可分离的共存于各种粒子中. 因此,任何黑洞的内部平衡都是其引力和热压力在各种不同条件下对抗达到其动态平衡的结果.

我们宇宙黑洞内,任何较稳定的原始星云和星系团中,在理想的球对称的条件下,任何一点的粒子 m_s 的引力与其热压力 P 说应当达到热动力平衡. ρ—密度, G—引力常数. κ—波尔兹曼常数, R—质量中心和 m_s 的距离, M—在 R 为半径的球内的总质量,

$$dP/dR = -GM\rho/R^2 \quad [8][2] \qquad (12)$$
$$P = n\kappa T = \rho\kappa T/m_s \quad [8][2] \qquad (13)$$

我们宇宙黑洞内, 公式(12) 和 (13) 可普遍地应用于星系和星系团的气态部分,与其中心有无超重级黑洞没有关系. 此二公式与其它边界条件公式一起曾被作者成功地用于解决了任何黑洞包括宇宙黑洞中的许多重大问题. [2] 此二公式表明, **在任何黑洞内, 热能的排斥力的增加永远地在对抗着能量物质的引力收缩.** 甚至白矮星和中子星都是在特殊条件下热能

的排斥力和能量物质的引力对抗达到平衡的结果(可参考 Tolman-Oppenheimer-Volkoff 方程). 在我们宇宙内,任何物体的解体的爆炸都是其内部的热压力大大地超过其引力的结果.

我们宇宙黑洞内,除了引力之外,还有其它的三种作用力,即电力,弱作用力和强作用力. 它们可在极短的距离内将粒子组成极坚实的物体,如金刚石, 白矮星和中子星等.**这些作用力的改变也会改变粒子的热状态即温度**。 然而,**只有引力和热压力在不同条件下的平衡才在宇宙的演变过程中起决定作用.** 足够大量的高密度能量物质能压垮任何坚实的物体而继续塌缩成为黑洞.一旦一个致密恒星塌缩成为黑洞,它不再收缩, 会因吞噬外界能量物质而膨胀.**在黑洞内,只有由于引力收缩所形成的高温压力才能对抗引力的进一步收缩**.

由此可见,**在我们宇宙内, 根本无需引进有排斥力的暗能量以对抗引力收缩.**

VIII. 下面将做进一步的分析和论证并得出一些有益的结论.

虽然前面的论证和计算多为定性分析,而远非是精确的完善的定量分析. 然而,只要观点的基础可靠,还是可以得出许多重要而有意义的结论.

A. 按照上面的计算, 我们宇宙黑洞现在的年龄A_u =13.7×10^9 年,其平均的**视界的膨胀速度V_{ub1}几乎达到 2C,**即 $V_{ub1}\approx$ 2C (在A_u内的平均值) 或者 $R_{ub} \le (C\times A_u = R_{uv})$. 这表明我们宇宙黑洞的质量中心有足够的时间将其中心引力传递到整个视界上的质点. 于是, $(R_{uv.} = C\times A_u \ge R_{ub})$ 就是现在我们宇宙黑洞存在的必要条件,这也就是我们宇宙或者说宇宙黑洞保持其平直性的必要条件. 一旦若 $R_{ub} > R_{uv}$, 这就表明宇宙黑洞内某些部分 $(R_{ub} - R_{uv})$的质点将不受中心引力的作用,而造成黑洞的不稳定.

B. 在我们宇宙黑洞的演变过程中,有两种不同的膨胀形式. (V_{ub1}> 2C)的膨胀可能仅由黑洞之间的碰撞或合并所产生的短暂地**空间膨胀**造成.例如, V_{ub1}>> C 就发生在大爆炸后的暴涨瞬间. 那时,极大量的最小引力黑洞(即 MGBH, 其单个质量 = 10^{-5}g)的合并造成了整个新生宇宙的空间大膨胀.[1] 这种空间膨胀完全不同于以后**黑洞吞噬外界能量物质的视界膨胀**.视界膨胀是不可能产生 (V_{ub1}> 2C) 和 ($R_{uv} < R_{ub}$)的情况. [参考 (6b), $V_b \le 2C$].

C. 由于$R_{uv.}$= C×A_u = 1.3×10^{28}cm, 这计算来自A_u =13.7×10^9 年. 然而, R_{ub} = 1.265×10^{28}cm 却来自哈伯常数H_o = (0.73±0.05) ×100kms^{-1}Mpc^{-1}. R_{uv} 和 R_{ub} 的数值相差是如此之小,这使我们无法准确地判断V_{ub1} 的膨胀速度现在是等于 2C还是稍小于 2C. 如果V_{ub1} = 2C, 这表明我们宇宙黑洞M_{ub} 外尚有充足的能量物质可供吞噬.如果V_{ub1} 稍小于 2C,这表明我们宇宙黑洞 M_{ub} 外的能量物质已经减少,以后就可能愈来愈少. [见公式(6b) 和 (6c)].

D. 当我们原始宇宙黑洞M_{ub1} 在与M_{ub2} 碰撞后,在 90 亿年间由于吞噬能量物质而增多的质量ΔM_{ub} 在通过黑洞视界后会完全转变成能量.按照公式 (10), $\Delta M_{ub} / M_{ub}$ = 65.7%, 和 M_{ub1}/ M_{ub} =34.3%. 那么,**所有由ΔM_{ub} 转变成的能量是否就是现在宇宙中有引力的暗能量呢?** 而现在宇宙中的可见物质和暗物质的总和是否就是来自我们原始宇宙黑洞M_{ub1}? 如果假想 我们原始宇宙黑洞M_{ub1} = 26% M_{ub} = $T^1\mu\nu + T^2\mu\nu$ (参见 II), 和 ΔM_{ub} = 74%M_{ub} = $T^3\mu\nu$,那将如何?

E. 不管M_{ub2} 现在仍有多少能量物质,它的总量终归是有限的.一旦在未来达到M_{ub} = M_{ub1} + M_{ub2} **而且** $R_{ub} = R_{ub1} + R_{ub2} = (M_{ub1} + M_{ub2})2G/C^2$ 时,就达到了V_{ub} = 0 的完全膨胀.而后就会发射霍金辐射并开始收缩, 直到最后收缩成为 10^{-5}g 的 MGBH而立即在最强烈的爆炸中消失.

IX. 我们与宙的膨胀模式。

A. (a) **如果 90 亿年前我们原始宇宙小黑洞M_{ub1}和宇宙大黑洞M_{ub2}没有发生碰撞,又如果M_{ub1}外边没有能量物质**, M_{ub1} 就会一直是一个孤立的宇宙黑洞, 它只能在大爆炸后由暴涨产生的余波而减速膨胀. 在充分膨胀后,按照公式(10),如果 $M_{ub1}/ M_{ub} \approx$ 34.3%, $R_{ub1}/R_{ub} \approx$34.3%, R_{ub1} 就会在 90 亿年前达到$R_{ub1} = 2GM_{ub1}/C^2$,此时$V_{ub1} = V_{ub11}$= 0 而停止膨胀. (b). 此后M_{ub1} 就不再膨胀,反而由于持续地发射霍金辐射而极其缓慢的收缩,减小其质量,直到最后M_{ub1} 收缩成为 10^{-5}g 的 MGBH而立即在最强烈的爆炸中解体和消失.我们原始宇宙小黑洞M_{ub1} 在暴涨后直到其最后消失就决不会再出现加速膨胀. 因此, **在这种模式不是我们宇宙的膨胀模式。**

B. 既然现在宇宙黑洞M_{ub}的$R_{ub} \approx C\times A_u$,而其视界的膨胀的平均速度$V_{ub1}$ 在宇宙年龄A_u内几乎达到V_{ub1}= 2C,**故必然会在长期的A_u 时间内,在不同的特别时期会出现 (V_{ub1}> 2C) 或 (V_{ub1} < 2C) 的情况. 宇宙黑洞视界的膨胀速度V_{ub1}> 2C情况的出现应有两次. (a).** V_{ub1}>>> 2C 的极大极快的膨胀出现在大爆炸后的暴涨瞬间, 因大量的原始小黑洞MGBH的合并造成整个宇宙的空间大膨胀. (b). V_{ub1}> 2C会出现在 90 亿年前,那时我们原始宇宙小黑洞M_{ub1} 的减速膨胀速度已经达到V_{ub1}= V_{ub11}= 0 而停止了膨胀.当M_{ub1} 与M_{ub2} 碰撞后,从那时起到现在,如要保持平均膨胀速度V_{ub1}=2C,就会由碰撞后产生的**空间膨胀**在一段短时间内必然由V_{ub1}= 0 达到V_{ub1}>2C,因为碰撞后一方面M_{ub2} 的膨胀造成M_{ub1} 的空间膨胀,另一方面, M_{ub1} 又从 M_{ub2} 吞噬大量的能量物质. (参考第 V节). 由此可见,**只有黑洞的碰撞和合并, 才有可能使黑洞产生空间膨胀和可能使黑洞视界膨胀速度加速到 (V_{ub1} > 2C)。**

(c). 既然 V_{ub1}>2C 已经两次发生在宇宙年龄 A_u,内, 为了能保持 $R_{ub} \approx C\times A_u$, 而原始宇宙黑洞 M_{ub1} 的[V_{ub1}< 2C 到 V_{ub1} →0]也必然会发生在暴涨后到 90 亿年前与 M_{ub2} 碰撞前的这段长时期内. 由于在此期间我们原始宇宙小黑洞 M_{ub1} 无能量物质可吞噬, 它只能靠大爆炸后的暴涨所产生的 V_{ub1}>>>2C 的膨胀余波减速到 V_{ub1}<2C 而后一直减速到碰撞前达到 V_{ub1}= V_{ub11}= 0 的完全膨胀.如果 M_{ub1} = 34.3% M_{ub} [见公式 (10)], R_{ub1} 将从暴涨后的 R_{ub1} <<<34.3% R_{ub} 将减速膨胀到两黑洞碰撞时的 90 亿年前,真好达到 R_{ub1} = 34.3% R_{ub} 而停止膨胀 。 (d).当我们原始宇宙小黑洞 M_{ub1} 在 90 亿年前与 M_{ub2} 碰撞后就会又产生一次 V_{ub1}>2C 视界的加速膨胀.如上面的(b)小节所述. (e). 当 V_{ub1}>2C 加速膨胀达到极限后,就会靠 V_{ub1}>2C 后的余波而减速膨胀,直到从 V_{ub1}>2C 的膨胀减速到在某一时间而达到 V_{ub1}= 2C (比如说在 70 亿年前)。 (f).从此以后, 我

们宇宙黑洞 M_{ub} (M_{ub} 是 M_{ub1} 与 M_{ub2} 在碰撞后转变而来)就会由于吞噬足够大量的能量物质而以 $V_{ub1} \approx 2C$ 的膨胀速度膨胀到现在.当然,这中间也可能出现由 $V_{ub1}>2C$ 到 $V_{ub1} \approx 2C$ 的几次反复震荡.但是无论如何, 视界的空间膨胀速度 V_{ub1} 的涨落必然应当符合 $R_{ub} \approx C\times A_u$ 的总的实际情况.

从上面的分析可知,正是由于我们原始宇宙黑洞 M_{ub1} 于 **90 亿年前在碰撞前的长期减速膨胀, 而在碰撞后有一段不短的加速膨胀时间,即从 $V_{ub1}= 0$ 加速到 $V_{ub1}>2C$ 的极限. 这就使科学界在 1998 年观测到了我们宇宙在碰撞后的加速膨胀.**

结论：上面从(c)到(f)的过程是符合我们宇宙的膨胀模式的。

C. 再假设当我们原始宇宙黑洞M_{ub1}在其出生时就等于现在的宇宙M_{ub}即 $M_{ub1}= 100\% M_{ub}$, 而在宇宙年龄A_u 内从未与其它宇宙黑洞发生碰撞,也无吞噬外界能量物质,其演变过程应是怎样呢? (a). 新生宇宙在大爆炸后的暴涨会导致我们宇宙视界 R_{uv}极其小于黑洞视界R_{ub},即 $R_{uv} <<< R_{ub}$. (b). 宇宙黑洞从暴涨后到现在就由暴涨的余波一路地减速,从$V_{ub1} >>> 2C$到$V_{ub1} << 2C$ 直到现在的$V_{ub1}= 0$ 达到$R_{ub} = 2GM_{ub}/C^2$ 的完全膨胀,因为现在正好是$R_{ub} = C\times A_u$. (c). 由于R_{uv} 正比于宇宙年龄 A_u,即$R_{uv} = C\times A_u$, 这将使R_{uv} 因M_{ub} 的余波减速膨胀终于在现在赶上R_{ub}, 即现在达到$R_{uv} = R_{ub} = C\times A_u$ 和 $V_{ub1}= 0$ 的完全膨胀. (d).从现在起, 宇宙黑洞M_{ub}的 R_{ub} 将不再膨胀而发射霍金辐射. M_{ub}会由于长期不断地发射霍金辐射而逐渐收缩和减少质量直到最后变成MGBH而在强烈的爆炸中消失. 这就是说,这个虚设的模式从暴涨后到现在应该是一路上地减速膨胀,而不会有任何加速膨胀出现. **这种模式不是我们宇宙的膨胀模式**

D. 再一种假想的宇宙演变模式是这样的.假设在大爆炸时,我们原始宇宙小黑洞M_{ub1} 非常的小,从大爆炸到现在的宇宙年龄A_u时间内,时时刻刻在吞噬外界的足够多的能量物质,使其能达到几乎$V_{ub1} \equiv 2C$. 这也可以使在现在达到$R_{ub} \approx R_{uv} = C\times A_u = 1.3\times 10^{28}$cm. 但这种演变模式就要否定暴涨,而且在整个演变过程中既无加速,也无减速. 这不符合实际情况,因为大爆炸不能没有暴涨. **这种模式也不是我们宇宙的膨胀模式**

从 A 段到 D 段,我们设想了好几种宇宙的演变模式.但只有 B 段的演变模式较复合实际情况. 这清楚地表明在 90 亿年前出现的宇宙加速膨胀可能确实是由两宇宙黑洞的碰撞造成的.

------全文完------

References:

[1]. Dongsheng Zhang: New Concepts to Big Bang And Black Holes—Both Had No Singularity at All (Part 1)

[2]. Dongsheng Zhang: New Concepts to Big Bang And Black Holes—Both Had No Singularity at All (Part 2) Two articles above were published on magazine "Nature and Science", 2(3), 2(4),3(1), or debate-001, 2004, ISSN:1545-0740, Published by Marsland Company, P.O.Box 753, East Lansing, Michigan, MI 48826 U.S.A. http://www.sciencepub.org/nature/debate-001 http://www.sciencepub.org/nature/0203 and 0204 http://www.sciencepub.org/nature/0301

[3].王义超: 暗能量的幽灵. 中国 <财经> 杂志, 总 176 期, 2007-01-08. http://www.caijing.com.cn/newcn/econout/other/2007-01-06/15365 .shtml

[4].卢昌海: 宇宙常数,超对称和膜宇宙论. http://www.changhai.org/2003-08-17

[5].对暗能量理论的挑战: 宇宙的加速膨胀不需要暗能量. http://tech.163.com/2005-04--25

[6].新发现对爱因斯坦的挑战: 暗能量可能不存在. http://tech.163.com/2006-05-17

[7].科学家首次绘出了宇宙的 3 维暗物质图. Web.wenxuecity.com/2007-05-21

[8]. 何香涛: 观测宇宙学. 科学出版社, 中国北京 2002

[9]. 约翰·格里宾: 大宇宙百科全书. 海南出版社, 2001,5.

[10]. 约翰-皮尔.卢米涅: 黑洞. 中国 湖南科学技术出版社, 2000.

[11].王永久: 黑洞物理学. 湖南师范大学出版社, 中国 湖南, 2002

[12]. Dongsheng Zhang: New Explanations to Hawking Radiation With Classical Theories. Nature and Science, 2006, 4(2). http://www.sciencepub.org/nature/0402

Note:

Primary version of this article was originally published in New York Science Journal [2008;1(2):30-35]. (ISSN: 1554-0200).

匪夷所思的电子

谭天荣

青岛大学 物理系 青岛 266071， 中国

ttr359@126.com

内容提要：电子的自旋与磁矩使人自然地联想到电子的电荷在旋转这样的直观模型，但这种模型有两个困难：第一，考虑到电子的线度，考虑到电子的边缘线速度不能超过光速，洛仑兹曾经对电子的刚球模型作过计算，电子的角动量的有一个上限，而这个上限小于其测量值。第二，如果电荷的在旋转，则电子会辐射电磁波，辐射将带走能量，而电子又没有外部能源，因此，电子会因为辐射失去能量，从而很快地崩溃。但事实上，电子却是经久不变的。我们知道，波尔从原子的卢瑟福模型看到了同一矛盾，并得出“原子世界有特殊规律”的论断。由于有这两个困难，量子物理学家们放弃了电子的直观模型。但我们即将看到，上述两个困难都可以在经典物理学的框架内予以排除。

先说电子的角动量的问题，洛仑兹在这里有一点疏忽：电子是一个带电系统，它会激发一个电磁场，它是电子的固有电磁场。由于电荷的旋转，电子的固有电磁场有角动量，它是电子的角动量的组成部分。而电子的电磁场分布在整个空间，不受电子大小的限制。考虑到这一点，电子角动量的大小就不再有洛仑兹所说的那种上限了。

再说波尔的论断：根据经典物理学，电子的内部运动满足麦克斯韦方程，至于它会满足哪一个特解，则必须根据实验事实来确定。容易证明，将麦克斯韦方程应用于电子的内部运动时，有这样一个特解：它表示当电子的电荷持续地旋转时，电子的能量却不会因此而流失。这个特解的存在表明波尔论断的原始依据是错误的，从而电子的直观模型并不是不可想象的。

对于一个静止的电子，麦克斯韦方程的上述特解表示一个“驻波场”。如果用复数表示，它由两个因子组成，一个仅含时间坐标，是时间的周期函数；另一个仅含空间坐标，表示一个静止的球面波场。如果电子作等速直线运动，则该时间因子表示一个单色平面波，而其空间因子则表示一个随着电子运动的固定波形。在一个电子束中，诸电子的固有电磁场相互迭加，形成该电子束的固有电磁场。如果电子束中的每一个电子都以相同的速度作等速直线运动，则这个电子束的固有电磁场由两个因子组成，一个因子表示单色平面波，另一个因子则是某一极为急剧变化的场函数，但其平均值却是一个常量。因此，该电子束的固有电磁场的测量值是一个单色平面波，它就是德布罗意波。由此得出结论：德布罗意波与光波都是由电子激发的电磁波，光波是离开了波源的电磁波，而德布罗意波则是伴随着波源的电磁波。

按照牛顿力学，一个物体的角动量在外界的作用下是可以改变的，从而它不可能有固定不变的角动量。但电子的角动量在外部作用下却保持不变。电子的这种行为表明，电子有一种自我调节的机制：当外部条件改变时，它总能保持不变的内部运动。例如，当电子绕原子核旋转时，电子的自我调节的机制将使得其轨道运动与自转运动相互协调，这就要求其轨道满足一定条件，满足这种条件的轨道称为“稳定轨道”。如果外界有小的扰动，电子会继续在轨道上运行。如果外界的扰动足够大，电子也会离开“稳定轨道”，进入一种不平衡状态，这时电子的自我调节的机制为了恢复电子的平衡，将迫使电子重新进入稳定轨道。如果回到了原来的稳定轨道，则不会显出宏观效果，如果过渡到另一稳定轨道，则电子经历了一个被人们称为“量子跃迁”的过程。这是电子的量子性的

最典型的表现方式。电子有磁矩，在磁场中会进入“进动”状态，为了使其进动状态与自旋相互协调，电子的自我调节机制将使得其自转轴与磁场方向保持特定的角度。电子的这种行为，称为“空间量子化”。对于电子束，诸电子的自我调节机制使得诸电子的位置分布与动量分布相互协调，电子束的这种行为的表现方式之一就是著名的海森堡关系。

所谓“不确定性”有多种含义，如果说电子的不确定性是指我们不能预言单个电子的行为，那么，这种不确定性只表明量子力学还不完备，而不表明电子的运动不是轨道运动。

[Academia Arena, 2009;1(1):79-91]. ISSN 1553-992X.

关键词：电子；自旋；磁矩；麦克斯韦方程；波粒二象性；量子性；不确定性；轨道运动；量子跃迁；量子力学

1. 引言

今天，人们非常熟悉“电子”这一用语：要看时间，手上带着电子表，墙上挂着电子钟；要看书，电子版各种书籍应有尽有，可以打开电子计算机在网上在线阅读，也可以下载下来慢慢看；要写信，可以写电子邮件，通过电子信箱投递，不仅节省了笔墨纸张，而且快得几乎没有时间延迟；要开车，驾驶台前电子仪表琳琅满目；要给孩子买生日礼物，超市的电子玩具目不暇接……。一言以蔽之，现代生活的任何一个环节似乎都少不了某种以“电子”命名的玩意。

然而，电子到底是一个什么东西，或许只有少数人才关心，也只有少数人才知道，电子的行为使人们绞尽脑汁。早在上世纪的二十年代，物理学家们就为了研究电子的行为建立了一个新的分支——量子力学，但这个量子力学却极为艰深难懂。对此，许多物理学家直言不讳。例如，美国物理学家费曼曾说：“没有人能理解量子力学。”前苏联物理学家兰道也说：“量子力学永远不可能被‘理解’，你们只须去习惯它。”或许，任何一门新的学科对于初学者都是困难的，但是量子力学的困难却不同一般，物理学领域里的一位王者，丹麦物理学家波尔曾说：“如果一个人说他可以思考量子力学而不会感到迷惑，这只不过说明他一点也不懂量子力学。”

关于量子力学的这种特殊性，中山大学的物理学教授，我的朋友关洪，有过极为精彩的描述。他对《老子》中的名言“道，可道，非常道；名，可名，非常名”作了如下重新诠释：“自然的规律和秩序是可以讲清楚的，但它们不是通常意义的规律和秩序；科学的术语和概念是可以给予称呼的，但它们不是通常意义的术语和概念。”他接着又说：“微观世界的规律是可以弄明白的，但它们不是我们习见的宏观世界的规律；量子力学的概念是可以弄明白的，但它们不是我们习用的经典物理学概念。”可见关洪教授上面说的“自然的规律”特指微观世界的规律，而他说的“科学的概念”则是特指量子力学的概念。

那么，电子的行为究竟怎样不同于宏观物体呢？我想，如下三点是特别引人注目的：

第一，波粒二象性：电子射线有时候显得是一束粒子，像由机枪射出的一粒一粒的子弹；有时候又显得是一种波动，像长江后浪推前浪的过程。

第二，量子性：电子往往从一种状态突变为另一种状态，似乎无法追溯其过渡阶段；

第三，不确定性：单个电子的行为是不能预言的，我们只能给出大量电子的统计规律。

电子的这些行为确实是非常奇怪的，而量子力学对电子的这些行为的说明则更匪夷所思。但是，从量子力学建立到今日已经八十多年了，不论量子力学的思维方式多么古怪，不论量子力学的语言多么晦涩，物理学家们也早已习惯了。而平易近人的经典物理学则被看作过时的“传统观念”。时至今日，如果有人想到要恢复经典物理学昔日的风光，肯定会被人们认为是痴人说梦。

然而，我在这里却要冒天下之大不韪：用经典物理学的规律来说明电子的奇异行为。特别是，我将根据经典物理学的原理，导出电子的与波粒二象性、量子性与不确定性。

2. 电子的卫星模型

一座城市，例如北京城，东城与西城的经度是不同的，北城与南城的纬度也不一样，但是，在地球仪上，这些区别不能表现出来，因为地球仪上的北京城只能表现北京城的位置，而不能表现其大小与形状。在这种意义下，我们把北京城看作了一个几何点。同样，在一定的条件下，我们也可以仅用一个几何点来表现一个物体的位置，而忽略其大小与形状。事实上，在表述牛顿力学的基本定律时，我们就把“物体”抽象为一个几何点，但同时考虑其质量，这种仅考虑其位置与质量的抽象物体，称为“质点”。1897 年汤姆逊发现电子时，他就把电子看成一个质点，但同时还考虑电子的另一“特征量”——电荷。这种同时考虑其位置、质量与电荷的抽象物体，就是“点电荷”。因此，电子是以点电荷的姿态最先出现在物理学的舞台上的。

到了二十世纪二十年代，物理学家们通过颇为复杂的途径发现，为了进一步描述的电子行为，必须考虑电子的另外两个特征量。一个是“角动量”，另一个是“磁矩”。角动量是一个物体的旋转运动的量度，由于它是一个力学量，人们似乎比较容易接受它，但对某些读者来说，磁矩这一物理量就显得有点陌生了。

粗略地说，磁矩是表现一个物体的磁性大小的物理量。说起物体的磁性，我们全都熟悉永久磁铁的如下行为：它能吸住铁钉等小物体，又能吸附在铁门等较大的物体上。从实质上说，这两种吸引是一回事。但在磁铁吸引铁钉时，我们把磁铁看作激发磁场的物体，在磁铁被铁门吸引时，我们却把磁铁看作在磁场中受力的物体。当我们把磁铁看作一个几何点时，它激发磁场的行为与它在磁场中受力的行为，都可由“磁矩”这一物理量来描述。

除了永久磁铁，电流也能产生磁性。例如，一个有电流通过的封闭线圈也会有磁矩，这就是说，像永久磁铁一样，它也会激发磁场，也会在磁场中受力。

那么，电子为什么有磁矩呢？是因为电子是一块小的永久磁铁，还是因为电子是一个小的封闭线圈呢？

1911 年，卢瑟福提出了原子的有核模型：原子有一个带正电的原子核，还有一些电子绕它旋转。形象的说，原子像一个小太阳系，原子核像太阳，绕原子核旋转的电子像行星。根据这种类比，我们很自然设想电子像一个由地球和月亮组成的系统。我们不妨设想得更具体一些：电子有两个“部分子”组成，一个像地球，我们称它为“定子”，一个像月亮，我们称它为“旋

子”。对于一个静止的电子，定子不带电，基本上是静止的，旋子带负电，以恒定的角速度绕定子作圆周运动。如果把原子核比作太阳，电子比作行星，则电子中的旋子就好比卫星，在这种意义下，我们把上面的电子模型称为“卫星模型”。这个模型对电子的结构刻画还相当粗糙，但已经远远超过实验数据能证实的程度。为什么我们要这么细致地想象电子的结构呢？因为我假定读者也像我一样，喜欢直观的、感性的、具体的模型，不喜欢那些玄之又玄的抽象概念。如果以后发现这个电子模型不能与实验事实吻合，那时再来修改还不迟。

根据经典电动力学，电子的卫星模型确实有磁矩，而且也有角动量，但这里有一个问题：角动量的计算值能不能与实验的测量值吻合？物理学领域里的另一位王者，荷兰物理学家洛仑兹，曾经对另一种电子模型作过计算，把他的计算结果用于我们的电子模型将得出结论：考虑到电子的大小，考虑到旋子的线速度不能超过光速，电子的角动量的计算值有一个上限，而这个上限小于其实验的测量值。

这个令人沮丧的矛盾引发了一场“物理学危机”，为了言简意赅，我们称它“洛仑兹危机”。我们不在这里详细叙述和评论这场危机，只想指出，洛仑兹在这里有一点小小的疏忽：由于旋子的旋转，电子会激发一个相应的电磁场，这个电磁场不能离开电子独立存在，在这种意义下它是“准静止的”。这个准静止的电磁场有角动量，它也是电子的角动量的组成部分。另一方面，准静止的电磁场分布在整个空间，不受电子大小的限制。考虑到这一点，电子角动量的大小就不再有洛仑兹所说的那种上限了。

还有一个问题，它与著名的“波尔论断”有关。

3. 波尔论断

1913 年，波尔提出原子的“波尔理论”，并提出“波尔论断”：“原子世界有特殊规律”，其原始依据是：根据经典电动力学，作加速运动的带电粒子必然辐射电磁波。把这个结论应用于卢瑟福的原子有核模型将得出结论：电子会因为辐射电磁波而落向原子核，从而原子会自动崩溃，而事实上原子却是经久不变的。

这一矛盾曾引发了另一场物理学危机，我们称它“波尔危机”，它迫使经典物理学退出了历史舞台。

同样，按照电子的卫星模型，由于旋子的旋转，电子除了会激发一个不能离开电子的准静止的电磁场以外，还会激发一个可以离开电子的周期性的电磁场，换句话说，电子也会“辐射电磁波”。电磁波的辐射将带走能量，而电子又没有外部能源，根据经典电磁学，我们立刻得出结论：电子会因为辐射失去能量，从而很快地崩溃。但事实上，电子却是经久不变的。这一矛盾是波尔危机的另一种表现方式。

然而，我们并不因为这一矛盾而放弃电子的卫星模型，相反，我们要重审一下物理学史上的这个旧案。问题在于：波尔危机能不能在经典物理学的框架下克服？这个问题可以这样提：按照电子的卫星模型，由于旋子的旋转，电子会激发一个球面电磁波的“波场”，在经典物理学的前提下，伴随着这个“波场”的电子是否可能经久不变？

“作加速运动的带电粒子必然辐射电磁波”这一结论是从经典电磁学的一个基本方程——麦克斯韦方程得出的，确切地说，是从麦克斯韦方程的某一个特解得出的。按照经典物理学，电子的内部运动满足麦克斯韦方程，至于它会满足哪一个特解，经典物理学却没有先验的规定，必须根据实验事实来确定。既然事实证明电子的能量不会流失，上面的疑难就归结为如下问题：将麦克斯韦方程应用于我们的卫星模型时，有没有这样一个特解：一方面，旋子持续地旋转，另一方面电子的能量却不会因此而流失。

回答是肯定的，麦克斯韦方程确实有这样一个特解，它表示电子的辐射与吸收达到平衡，我们称它“平衡解”。这个特解的存在表明波尔危机的原始依据可以在经典物理学的框架下得到克服，同时也表明我们的卫星模型就不再与经典物理学相冲突，在这种意义下，它是一个电子的经典模型。

但是，人们之所以坚信波尔论断，与其说是由于其原始依据，倒不如说是由于实验事实一再地证实它。因此，我们的上述论证远不能驳倒波尔论断。这里，我们提出另一论据。首先提一个问题：

“如果原子世界没有特殊规律，电子应该怎样运动？”

汤姆逊当年发现电子，即发现阴极射线是一束“电子流”时，他默认了一个前提：电子在外电磁场中的行为和点电荷一样。而按照经典力学，点电荷在外电磁场中的行为像点电荷一样。不久以后，人们还根据这一前提发现电子的质量与速度之间的相对论关系。由此可见，自从发现电子以来，人们一致认为：如果原子世界没有特殊规律，则电子在外电磁场中的行为和点电荷一样。”

另一方面，根据牛顿第二定律，一个带负电的点电荷在一个质量大得多带正电的点电荷的有心力场中，将作椭圆轨道运动。我们立刻得出结论：

A： 如果原子世界没有特殊规律，则对于原子有核模型来说，电子将绕核作椭圆轨道运动。

量子力学建立以后，人们发现：在普朗克常量趋于零的极限情况下，薛定谔方程蜕化为经典力学的雅可比方程。将这一方程应用于原子的有核模型，将得出与牛顿第二定律相同的结论。可见即使在量子力学建立以后，命题 A 仍然是人们深信不疑的结论。

可是，当波尔提出它的原子理论，并断言原子世界有特殊规律时，他的前提却是：

B：如果原子世界没有特殊规律，则对于原子有核模型来说，电子的运动不是绕核作椭圆轨道运动。

即使电子是一个百依百顺的女孩子，任我们梳妆打扮，她也会无所适从。她会问：

“我不可能既满足命题 A 又满足命题 B，你们到底要我怎样运动？”

但是，胡适的原理在这里似乎不适用。电子非常不听话，一再让人们得出“原子世界有特殊规律”的结论。不过这也难怪电子，无论电子怎样运动，它都会不断地证明这一结论。就说电子在原子中的运动吧，如果电子绕核作椭圆轨道运动，它就违背了经典电动力学，这就表明原子世界有特殊规律；如果电子不绕核作椭圆轨道运动，它就违背了经典力学，这也表明原子世界有特殊规律。

由此可见，波尔论断之所以不断被证实并不是由于它符合实验事实，而是因为经典物理学

本身自相矛盾。因此，我们的任务不是放弃经典物理学，而是首先清理经典物理学，使它成为一个自洽的理论，然后再用它来说明新的实验事实。

4. 电子衍射与德布罗意波

回到电子的卫星模型，电子的状态经久不变表明，对于一个静止的电子，旋子绕定子旋转激发一个驻波场，对应于麦克斯韦方程的平衡解。如果用复数表示，这个解由两个因子组成，一个仅含时间坐标，是时间的周期函数，我们称它为“时间因子”；另一个仅含空间坐标，表示一个静止的球面波场，我们称它为“空间因子”。

如果一个电子作等速直线运动，则其时间因子变成了一个单色平面波的“波函数”，而其空间因子则表示一个随着电子运动的固定波形。下面，对于作等速直线运动的电子，我们仍然把表示单色平面波的因子称为“时间因子”，把表示随着电子运动的固定波形的因子称为“空间因子”。

电子束是由大量电子组成的电子群体，在这个群体中，每一个电子都有一个准静止的电磁场和一个驻波场，这些场相互迭加，合成一个统一的电磁场，它是电子束的固有电磁场，这个场的场函数随位置与时间剧烈变化，其测量值将是它的平均值。

考虑一种特殊的电子束，其中的每一个电子都以相同的速度作等速直线运动，即该电子束诸电子的动量是一致的，人们称这种电子束为“单色电子束”。这个电子束中的诸电子的固有电磁场的场函数是诸电子的固有电磁场的场函数的迭加。如果表成复数，则诸电子的固有电磁场的场函数有一个相同的时间因子，即单色平面波的波函数，因此，单色电子束的固有电磁场的场函数有一个单色平面波的因子。

实验证明，电子束的位置分布与速度分布有一一对应的关系，特别是，对于单色电子束，它的诸电子的位置在整个空间均匀分布。这样，单色电子束的固有电磁场的平均值的空间因子不再随位置与时间改变，成了一个常量，换句话说，单色电子束的固有电磁场中的空间因子消失在平均值中了。这样，从宏观的角度来看，单色电子束的固有电磁场是一个单色平面波，这个单色平面波就是大名鼎鼎的“德布罗意波”。

由此我们得出结论：

第一，德布罗意波是单色电子束的固有电磁场。

第二，德布罗意波是一种电磁波。

然而，德布罗意波不是光波那样的电磁波：德布罗意波与光波的波源都是电子，但两种波有一显著的区别：德布罗意波作为电子束的固有电磁波，总是伴随着电子束，也就是伴随着波源。而光波却已经离开了作为波源的电子。由于有这一区别，这两种电磁波所满足的波动方程是不同的。光波满足“齐次波动方程”：

$$\frac{\partial^2\psi}{\partial x^2}+\frac{\partial^2\psi}{\partial y^2}+\frac{\partial^2\psi}{\partial z^2}-\frac{1}{c^2}\frac{\partial^2\psi}{\partial t^2}=0;$$

德布罗意波则满足如下“广义波动方程”：

$$\frac{\partial^2\psi}{\partial x^2}+\frac{\partial^2\psi}{\partial y^2}+\frac{\partial^2\psi}{\partial z^2}-\frac{1}{c^2}\frac{\partial^2\psi}{\partial t^2}=\left(\frac{2\pi m_0 c}{h}\right)^2\psi。$$

除了单色电子束以外，其他电子束也有固有电磁波，我们仍然称它为德布罗意波。按照这一规定，一般地说，德布罗意波是电子束的固有电磁波。

这样，电子的波粒二象性就不再难以理解：例如，在电子的散射实验中，可以用盖革计数器为射向某一方位的诸电子计数，从而显示出电子束的粒子性；而在电子衍射实验中，电子束的固有电磁场——德布罗意波——作为电磁波，在通过单缝、双缝或小孔时，将像光波一样衍射，并通过电子的数密度表现出来，从中可以看到德布罗意波的衍射图形，从而显示出电子束的“波动性”。

5. 电子的量子性

从牛顿力学的角度来看，电子肯定有确定的质量，但是它有确定的角动量却难以理解，我们不妨用一个日常生活的例子来阐明这一点。小孩玩的陀螺有一定的质量，这使得当它的平移运动有所改变时有某种“惯性”。陀螺不仅能平移，而且还特别能旋转，它的旋转运动也有某种“惯性”，用一个称为“转动惯量”的力学量来描述。在小孩玩陀螺的过程中，不断地用鞭子抽它，每抽它一下，陀螺就转的更欢。用力学的术语来表达，用鞭子抽陀螺，就是给它施加力矩，陀螺转的更欢，就是它的角动量增加了，因此，一个陀螺有固定不变的质量和转动惯量，却不可能有固定不变的角动量，它的角动量在外界的作用下是可以改变的。一般地说，牛顿力学意义下的物体都不可能有固定不变的角动量。但是，电子自旋（电子的角动量）是电子的一个特征量这一事实表明，电子有固定不变的角动量，因此，电子不是一个牛顿力学意义下的物体。

由于电子有磁矩，可以通过磁场对电子施加力矩，但电子的角动量不会因此而改变。电子的这种行为虽然是微观世界的特征，但宏观世界也有类似的现象。例如，我们的体温是一定的，天气突然变冷时，体温会降低一点点；天气突然变热时，体温也会稍稍增高，但我们的身体随之就会进行自我调整，恢复到原来的体温。这种情况表明我们的身体有一种自我调节的机制。电子有固定不变的角动量表明，电子也有一种自我调节的机制：当外部条件改变时，它总能保持自己内部运动不变。

19 世纪德国生物学家海克尔曾说，原子是“有意识的”。根据上下文，海克尔在这里是说：原子等微观物体不同于牛顿力学意义下的物体，它不是被动地接受外界作用，而是有着内部的、必然的、自己的运动的一种新型物体。或许，“意识”这一用语未必恰当，微观物体与其说是“有意识的”，还不如说是“自动的”。然而，海克尔关于原子等微观物体不同于牛顿力学意义下的物体的论断却是天才的预言，物理学家们要是早听了他的这一预言，或许就不会有今天的量子力学。

如果考虑到电子的自我调节的机制，电子的量子性就不难理解了。下面，我们举三个例子。

第一，当电子绕原子核旋转时，电子的自我调节的机制将使得其轨道运动与自转运动相互协调，这就要求其轨道满足一定条件，满足这种条件的轨道称为“稳定轨道”。德布罗意发现，

当电子在原子中运行时，只有德布罗意波即他说的“物质波”在轨道上形成驻波时，才是“稳定轨道”。用我们的语言来表述：在原子中运行的电子的“稳定轨道”对应于该电子的固有电磁场的时间因子在轨道上形成驻波。在这里，“稳定”这一用语的含义是：如果外界有小的扰动，电子会继续在轨道上运行。但“稳定”并不意味着绝对不变，如果外界的扰动足够大，电子也会离开“稳定轨道”。电子离开某一稳定轨道以后，将进入一种不平衡状态，这时电子的自我调节的机制将恢复电子的平衡，从而使得电子重新进入稳定轨道。如果回到了原来的稳定轨道，则不会显出宏观效果，如果过渡到另一稳定轨道，则电子经历了一个被人们称为“量子跃迁”的过程。这是电子的量子性的最典型的表现方式。

第二，当陀螺在水平的地面快速旋转时，如果它的转轴不与地面垂直，则这个转轴会与垂直轴保持不变的角度的前提下绕垂直轴旋转，这种运动称为陀螺的“进动”。按照经典物理学，当一个有磁矩与角动量的物体落在外磁场中时，将会进入绕磁场方向“进动”的状态。电子有磁矩与角动量，因此它在外磁场中肯定会“进动”。但是，当电子进入外磁场以后，会立即进入进动状态，而电子的自我调节的机制将力求其“进动”与“自转运动”相互协调，只有这样的“进动状态”才是稳定的。实验证明： 电子在外磁场中恰好有两种稳定的“进动状态”，这意味着电子在外磁场中，总与外磁场方向保持两种不变的角度之一，电子的这种行为称为“空间量子化”，它是电子的量子性的另一种表现方式。

第三，当一个孤立的电子遇到外界扰动时，电子的自我调节机制力求使保持电子的内部运动不变，其中包括是旋子的圆周运动与电子的驻波场之间的相互协调。当大量电子形成电子束时，诸电子的固有电磁场相互迭加，形成一个统一的电磁场，这时电子的自我调节机制将要求每电子中的旋子运动与这个统一的电磁场相协调。对于电子束，诸电子的自我调节机制要求诸电子的位置分布与动量分布满足某种一一对应的关系。一般地说，电子束的动量分布是比较稳定的，诸电子的自我调节机制主要是调节诸电子的位置分布。以单色电子束为例，这种电子束诸电子的动量一致，诸电子的自我调节机制将力求它们的位置在空间均匀分布。这也是电子的量子性的一种表现方式。

6. 电子在云雾室中的径迹

在量子力学中，“不确定性”这一用语有各式各样的含义，这些含义彼此混淆造成许多概念混淆。在这里，我们先考察这些概念混淆中的一个。

电子衍射实验曾经使物理学家们大为震惊，时至今日，让我们静下心来仔细想一想，当年人们为什么会那样震惊？如果说这个实验事实出人意外，那么，当时人们意料的究竟是什么？如果说这个实验事实违背了经典物理学的预期，那么，经典物理学究竟预期什么样的实验结果？

电子被发现以后，人们曾一度把电子看作点电荷，如果在电子的小孔衍射实验中把每一个电子换成一个点电荷，则诸点电荷将落在屏幕上的同一位置（最多有实验误差允许的小偏差）。因此，在一个点电荷刚通过小孔时，我们就能预言它将落在屏幕上的什么位置，在这种意义下，我们说“单个点电荷落在屏幕上的位置是确定的”。但电子不是这样，它们不是集中在屏幕上同

一位置，而是分散成为衍射图形。因此，在电子刚通过小孔时，我们不能预言它将落在屏幕上的什么位置，正是在这种意义下，人们说“单个电子落在屏幕上的位置是不确定的”。电子的这种不确定性是一种“量子现象”，它可以追溯到海森堡的“测不准关系”。

但是，在同一实验中，电子的“不确定性”还有另一种含义：单个电子落在屏幕上留下一个痕迹，这个痕迹的线度远远大于电子本身的线度，因此，某一电子在屏幕上留下的痕迹不能给出这个电子落在屏幕上的确切位置。在这种意义下，我们也可以说“单个电子落在屏幕上的位置是不确定的”。这种不确定性并不是什么量子现象，它与测不准关系无关。

按照海森堡的用语，在上面的两种“不确定性”中，第一种不确定性来源于预告性测量的误差，我们称它为“预告不确定性”；第二种不确定性来源于回溯性测量的误差，我们称它为“回溯不确定性”。海森堡一再强调：回溯性测量是没有意义的；而英国哲人波普尔却认为回溯性测量极为重要，回溯性测量达不到一定的精确度，就无法检验对预告性测量的预言。在判定波普尔与海森堡的上述争论谁是谁非之前，请允许我先提出一个问题：怎样划分预告性测量的误差与回溯性测量的误差，即怎样划分预告不确定性和回溯不确定性？我想，人们会异口同声地说：“多么幼稚的问题”。尽管如此，我还是要为这一幼稚的问题提供一个或许是更加幼稚回答：以电子小孔衍射过程为例，如果设想整个实验装置的线度（包括装置本身的大小和装置之间的距离）增加一倍而各种部件的材料的性能保持不变，则有，第一，屏幕上任意两个电子的距离增加了一倍，从而Δx 这一预告性测量的误差增加了一倍；第二，屏幕只改变大小而不改变性能，因此，单个电子落在屏幕上留下的痕迹的线度不变，从而Δx 的回溯性测量的误差保持不变。一般地说，当实验装置的线度改变时，与距离有关的预告不确定性将随着改变，而回溯不确定性则保持不变。

实验证明，当电子经过威尔逊云雾室时，将留下一条径迹。由于有某种不确定性，这条径迹不能确切地给出电子的轨道。现在我们问，这里的“某种不确定性”是“预告不确定性”还是“回溯不确定性”。

如果一束电子通过一个小孔进入一个云雾室，则每一个电子将在该云雾室中形成一条径迹，这些径迹将是相互分散的。现在让我们设想，把云雾室的线度增加一倍（从而小孔的直径也增加一倍），但不改变云雾的物质颗粒的大小，结果会怎么样？我们可以立刻回答：第一，则根据测不准关系，大量进入云雾室的电子留下的径迹将更加分散，从而Δx 的预告性测量的误差增加了一倍；第二，每一条径迹的粗细保持不变。从而Δx 的回溯不确定性保持不变。那么，海森堡所说的“云雾室中的电子的轨道不确定”是哪一种不确定性呢？他说的是：由于云雾室的雾珠太大，不能精确确定电子的轨道，这分明说的是回溯不确定性，它与测不准关系无关。

为了区分上面两种“不确定性”，找出它们的反义词或许是有益的。命题“单个电子落在屏幕上的位置是不确定的”的对立命题是“单个电子落在屏幕上的位置是确定的”。

按照不确定性的第一种含义，“单个电子落在屏幕上的位置是确定的”是指在电子的小孔衍射过程中，所有通过小孔的电子基本上都落在屏幕上的同一位置；而按照不确定性的第二种含义，同一命题是指在单个电子落在屏幕上留下的痕迹的线度与电子的线度相差无几。我想许多人会对这种指出反义词的作法极为反感，他们会提出抗议：“为什么要说这种与事实不符的话

呢？”诚然，“单个电子落在屏幕上的位置是确定的”的上述两种含义确实都与事实不符，但是，我们在这里不是问这个命题是否符合事实，而是问它有没有歧义。我们看到，这个命题与两种不同的事实不符，从而它是有歧义的。它的第一种含义“所有通过小孔的电子都落在屏幕上的同一位置”虽然与事实不符，但当人们把电子看作点电荷时，他们正是这样预期的。他们这样预期，是因为他们还不知道测不准关系。而它的第二种含义，即“单个电子落在屏幕上留下的痕迹的线度与电子的线度相差无几”，不仅与事实不符，而且根本就没有人这样想过，无论是在知道测不准关系之前还是之后，这一事实明显地表明命题的第二种含义与测不准关系无关。

同样，由于有某种不确定性，电子在威尔逊云雾室留下的径迹不能确切地给出电子的轨道。这一事实可以表成：“电子的轨道是不确定的。”其对立命题是“电子的轨道是确定的”。

和“单个电子落在屏幕上的位置是确定的”一样，“电子的轨道是确定的”也有两种含义，第一种含义是，云雾室中的每一个电子都留下同一径迹；第二种含义是，电子在云雾室中的留下每一条径迹都和电子的真实轨道一样细。诚然，根据观察，我们知道该命题的第一种含义与事实不符，但只有知道了测不准关系以后，我们才知道这种含义的命题在理论上是不成立的。因为根据测不准关系，一个电子束中的诸电子不可能在同一轨道上运行。至于该命题的第二种含义，它也与事实不符，与第一种含义不同的是，无论是在知道测不准关系之前还是之后，谁也没有想过电子在云雾室中的留下径迹和电子的真实轨道一样细。这也可以看出该命题的第二种含义与事实不符这件事与测不准关系完全无关。

或许没有人曾混淆命题“单个电子落在屏幕上的位置是不确定的”的两种含义，但是，似乎没有人不会混淆命题“电子的轨道是不确定的”的两种含义，人们多么健忘！

在电子衍射过程中，由于回溯不确定性，单个电子在屏幕上留下的痕迹不能给出该电子的确切位置，但是这个痕迹足以表明，该电子在屏幕上有一个“位置”；同样是由于回溯不确定性，单个电子在云雾室中留下的径迹不能给出该电子的确切轨道，但是这条径迹的存在足以表明，该电子运行在云雾室中有一条轨道。换句话说，这条径迹的存在足以表明，电子的运动是轨道运动。

爱因斯坦与玻尔的所谓“世纪之争”中的一个重要问题是：“量子力学的描述是否完备？”现在我们可以简单地回答这一问题：量子力学不能给出单个电子的轨道运动，从而不能描述电子在云雾室中留下的径迹，因此是不完备的。

7. 结束语

综上所述，我们得出结论：

第一，电子的波粒二象性原来是经典物理学的必然结论。例如，单色电子束伴随着一个单色平面波，这个单色平面波是该电子束的固有电磁场（测量值）。

第二，电子的量子性乃是电子的自我调节机制的表现。诚然，从经典物理学不能导出电子具有自我调节的性质，但是，电子的这种性质并不与经典物理学相矛盾。我们知道，从牛顿力学不能导出电动力学的方程，但电动力学的方程并不与牛顿力学相矛盾，从而这个方程的导出

不意味着推翻了经典物理学，而是把经典物理学发展到了一个新阶段。同样，电子的量子性并不与经典物理学相矛盾，这种性质的存在不意味着推翻了经典物理学，相反，它把经典物理学发展到了一个新阶段。

第三，如果说电子的不确定性是指我们不能预言单个电子的行为，那么，这种不确定性只表明量子力学还不完备，而不表明电子的运动不是轨道运动。

在近代的思想史上，数学和物理学一样，也经历过从“经典”阶段向“现代”阶段的过渡，如果说对于物理学，这一过渡以爱因斯坦的相对论的建立为标志，那么对于数学，同样的过渡的标志或许可以算是罗巴切夫斯基建立非欧几何学。这一早一晚的两个过渡都经历了光辉而又苦涩的历程，但两者的发展进程却有一个明显的区别：现代数学的建立使数学家们发现，过去的数学中的逻辑形容枯槁、惨不忍睹。人们伤心地看到：数学中包括错误的证明，推理的漏洞，还有稍加注意就能避免的疏忽，这样的大大小小的错误比比皆是。此外，还有对概念的不充分理解，不清楚逻辑所需要的原理，在某些已经给出的证明中，直觉、实证和借助于几何图形的证明取代了逻辑的证明。等等，等等。诸如此类，不一而足。

那么，在从“经典”阶段向“现代”阶段的过渡中，物理学的情况又怎样呢？由于物理学是一门实验的科学，人们重视实验事实超过重视逻辑推理，因此从“经典”阶段向“现代”阶段的过渡并没有促使物理学家们去检查物理学有没有和数学一样的随处可见的错误；相反，这种过渡使物理学家们相信，在物理学的不同的领域，特别是高速领域与微观领域，有新的物理学规律。

在我看来，与数学相比，物理学的现状更加惨不忍睹：和数学一样，物理学也有错误的证明，推理的漏洞以及稍加注意就能避免的疏忽，正是这种类型的错误导致上面我们所说的“洛仑兹危机”和“波尔危机”。此外，物理学中还有一些在数学中罕见的概念混淆，上面说的对“不确定性”这一概念的两种含义的混淆就是一例。更令人伤心的是，物理学中还充满了古怪新奇而又令人啼笑皆非的幻想，人们把这些幻想称为“新颖观念”。

在二十世纪，几乎物理学的每一个划时代的发现都伴随着某种空前的“新颖观念”。现在，这些“新颖观念”已经如此深入人心，人们已经把它们当作天经地义，竟然没有发现，这种由一个又一个“新颖观念”所形成的思维方式，已经使得一度辉煌的物理学蜕化成为一门边缘学科。不幸的是，失去了神圣光环的物理学家不是反躬自问：物理学的思想方法是不是出了问题。相反，人们仍然一味把物理学中的每一个困难都归结为经典物理学的传统观念作祟。

Unimaginable Electrons

Tan Tianrong

Qingdao University, Physics department, 266071

ttr359@126.com

Abstract: It is natural to associate the argument that an electron has angular momentum and magnetic moment with an intuitive electron modal in that the charge is revolving, but such an electron modal has two difficulties: Firstly, considering the dimension of the electron, and the requirement that the linear velocity of the electron border cannot large than light velocity, Lorentz has concluded that the electron angular momentum has a superior limit, but which is clearly less than the measurement value. Secondly, if the charge is revolving, an electron is bound to emit electromagnetic wave and thus would collapse because of losing energy, but the state of the electron is prolonged constant actually. It is well known that Bohr found the same contradiction in the Rutherford atom model, and for this reason he asserted that "there are special laws in micro world". Due to the above two difficulties, any intuitive modal in micro world are abandoned by quantum physicists. However, it is about to see that the very two difficulties are eliminable in the framework of classical physics.

Firstly, it must be pointed out that Lorentz advanced his argument through an oversight. An electron is a charged system, and thereby it certainly excites an electromagnetic field, which is the "intrinsic electromagnetic field" of the electron. This field possesses angular momentum and that is a component part of the electron angular momentum. On the other hand, the intrinsic electromagnetic field of the electron distributes over the whole space. Considering this argument, the electron's angular momentum has not the superior limit as Lorentz given any longer.

Secondly, if there are no special laws in micro world, the internal motion of electron satisfies Maxwell functions, but the question which special solution herein ought to be choosed must be answered by experimental facts. It is easy to prove that applying Maxwell functions to the internal motion of electron, there exists a special solution indicating that the energy of the electron will not be washed away when its charge sustained revolve. It is thus seen the original foundation of Bohr's thesis that "there are special laws in micro world" is wrong, and thereby the intuitive electron modal in that the charge is revolving is imaginable.

For a still electron, such a special solution of Maxwell function expresses a standing wave field, of which the wave function signified as a complex number consists of two factors, one merely contains the coordinate of time; the other only contains that of space. It is concluded that the first factor of for an electron moving in a straight line and constant velocity state becomes a singer-frequency plan wave, and the second factor becomes a fixed wave shape following the electron.

In an electron beam, the intrinsic electromagnetic field of its electrons forms the intrinsic electromagnetic field of the beam. If all electrons belong to the beam are in a same straight line and constant velocity state, the intrinsic electromagnetic field of the beam has two factors, one is a singer-frequency plan wave, and the other as a function of time and space rapid changes, but its mean value is a constant. So, the measurement value of the intrinsic electromagnetic field of this beam is a singer-frequency plan wave, which is exactly de Broglie wave. It is thus seen that both de Broglie wave and light wave are electromagnetic waves radiated by electrons, merely a light wave is one departed from wave source while a de Broglie wave is one in company with wave source.

According to Newton mechanics, the angular momentum of a given body is variable, namely, a body in the Newton mechanics sense has not fixed angular momentum. On the other hand, it is well known that

the angular momentum is a characteristic quantity of the electron. This fact means that the angular momentum of an electron is able to keep invariant under the external action. In other words, this fact indicates that the electron has a certain self-regulation mechanism, by means of which it is always able to keep its internal motion constant while the external condition is changing. For instant, when the electron revolves round the atom nuclear, its self-regulation mechanism will harmonize its orbital motion with rotation, so that requires its orbit satisfies a certain condition. An orbit satisfying such condition is called “stable orbit”. If there is small external turbulence, an electron in stable orbit will continue move in the orbit. Conversely, if the external turbulence is large enough, the electron will depart from stable orbit, enter an unbalance state, and at this moment the self-regulation mechanism will make it reenter stable orbit for the purpose of recovering balance state. If returning to the original orbit, this process has not macro effect. Conversely, if enters a new orbit, it will undergo a process that is called “quantum transition”. That is a typical example of so-called “quantum behavior”. Having magnetic moment, an electron will enter precession in a magnetic field and its self-regulation mechanism will make its rotation axis form a certain angle with the magnetic field. Such a behavior of the electron is called “space quantization”. For an electron beam, the self-regulation mechanism of each electron will harmonize the position distribution of electrons with the momentum distribution. So-called Heisenberg relation is one of the expressions of such a behavior of the electron beam.

So-called “uncertainty” has variable meanings. If “the uncertainty of the electron” means that it is impossible to predict the behavior of a single electron, then the “uncertainty” only indicates that quantum mechanics is not complete instead of electron motion is not orbital motion,

Key words: electrons; spin; magnetic moment; Maxwell function; wave particle duality; quantum properties; uncertainty; orbit motion; quantum transition; quantum mechanics

Note:
Primary version of this article was originally published in New York Science Journal [2008;1(2):36-48]. (ISSN: 1554-0200).

Academia Arena

http://www.sciencepub.net

ISSN: 1553-992X

The international academic journal, "Academia Arena" (ISSN: 1553-992X), is registered in the United States, by English and Chinese language, and invites you to publish your papers.

The valuable papers in all fields that describe your researches or opinions on natural phenomena and existence are welcome. Papers submitted could be reviews, objective descriptions, research reports, opinions/debates, news, letters, and other types of writings that are nature and science related. Manuscripts will be processed in a professional peer review. After the peer review, the journal will make the best efforts to publish all the valuable works as soon as possible.

This journal will be no charge for the manuscript contributors. If the author needs hard copy of the journal, it will be charged for US$60/issue to cover the printing and mailing fee. Here is a new avenue to publish your outstanding reports and ideas. Please also help spread this to your colleagues and friends and invite them to contribute papers to the journal. Let's work together to disseminate our research results and our opinions.

Papers in all fields are welcome, including articles of natural science and social science.

Please send your manuscript to: aarenaj@gmail.com

For more information, please visit: http://www.sciencepub.net/academia

Academia Arena
Marsland Press
525 Rockaway PKWY, #B44
Brooklyn, New York 11212, USA
Telephone: (347) 321-7172
Email: aarenaj@gmail.com
Website: http://www.sciencepub.net/academia

Academia Arena

学术争鸣

http://www.sciencepub.org

ISSN: 1553-992X

Marsland Press

Lansing, Michigan, The United States

ISSN 1553-992X

9 771553 992012